Investigating and Exploiting the Electrocatalytic Properties of Hydrogenases

Kylie A. Vincent, Alison Parkin, and Fraser A. Armstrong*

Inorganic Chemistry Laboratory, Department of Chemistry, University of Oxford, South Parks Road, Oxford OX1 3QR, United Kingdom

Received February 23, 2007

Contents

1. Hydrogen as an Energy Store

Hydrogen is the most abundant element in the universe and the tenth most abundant element on Earth, but we encounter only a tiny amount as molecular H_2 (0.5 ppm in

10.1021/cr050191u CCC: $65.00
Published on Web 09/11/2007

Kylie Vincent is a graduate of the University of Melbourne, Australia (BA/BSc Hons, Ph.D.), and since 2002 has carried out postdoctoral research at the University of Oxford with Fraser Armstrong. She holds an R. J. P. Williams Junior Research Fellowship at Wadham College, Oxford. Her research interests include the application of electrochemical and spectroelectrochemical methods to biological systems, in particular enzymes involved in energy cycling.

Alison Parkin was born in Beverley, U.K., and grew up in East Yorkshire. She is a graduate of the University of Oxford (MChem) and is now completing her doctorate in the Armstrong group. Her studies have focussed on applications of protein film voltammetry to elucidate mechanistic details of complex enzymes. Many of these catalyze technologically relevant reactions.

Fraser Armstrong is a Professor of Chemistry at Oxford University and a Fellow of St. John's College. He obtained his Ph.D. at the University of Leeds with Geoff Sykes and then carried out postdoctoral research with Peter Kroneck (Konstanz), Ralph Wilkins (New Mexico), Helmut Beinert (Madison), and Allen Hill (Oxford). In 1983 he was awarded a Royal Society University Research Fellowship which he held in Oxford until 1989, when he joined the Chemistry Faculty at the University of California, Irvine. He moved to his present position in 1993. His interests are in biological redox chemistry, in particular the application of dynamic electrochemical techniques in studies of complex electron-transfer and catalytic reactions in proteins, and most recently the mechanisms and exploitation of biological hydrogen cycling. He was awarded the 1998 European Medal for Biological Inorganic Chemistry, the 2000 Royal Society of Chemistry award for Inorganic Biochemistry, the 2003 Carbon Trust Academic Innovation Award (with Kylie Vincent), the 2004 Max-Planck "Frontiers in Biological Chemistry" Award, and the 2006 Royal Society of Chemistry Medal for Interdisciplinary Chemistry.

the lower atmosphere[1]) because it escapes easily into space. Although H_2 has a strong chemical bond, the hydrogen atom forms an even stronger bond to oxygen, and H_2O, being relatively nonvolatile, is the dominant compound on Earth's surface. Reaction of H_2 with O_2 (1) releases a large amount of energy, and most mixtures explode upon ignition.

$$2H_2(g) + O_2(g) \rightarrow 2H_2O(l) \qquad \Delta H^\circ = -286\ \text{kJ mol}^{-1} \tag{1}$$

In both biology and technology, H_2 is a fuel (an energy carrier).[2] In technology, some important advantages of H_2 are (i) its high specific enthalpy of reaction with O_2 (ΔH° per gram), which lends itself to uses where weight is important, such as rocket propulsion, and (ii) the fact that the explosive reaction 1 with O_2 is ignited simply by a spark and produces only water. In both biology and technology, as the reduction product of water, H_2 is the strongest reducing agent to be thermodynamically stable in aqueous solution. But H_2 also has notable disadvantages. Its low solubility in water limits its availability as an energy source in that medium, although its large diffusion coefficient enables it to move rapidly to replenish areas where it has been depleted. Most importantly, because it is so highly volatile, H_2 is difficult to store—a point that has been emphasized by critics of a future "hydrogen energy economy". The biological solution to trapping H_2 has been to lock it up in organic molecules and supply it as the hydride carriers NADH and NADPH (nicotinamide adenine dinucleotide and the phosphate derivative).

Reaction 1 occurs extremely rapidly by a radical chain mechanism, but H_2 is otherwise quite an inert molecule and is oxidized slowly without a catalyst. Equally, it is not easy to reduce water (H^+_{aq}) to form H_2 without a catalyst (although clean, four-electron reduction of O_2 to form H_2O is even more difficult). Under mild conditions, up to 150 °C, the most effective catalyst is platinum, but very fast interconversion of H_2 and H^+ is also a key aspect of microbial energy cycling in reactions that do not involve any precious metal. In microbes, production and oxidation of H_2 are catalyzed under ambient conditions at iron or nickel and iron catalytic centers contained in highly active enzymes called hydrogenases.[2]

1.1. The Hydrogen Half Cell Reaction

The energy released when H_2 is oxidized is also expressed in electrochemical terms, beginning with the standard half cell reaction (eq 2A) and the Nernst equation (eq 2B), which shows how the electrode potential E measured for an aqueous solution in equilibrium with H_2 gas depends on pH ($-\log(a\text{H}^+)$, where $a\text{H}^+$ is the activity of H^+), and the H_2 partial pressure, $\rho(H_2)$.

$$2H^+ (pH = 0) + 2e^- \rightarrow H_2 (1\ bar) \qquad E^\circ = 0\ V \quad (2A)$$

$$E = E^\circ + 2.3RT/nF \log\{(aH^+)^2/\rho(H_2)\} \qquad (2B)$$

In eq 2B, R is the gas constant, T is the absolute temperature, n is the number of electrons involved (=2 for reaction 2A), and F is the Faraday constant. The standard reduction potential (E°) in this case is the standard hydrogen electrode (SHE)—the potential provided by an aqueous solution at pH 0, 25 °C, in equilibrium with H_2 gas at 1 bar pressure—and is a common reference for other redox couples. In biochemistry, electrochemical measurements are made at higher pH values that have greater physiological relevance, and "standard" reduction potentials under these conditions are replaced by terms such as $E^{\circ\prime}$ (a "formal potential") or E_{m7} (a "midpoint potential", in this case determined from potentiometry carried out at pH 7). Reduction potentials reflect reducing power—the more negative the potential, the more potent is the electron donor. Some misconceptions arise: at pH 7, under 1 bar H_2, the reduction potential of the proton is −413 mV vs SHE, but this value is considerably more positive under the much lower H_2 partial pressures that are physiologically and environmentally relevant (see section 2.1). Figure 1 shows how E for the H^+/H_2 redox couple varies with pH and $\log\{\rho(H_2)\}$.

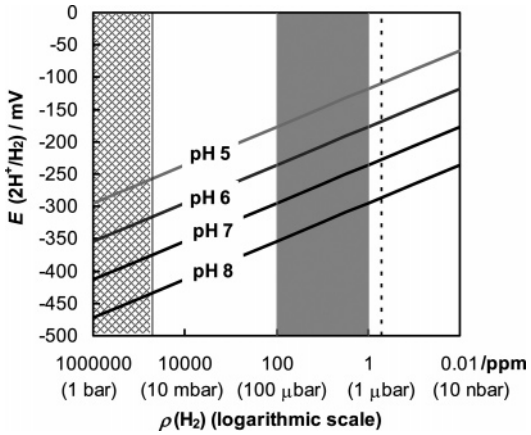

Figure 1. Plot of $E(H^+/H_2)$ vs $\rho(H_2)$ (logarithmic scale) according to eq 2B for pH 5−8, 25 °C. H_2 levels are provided as parts per million (ppm) in the lower atmosphere or as partial pressure in bar at atmospheric pressure. The gray area shows the levels of H_2 that are likely to be encountered by soil bacteria;[3] the dashed line corresponds to the level of H_2 in the lower atmosphere;[1] the hatched area indicates typical levels of H_2 employed in solution assays or electrochemical studies of hydrogenases.[2]

The abundance of H_2 in the lower atmosphere (0.5 ppm) sets a realistic lower limit on its thermodynamic reducing power, and $E = -227$ mV at pH 7 (Figure 1). At pH 7, 0.1% H_2 (1000 ppm, about μM) is in equilibrium with a 50% NAD^+/NADH mixture ($E = -320$ mV), a fact that has implications for soluble hydrogenases that catalyze formation of NADH from very low amounts of H_2. Conversely, NADH in water at pH 7 would evolve H_2 if there were no H_2 present to start with (provided an appropriate enzyme is present to catalyze what is otherwise an extremely slow reaction). Figure 1 is not a reflection of the redox potential in a living cell, only an expression of the inherent electrochemical properties of H_2 itself as its partial pressure is varied. As we discuss in sections 6 and 7, a certain level of H_2 is also important in protecting the active sites of hydrogenases against formation of inactive states.

At very low levels, H_2 not only loses its thermodynamic potency, but the kinetics of reaction are slowed down. These disadvantages are partly offset by its high diffusion coefficient, which is the largest of any molecule, and since diffusion rates scale as the square root of molecular mass, the H_2 molecule travels about four times faster than an O_2 molecule and 18 times faster than NADH. The fact that a H_2 molecule will travel faster than any other molecule has relevance both for cell physiology and electrochemistry because it can escape quickly from its site of production.

1.2. Why Study Hydrogenases on an Electrode?

This Review describes how much can be learnt about the properties of hydrogenases by applying a variety of dynamic electrochemical techniques. Aside from scientific curiosity, we will be interested to see how well these enzymes or their inspired mimics could function as electrocatalysts in future hydrogen technologies such as novel H_2 fuel cells, "green" H_2 production, or H_2 sensing.

Protein film voltammetry (PFV) is a term used to describe the application of a suite of dynamic electrochemical techniques to interrogate redox-active protein molecules attached to an electrode. It is now well established that proteins ranging from small electron carriers to large, complex enzymes can be adsorbed on electrode materials such as carbon and exhibit high rates of electrode−protein (interfacial) electron transfer.[4−7] In these experiments, diagnostic current signals arise as electrons are exchanged between the enzyme and electrode as a result of catalytic turnover and variations in electrode potential. The experiment is depicted as a cartoon in Figure 2.

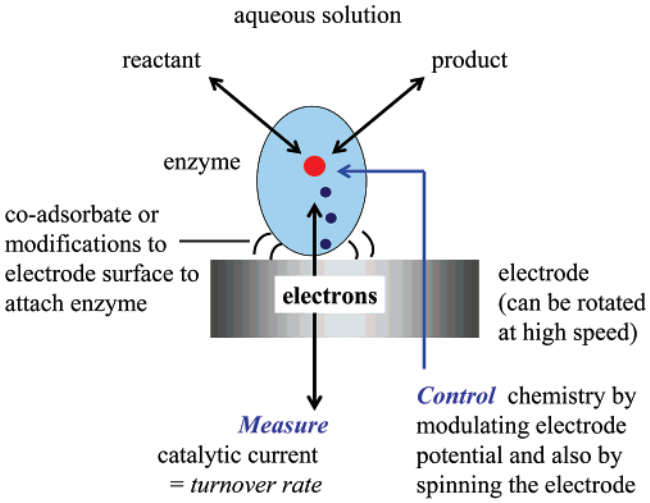

Figure 2. Cartoon showing the configuration of an enzyme in a protein film voltammetry experiment. Adapted with permission from ref 5a. Copyright 2003 American Chemical Society.

Dynamic electrochemical techniques are very different from potentiometry[8] because the focus is on recording *current* (electron transfers and catalytic activity) as a function of electrode potential rather than measuring the ratio of oxidized to reduced components of a system that is at equilibrium with a particular electrode potential. Techniques such as cyclic voltammetry which have been used for over 40 years to measure the redox properties of small molecules in solution (their reduction potentials and stabilities) acquire a fresh significance when dealing with complex enzymes that are attached to an electrode surface. As we will show later,

hydrogenases are not directly electroactive at an electrode until they have become attached to (adsorbed on) the electrode surface (Figure 2). A useful aspect of protein film voltammetry is the minimal sample requirement: whereas extensive spectroscopic measurements require quite large amounts of material (a typical EPR sample may contain several milligrams (tens of nanomoles) of enzyme), detailed electrochemical results are obtained from less than a picomole of enzyme on an electrode. This advantage is particularly important for hydrogenases because preparation yields are low (often no more than a few milligrams from 100 g cells) and heterologous (over-)expression is challenging due to the genetic complexity of hydrogenase assembly.[2,9]

Protein film voltammetry allows extensive exploration of properties, and it can both complement and "trailblaze" spectroscopic and structural investigations. We emphasize in this Review that fast and direct control over the electrode potential is critical in studies of hydrogenases—enzymes that exist in numerous active and inactive states. As an example, it has recently become apparent that uncertainty over the presence of a sulfur-based bridging ligand in the active site of [NiFe]-hydrogenases can be attributed in part to the difficulty in achieving control over the redox state of protein molecules in crystallographic experiments (see section 7.3).[10] The importance of potential control is also appreciated by considering the structural information that can be obtained from infrared spectroelectrochemical studies, described in the Review by Fernández et al. in this Issue, in which a gold electrode in conjunction with soluble mediators is used to produce specific redox states of a hydrogenase.[11,12]

1.3. Challenges and General Visionary Outlook

Hydrogen is heralded by many as a "fuel of the future", but more accurately, it is a form of stored energy and a transportable fuel. Three major challenges are how to obtain H_2 in large amounts, how to store it, and how to release its energy. The latter is the best developed because fuel cells, albeit expensive, are becoming an accepted technology. At present, H_2 is stored by compression or liquefaction, although there is intense interest in finding low-cost lightweight materials that, like Pd, can reversibly absorb high volumes of H_2 but without the disadvantages of cost and prohibitive weight (for transport).[13] Only in rare cases, such as Iceland, does H_2 exist as a mineable resource, otherwise it must, in the future, be obtained by splitting water.[14] Whether this is carried out electrolytically, photolytically, thermolytically or "biolytically", the catalyst is a prime consideration. At present, most H_2 is obtained from fossil fuels by reacting methane with water at high temperatures (the "steam reforming" reaction). But for those anxious to promote the development of "green" H_2 technologies, steam reformation is really to be seen only as bridging the gap until H_2 is obtained from nonfossil sources without CO_2 as a byproduct. "Reformed" H_2 is contaminated with H_2S and CO—gases that poison Pt catalysts. Pure H_2 is obtained mainly by electrolysis, where, significantly, Ni and Fe electrodes are used to electrolyze a concentrated alkali solution, although a large overpotential is required.

"Bio-hydrogen" is the production of H_2 using microbes,[15] and two routes are available, fermentation or photosynthetic production. Fermentation involves providing bacteria with suitable carbon sources such as domestic waste.[16] Photosynthetic H_2 production is potentially more attractive since primary energy is captured, but it is complicated by the need to avoid O_2 damaging the active site of the enzymes. Phototrophic microbes such as cyanobacteria and green algae use energy from sunlight to oxidize water, generating a transmembrane proton gradient and producing energetic electrons. Although the electrons are usually used in NADPH generation, under certain adverse growth conditions, particularly deprivation of sulfur, the green algae are able to sustain photosynthetic ATP synthesis by diverting the electrons to a hydrogenase that generates H_2.[17,18] This hydrogenase, which is of the [FeFe]-type (see later), is highly sensitive to the O_2 that is released during water splitting, and this process therefore does not persist under conditions of illumination.[19] Okura, Friedrich, and co-workers recently fused a subunit of Photosystem I (PSI) from the cyanobacterium *Thermosynechococcus elongatus* to the O_2-tolerant [NiFe] membrane-bound hydrogenase of *Ralstonia eutropha* H16.[20] They demonstrated by gas chromatographic detection of H_2 that the spontaneously assembled composite hydrogenase−PSI system catalyzes light-driven H_2 production. Direct electron transfer between PSI and the hydrogenase side steps the physiological ferredoxin-mediated electron transfer between PSI and *T. elongatus* hydrogenase. The electrochemical potential, whether pertaining to the biological cell or a voltammetry experiment, is an important variable for tuning catalytic activity: it not only controls catalytic activity but it also determines the sensitivity of enzymes to inhibitors and destructive agents such as O_2.

Synthetic electrocatalysts for H-cycling are coming under increased attention and might ultimately be based on the active sites of the enzymes. If synthetic catalysts could be attached to electrodes, new avenues could be opened up for cheap electrolytic H_2 production. Once again, a key issue is likely to be O_2 sensitivity, because it will be difficult to substitute the "supramolecular" protection that is provided by the protein environment to filter or neutralize attacks by this aggressor.

2. Hydrogen and Its Redox Chemistry in Biology

2.1. Hydrogen Cycling in Biology

Atmospheric models predict that extensive future use of H_2 as a fuel will lead to increased atmospheric H_2 levels due to leakage during storage and transportation and to incomplete fuel conversion.[21] At the present time, the level of H_2 in the lower atmosphere, 0.5 ppm, is influenced mainly by H_2 released during fossil fuel combustion and microbial production, atmospheric photochemical reactions that convert H_2 into H_2O and CH_4, and uptake of H_2 by soil.[21] In the 1980s and 1990s, Conrad and co-workers determined details of soil H_2 cycling and showed that the sub-ppm atmospheric H_2 levels are too low for uptake by soil micro-organisms.[22] Thus, microbial H_2 uptake from soil relies upon supplemented levels from geological and other biological activity. In upland soils, N_2-fixing root nodules release H_2 as a byproduct of ammonia formation catalyzed by nitrogenases. In O_2-poor wetland soil and submerged sediments, H^+ ions are important electron acceptors and H_2 is produced by hydrogenase action in fermentative bacteria.[23] Dihydrogen is also produced by algae and cyanobacteria that under certain conditions use hydrogenases to consume electrons produced by photosynthesis.[15,24]

Conrad defined zones in submerged wetland soils according to a vertical redox gradient of microbial substrate reduction reactions coupled to H_2 oxidation (Figure 3).[22]

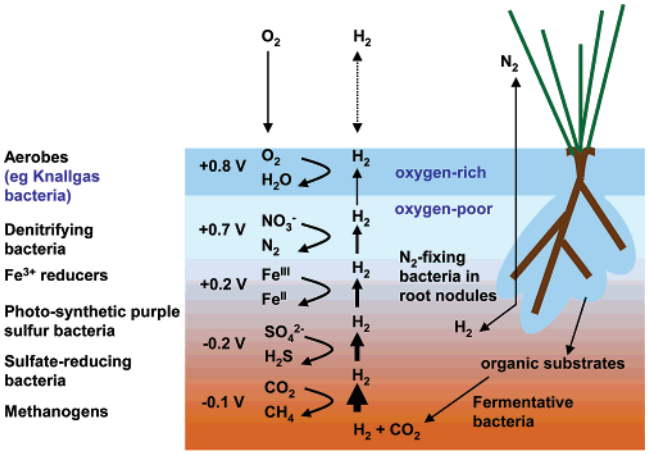

Figure 3. Schematic representation of the vertical distribution of redox reactions that contribute to the flux of H_2 and other trace gases in submerged wetland soil. Only trace levels of H_2 reach the O_2-rich environment at the surface where aerobic Knallgas bacteria are able to oxidize H_2. Higher levels of H_2 are available to anaerobes. Depletion of H_2 toward the surface is indicated by the thickness of the vertical arrows. The potentials indicated are for pH 7. Adapted from ref 3 with permission of the author and the American Society for Microbiology Journals Department.

Gradients of H_2 and O_2 concentration also exist in this environment, and the range of H_2 levels likely to be encountered is highlighted by the gray box in Figure 1. In the anaerobic fermentation zone, dissolved H_2 is present at a steady-state concentration in the 10−180 nM range (equivalent to an atmosphere containing approximately 10−180 ppm) and it is taken up by methanogens that couple H_2 oxidation with the reduction of CO_2 to CH_4.[22] Microbial utilization of trace gases is defined by threshold concentrations below which they are no longer consumed.[3] Lovley[25] and Conrad[3] report that cultures of methanogens in sediments are only able to oxidize H_2 if it exceeds a threshold partial pressure of about 70 ppm (corresponding to ca. 70 nM dissolved H_2). Some H_2 diffuses upward to the sulfate reduction zone, where sulfate-reducing bacteria (e.g. *Desulfovibrio*) couple H_2 oxidation to sulfate reduction. They have a higher affinity for H_2 than methanogens and lower its steady-state concentration to ca. 2−10 nM. Levels of H_2 are further depleted by the action of Fe^{3+} reducers and denitrifying bacteria in the upper levels of submerged soil.

Dioxygen at the soil surface is consumed by aerobic microorganisms and is therefore depleted rapidly with depth. The uppermost, O_2-rich niches are inhabited by aerobic Knallgas bacteria (eg *Ralstonia*, formerly *Alcaligenes*) that are able to grow on H_2, O_2, and CO_2 as the sole sources of energy and carbon.[3] Only trace levels of H_2 reach the surface, and Knallgas bacteria have thresholds for H_2 uptake of >1 ppm by volume (approximately 1 nM dissolved H_2) and have needed to adapt to considerable variation in levels of both H_2 and O_2.[22,26] A question thus arises which can be addressed by electrochemical methods: how compatible are hydrogenases, ancient enzymes that preceded O_2 on earth, with ambient levels of O_2 and oxidizing conditions in general?

Arras et al. have considered the cellular levels of O_2 likely to be maintained by aerobes. They monitored the growth of *Pseudomonas putida*, an organism that is physiologically similar to *R. eutropha*, on different organic substrates at various partial pressures of O_2, $\rho(O_2)$.[27] Growth becomes severely limited at $\rho(O_2)$ below 10 mbar, particularly for growth on aromatic substrates which the authors show are only partially metabolized under microaerobic conditions. Even at extracellular $\rho(O_2)$ as low as 1 mbar, the cytoplasmic O_2 concentration is maintained at the same level as that outside the cell. The growth limitation must therefore arise because the oxygenases required for organic substrate oxidation have relatively high K_M values for O_2 (K_M = Michaelis constant, a measure of the affinity of an enzyme for its substrate, where a high K_M indicates a low affinity).[27] Thus, it can be assumed that O_2 levels above ca. 1 mbar are maintained in actively growing cultures. In this Review we will consider the challenge that these levels of O_2 would pose for aerobic H_2 oxidation and show how electrochemical experiments can assist in understanding the chemistry in a quantitative manner (sections 7.1 and 8).

Interesting examples of hydrogen cycling arise in unusual or extreme environments. Most strikingly, the H_2 that is released through geological action at volcanic vents is taken up by thermophiles and hyperthermophiles.[2] Closer to home, the anaerobic environment of the human large intestine houses methanogens and sulfate-reducing bacteria that compete for H_2 formed by fermentation of carbohydrates.[28] An average H_2 level of 43 μM has been measured in the mucus layer of the mouse intestine, and it is becoming apparent that high affinity hydrogenases expressed by bacteria such as *Helicobacter pylori* (whole cell $K_M \sim 1.8$ μM) assist these human gastric pathogens to colonize the niche environment of the stomach.[29] High levels of H_2 in the breath have been used to diagnose carbohydrate maladsorption and may reach >70 ppm following lactose ingestion by lactose-intolerant patients.[30]

Challenges to biological H_2 oxidation and production arise not only from O_2 but also from other small molecules that are expected to bind at H_2 activation sites, including CO, H_2S, and even NO. Carbon monoxide may be present in soil at nanomolar levels, arising from chemical conversion of organic carbon and as an intermediate of microbial metabolism, and it is consumed by bacteria including carboxydotrophs.[3] Hydrogen sulfide is produced by sulfate- and sulfur-reducing bacteria, and H_2S can be formed at millimolar levels in laboratory cultures of sulfate-reducing bacteria.[31,32] Nitric oxide is an intermediate in nitrogen cycling, and its concentration is balanced by the action of nitrifiers and denitrifiers that have K_M values < 8 nM.[3] A strong electrochemical connection arises because the degree to which any of these small molecules may inhibit a particular hydrogenase should depend on the redox level of the active site prevailing during catalysis under given conditions.

Electrochemical studies of H_2 oxidation by hydrogenases and solution assays for H_2 uptake activity have focused on high H_2 levels under anaerobic conditions, usually 0.05−1 bar H_2, indicated by the hatched region in Figure 1. The high levels of H_2 are far above physiological levels,[3,33] and we include in this Review some recent observations of interesting effects in the voltammetric behavior of hydrogenases at very low levels of H_2 under both anaerobic and aerobic conditions.

2.2. Types of Hydrogenases

Utilization of H_2 for energy was probably a crucial feature of very early life on Earth and occurs everywhere—in bacteria, archaea, and lower eukaryotes. Convergent evolution led to three classes of hydrogenases that are able to catalyze interconversion of molecular H_2 and protons. Although they share no sequence similarity,[34] all three types of hydrogenases utilize metal carbonyl active sites that are

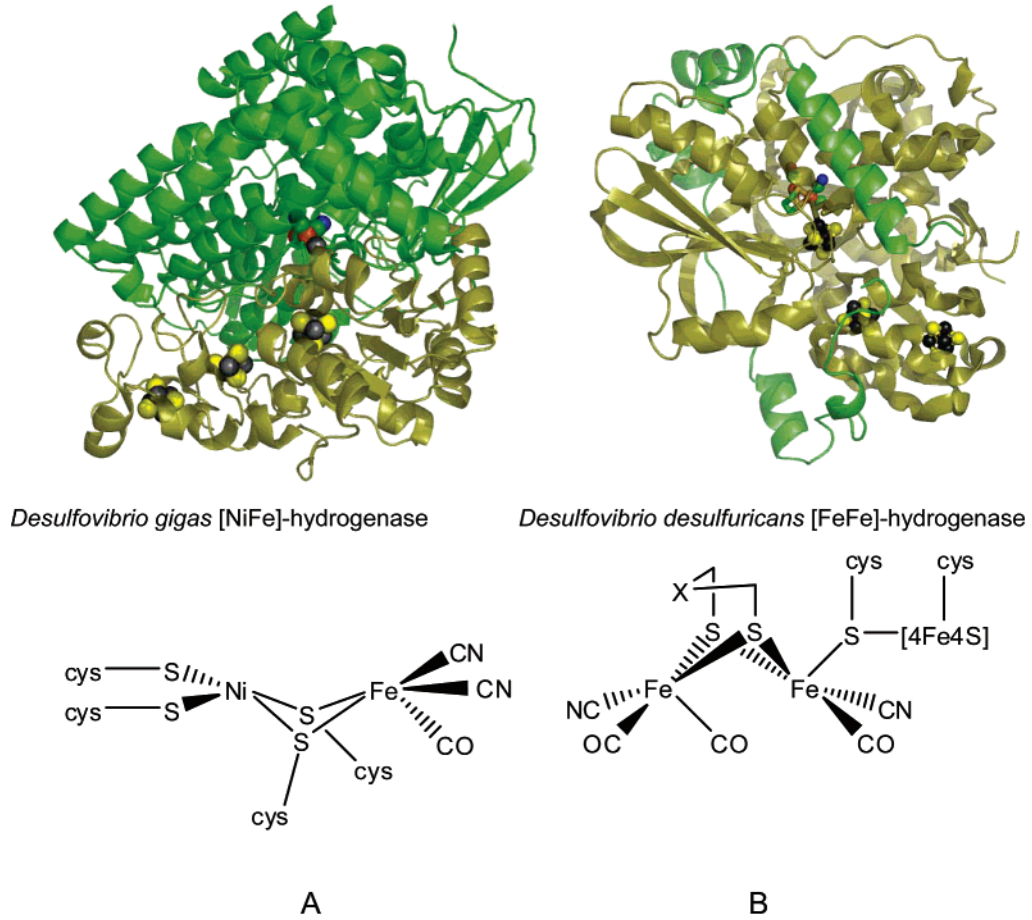

Figure 4. Representations of the X-ray crystallographic structures (constructed using Pymol) and active forms of the active sites of (A) *Desulfovibrio gigas* [NiFe]-hydrogenase (PDB code: 1YRQ)[39] and (B) *Desulfovibrio desulfuricans* [FeFe]-hydrogenase (PDB code: 1HFE).[40] The identity of the bridgehead atom X in the *D. desulfuricans* structure remains uncertain: it may be C, N, or O. Note how in either case the electrons are transported through the enzyme molecule by a special relay system comprised of Fe−S clusters (shown as spheres).

unknown elsewhere in biology. The [FeFe]- and [NiFe]-hydrogenases are named according to the metal composition of their active sites, each being bimetallic centers with CO and CN^- ligands (Figure 4). The active sites are intriguing in both biological and chemical terms: it is rare to find CO and CN^- as endogenous ligands in biology, and the metals cycle through oxidation states that are unusual in coordination chemistry. A subset of the [NiFe]-hydrogenase family, the [NiFeSe]-enzymes, incorporate a selenocysteine coordinated to the Ni in place of one of the terminal cysteine residues of the standard [NiFe]-enzymes.[35] In the third class of hydrogenases, recently termed [Fe]-hydrogenases[36] and found only in methanogens, H_2 is split at a mononuclear iron-carbonyl center to release a proton and transfer a hydride to the hydride carrier, N^5,N^{10}-methenyltetrahydromethanopterin.[37,38]

In this Review we focus on the [FeFe]- and [NiFe]-hydrogenases that rely upon an electron relay chain for fast electron transfer between the buried active site and the protein surface. The active sites of these enzymes have certain similarities as well as differences, and we will see how, despite being products of convergent evolution, the [NiFe]- and [FeFe]-hydrogenases show very similar chemical characteristics, even in their respective behavior toward inhibitors such as O_2 and CO. The turnover rate for H_2 oxidation relative to the reverse reaction, H^+ reduction (the inherent preference for catalysis in one direction as opposed to the other is known as the *catalytic bias* of the enzyme), varies among different hydrogenases (in section 5.6 we discuss how this is quantified), but in general, [NiFe]-hydrogenases have been classed as H_2-oxidizers, whereas [FeFe]-hydrogenases have been considered mainly to be H_2-producers.

An issue familiar to organometallic chemists is the significance of valence shell electron counting, particularly when it is applied to carbonyl compounds. The so-called "18-electron rule" (which predicts that a d-block organometallic compound should be stable if the total number of electrons involved in bonds between the metal and its ligands totals 18) applies most commonly to those elements located in the middle of the d-block.[1] These rules ought to apply to the active sites of hydrogenases. Thus, in Figure 4, if the iron atoms were assigned as Fe^{II}, they would each possess 16 valence electrons (presuming there is no Fe−Fe bond) and be susceptible to attack by an additional ligand, taking the electron count up to 18.

Although hydrogenases first evolved in an anoxic environment, the gradual accumulation of O_2 in Earth's atmosphere (after the establishment of oxygenic photosythesis) and the subsequent emergence of O_2 respiration led to microbes able to couple H_2 oxidation to O_2 reduction. Even so-called "strict anaerobes" such as sulfate-reducing bacteria, *Desulfovibrio*, are often found in microbial mats at the interfaces of oxic and anoxic environments and may even utilize the oxidizing power of O_2 under certain conditions.[41] Oxygen-rich conditions present a series of challenges for microbes that utilize or produce H_2. The sulfur-rich and often coordinatively unsaturated metal sites at the active centers of hydrogenases

render these enzymes sensitive to attack by O_2. Like H_2, both O_2 and CO utilize π-back-donation in their bonding with transition metal atoms, making them potential competitors for H_2 binding sites. Once bound, O_2 can react further as an oxidant, leading to a variety of possible products, including peroxides and oxygenated sulfur species such as sulfenic acids (−S−O−H) and sulfoxides (>S═O).[42,43] As discussed below, channels identified in the protein framework of both [NiFe]- and [FeFe]-hydrogenases probably facilitate access of these gases to the active site. Further, the [NiFe]- and [FeFe]-hydrogenases rely upon iron−sulfur clusters as electron relay stations, and these centers are inherently unstable in the presence of O_2.

2.3. Redox Partners for [FeFe]- and [NiFe]-Hydrogenases

2.3.1. In vivo Redox Partners

Hydrogenases have a complex range of cellular functions, and sometimes several enzymes within one organism are active in energy cycling. Indeed, the recently published genome for *Desulfovibrio vulgaris* Hildenborough encodes six hydrogenases, although only three are normally expressed sufficiently to be detected.[44,45] Periplasmic "uptake" hydrogenases link H_2 oxidation to reduction of various electron acceptors including CO_2, SO_4^{2-}, NO_3^-, fumarate, or O_2 (see Figure 3) and contribute to the establishment of a transmembrane proton gradient.[34] The [NiFe]-hydrogenases of this type (see Figure 4A) comprise a large subunit that incorporates the [NiFe]-active site and a small subunit that houses an electron relay chain of FeS clusters which "wires" the buried active site to the surface. Periplasmic uptake hydrogenases may be anchored to the membrane via a *b*-type cytochrome that mediates transfer of electrons from H_2 to the respiratory chain quinone pool (Figure 5A): examples are the [NiFe]-membrane-bound hydrogenases (henceforth, we will use the term "MBH" where a hydrogenase is believed to be membrane bound in the cell) from *R. eutropha* or *Ralstonia metallidurans* and *Allochromatium vinosum*.[46] Other bacteria, such as *D. gigas* and *D. desulfuricans*, express soluble [NiFe]-hydrogenases that interact with a *c*-type cytochrome (Figure 5B). All these [NiFe]-hydrogenases appear to be particularly well-suited for protein film voltammetry, probably because electron transfer to the electrode (Figure 5C) is not dissimilar to electron transfer to their large and often membrane-bound redox partners: in both cases, an extensive contact area must be available at a point where electrons can enter or leave the protein (see section 3.2.1). An important assumption here is that the catalytic parts of the enzyme molecule have dissociated from the membrane "anchor" in order to form a good "conducting" contact with the electrode surface.

A group of multi-subunit soluble hydrogenases incorporate additional domains with flavin cofactors and diaphorase ($NAD(P)^+$ reducing) functionality. They may utilize the reducing power of H_2 to produce NAD(P)H, or to restore redox balance by removing NAD(P)H and generating H_2 from water.[34] An example is the cytoplasmic bidirectional "soluble hydrogenase" of *R. eutropha*.[47]

D. vulgaris and *D. desulfuricans* express a soluble periplasmic [FeFe]-hydrogenase that is thought to be a H_2 uptake enzyme.[48] These hydrogenases are analogous to the *D. gigas* [NiFe]-hydrogenase shown in Figure 5B and pass electrons to soluble cytochrome *c*. In contrast, the highly O_2-sensitive [FeFe]-hydrogenase I of *Clostridium pasteurianum* is cytoplasmic and is a H_2-producer, with the net reaction being the oxidation of glucose by protons.[49] The electrons are supplied by ferredoxins, under iron-rich growth conditions, or flavodoxins under conditions of iron starvation.[50] In green algae such as *Chlamydomonas reinhardtii*, [FeFe]-hydrogenases may be located in the chloroplast stroma and catalyze H_2 production linked to photosynthetic electron transfer via interaction with a ferredoxin.[51]

2.3.2. In vitro Redox Partners

In vitro hydrogenase activity is usually detected and quantified through H_2 uptake or production assays that involve a soluble redox partner such as methyl viologen (E_{m7} = −446 mV), benzyl viologen (E_{m7} = −358 mV), or methylene blue (E_{m7} = 11 mV).[8] Indeed, Stephenson and Stickland first identified hydrogenase activity in the 1930s after noting that they had a culture capable of reducing methylene blue in the presence of H_2.[52] The reaction can be followed spectrophotometrically by monitoring the change in concentration of the redox dye[53,54] or by using a Clark electrode to follow changes in H_2 concentration.[2] Viologens are also used as titrants in potentiometry, and in spectroelectrochemistry and mediated electrochemistry,[55−57] where the protein is not interacting directly with the electrode. Certain cytochromes—physiological redox partners of some hydrogenases—have also been employed as mediators.[56−58]

In protein film voltammetry, the electrode acts as the direct redox partner of the hydrogenase (Figure 5C), providing a continuous flow of electrons, back and forth, as the potential is varied. The advantage of having electrons "on-tap" will be discussed in section 4. A redox center in the hydrogenase (the electron entry/exit point) is held in close contact with the electrode surface, and there is no need for mobile

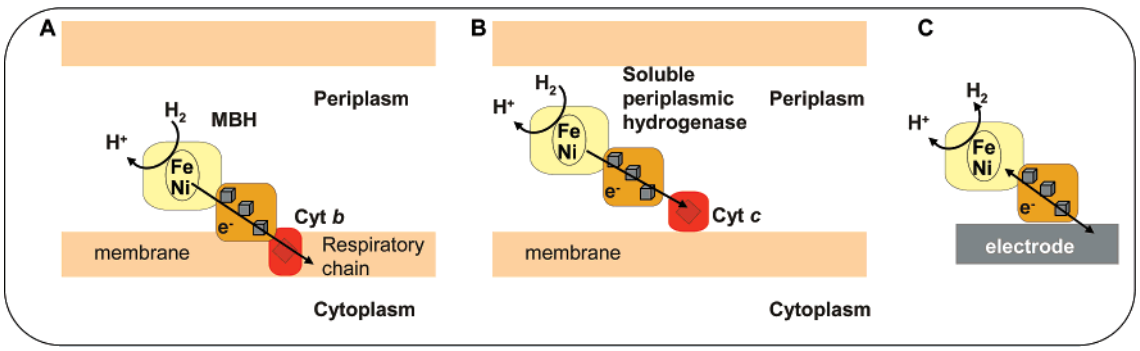

Figure 5. Schematic representation of two-subunit periplasmic [NiFe]-hydrogenases with their *in vivo* redox partners: (A) a membrane-bound hydrogenase (MBH); (B) a soluble periplasmic hydrogenase (this could also be an [FeFe]-hydrogenase); (C) an isolated hydrogenase adsorbed on an electrode.

electron-transfer mediators. However, in cases where the protein is entrapped on the electrode as a multilayer film or where the sample contains impurities that block sites on the electrode, some enzyme molecules may be unable to exchange electrons rapidly with the electrode and will only undergo electrocatalysis in the presence of mediators. The conditions required for direct adsorption of hydrogenases in electroactive conformations remain unclear, but they are discussed further in section 3.2.

2.4. Hydrogenase Structures: Biological Plumbing and Wiring

2.4.1. Electron Relay Centers

The protein environment provides more than just a protecting scaffold for the fragile and sensitive catalytic centers. Both [NiFe]- and [FeFe]-hydrogenases incorporate iron−sulfur clusters as electron relay centers to connect their buried active sites to the protein surface (see Figure 4), and in both classes of enzymes the clusters are typically positioned 12−14 Å apart. Dutton and co-workers have suggested that this type of spacing allows electron transfer to be sufficiently fast as to not limit the rate of catalysis of an enzyme,[59] although this need not be the case when relay centers are altered by deliberate mutations, as discussed in section 5.7.

The combination of different iron−sulfur clusters found in the relay varies between different types of hydrogenases, and this may have important implications for catalytic activity and bias. [FeFe]-hydrogenases have a [4Fe-4S] cluster bound directly to the di-iron site via a bridging cysteine ligand (Figure 4). As well as shortening the path for long-range electron transfer, this iron−sulfur cluster must also be regarded as an integral part of the active site, contributing directly to the electronic and catalytic properties. X-ray crystallographic studies show that the *D. desulfuricans* [FeFe]-hydrogenase contains two [4Fe-4S] clusters in a ferredoxin-like domain, whereas the *C. pasteurianum* [FeFe]-hydrogenase I contains an *N*-terminal [2Fe-2S] ferredoxin-like module and an additional [4Fe-4S] cluster. The [NiFe]-hydrogenases from *D. gigas* and *D. fructosovorans* each contain two [4Fe-4S] clusters and one [3Fe-4S] cluster, whereas the [NiFeSe]-hydrogenase from *Desulfomicrobium bactulatum* contains three [4Fe-4S] clusters.[35] An interesting feature of the [NiFe]- and [NiFeSe]-hydrogenases is the presence at the distal [4Fe-4S] cluster (the cluster furthest from the active site) of a histidine ligand rather than a cysteine at one Fe subsite. The significance of this unusual substitution is discussed in section 5.7.

2.4.2. Gas Channels May Control the Activity of Hydrogenases

Hydrophobic channels sufficiently large to allow access for gas molecules have been identified crystallographically in a [NiFe]-hydrogenase (*D. fructosovorans*) by the trapping of Xe atoms within the protein at high Xe pressures.[60] Modeling of gas access within the *D. desulfuricans*[40] and *C. pasteurianum*[61] [FeFe]-enzymes suggests that gas channels may also exist in this class of hydrogenases. Molecular dynamics (MD) simulations indicate that although H_2 easily enters the protein, there is preferential occupation of certain gas channels and, on the time scale (9 ns) of the MD simulations, H_2 accesses the active site via these channels.[62] Similarly, X-ray crystallography studies of O_2 and CO movement in myoglobin have shown that protein cavities (formed by introducing internal packing defects) are used as pathways for ligand migration.[62] In [NiFe]-hydrogenases with H_2-sensing and gene regulation roles, it has been suggested that bulky isoleucine and phenylalanine residues gate the end of a channel close to the Ni atom and hinder access of larger neutral molecules (eg O_2, CO, or H_2S) to the active site. Support for this hypothesis stems from experiments on the O_2-tolerant regulatory hydrogenases (RH) from *R. eutropha* H16 or *Rhodobacter capsulatus* in which replacement of these amino acids by less bulky valine and leucine residues confers O_2 sensitivity.[63,64] We return to the question of gas channels in [NiFe]-hydrogenases in section 7, where we discuss access of CO and O_2 to the active site of the membrane bound hydrogenase of *R. eutropha*.

2.5. Complexity of Hydrogenase States

Newcomers to hydrogenase research are naturally overwhelmed by the number of different states that have been detected and sometimes characterized sufficiently to provide a basis for a good molecular understanding. Chemical features which are common to both [NiFe]- and [FeFe]-hydrogenases include (a) the presence of one or more oxidized states that are catalytically inactive but may serve a purpose in being "resting states" that are unreactive to destructive ligands such as O_2, and (b) involvement of uncommon oxidation states, such as Ni(III), Ni(I), and Fe(I). For both classes of hydrogenase, strong IR absorption bands from active-site CO and CN^- ligands are very helpful

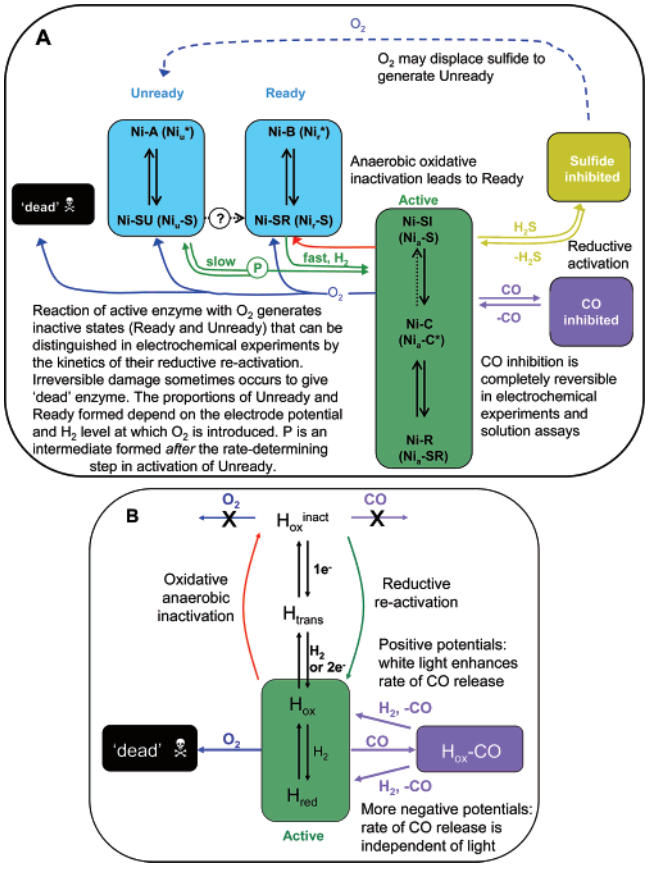

Figure 6. Inactive and active states of (A) "standard" [NiFe]-hydrogenases (e.g. *D. gigas* or *A. vinosum*) and (B) [FeFe]-hydrogenases (specifically, the enzyme from *D. desulfuricans*). Interconversions that have been detected in electrochemical experiments are highlighted by colored arrows.

for distinguishing between different states, including those that are EPR-silent, whereas a potentially serious shortcoming is the difficulty in locating H atoms and dealing with the possibility of coordinated H_2 when assigning oxidation levels.

Figure 6 summarizes the interconversions so far reported for [NiFe]- and [FeFe]-hydrogenases, emphasizing (with colored arrows) the reactions that can be studied by protein film voltammetry. The situation is further confused because different researchers have used different terms to identify the same states. For example, in referring to inactive states of [NiFe]-hydrogenases, the "Ready" state is also known as Ni-B or Ni_r* and the "Unready" state is also known as Ni-A or Ni_u*. In fact Ready and Unready are labels that relate to their rates of reductive reactivation, whereas the corresponding labels Ni-B/Ni_r* and Ni-A/Ni_u* are assigned to specific active-site EPR or IR spectroscopic signatures (the asterisks denote EPR detectability). These states are relevant to [NiFe]-hydrogenases from *Desulfovibrio* species, or *A. vinosum*, and it remains to be seen whether analogous states are formed with other [NiFe]-hydrogenases. Similar inconsistencies in nomenclature have arisen for the [FeFe]-hydrogenases. We stress that Figure 6 shows only states that persist long enough to have been detected. Observation of very high catalytic rates for both [NiFe]- and [FeFe]-hydrogenases means that true catalytic intermediates remain uncharacterized. The green boxes depicting active states are thus oversimplified (for example, it is reported that only the interconversion between Ni-C and Ni-R is reversible and this reaction probably involves several intermediates).[36,65]

2.5.1. The Role of Protein Film Voltammetry in Navigating between States of Hydrogenases

Dynamic electrochemistry of hydrogenases should be considered as a complementary approach, working alongside and in harmony with other physical methods. A possible complication with interpreting crystal structures of redox enzymes is that the oxidation level of the active site might be unknown; moreover, two or more oxidation states might coexist in the crystal. Spectroscopic methods can provide more detailed information to help characterize a particular state: this is because, compared to crystals, solution samples for spectroscopy are easier to obtain in well-defined states by titration and rapid quenching. Equilibrium electrochemical measurements (titrations with mediators) link spectroscopic characteristics to reduction potentials. In contrast, dynamic electrochemical methods in general do not link directly with spectroscopy but instead measure, simultaneously, (a) the potentials at which reactions occur (both during catalysis and when the enzyme is inhibited) and (b) the rates at which these reactions occur over a variable potential range.

In protein film voltammetry, both oxidized and reduced forms of a redox couple can be present simultaneously in the cell solution and the rate of reaction in either direction is controlled by the thermodynamic bias provided by the electrode potential and the kinetic bias of the enzyme. The electrode can also be considered as a reaction partner, able to donate or accept electrons over a continuous range of potential (electrochemical driving force).

3. Dynamic Electrochemical Methods for Studying Hydrogenases

3.1. Electrochemical Equipment

A standard three-electrode setup is generally employed for protein film voltammetry experiments. The counter electrode is a platinum wire or gauze, and the reference is generally a saturated calomel electrode (SCE) or a Ag/AgCl electrode. The working electrode is typically carbon (particularly pyrolytic graphite), but it can be gold modified with an alkanethiolate self-assembled monolayer (SAM) that will enable the protein to bind in a productive manner. There are many possible configurations for the three electrodes, and Figure 7 illustrates a selection of cell configurations that have been used in electrochemical studies of hydrogenases. In Figure 7A, the cell is open and consists of a main compartment that houses the working electrode and the counter electrode, and a reference compartment that is connected to the cell via a luggin capillary, the tip of which is located close to the working electrode. The working electrode is a rotating disc electrode (RDE) that can be rotated rapidly (500−10,000 rpm depending on the motor) to provide a well-controlled flux of substrate and product to and from the surface. As explained in section 4.2, the rotating disc electrode is particularly important for highly active enzymes such as hydrogenases, and its use is discussed further in section 3.1.1. The cell is surrounded by a water jacket for temperature control, whereas the reference electrode is always held at an ambient standard temperature. The primary gas atmosphere is controlled by bubbling gas into the cell solution. A short-lived concentration of another gas is achieved by injecting an aliquot of gas-saturated solution and then allowing it to flush out of the cell solution: this is the essence of a novel approach to extracting detailed information on kinetic constants (see sections 5.3 and 7.1.1).[66,67] Since hydrogenases are generally O_2-sensitive, the use of an open cell usually necessitates confinement in an anaerobic glove box.

Better control over the gas concentration is achieved by sealing the glass cell onto the electrode rotator and flowing gases through the headspace as shown in Figure 7B. This design also incorporates a manifold for preparing gas mixtures, and gases are passed through a purifier before reaching the cell. In most cases, it is still desirable to house the cell within an anaerobic glove box. Placing the counter electrode in the same compartment as the working electrode presents a possible source of contamination, since an oxidative reaction at the working electrode results in a corresponding reductive current at the counter electrode and vice versa, and in some circumstances, O_2 may be evolved at the Pt electrode. Location of the counter electrode in a compartment separated by an ionically conducting frit (e.g. Vycor) may be necessary in some cases. The electrode surface may also be illuminated.

Alternative electrode configurations have been developed for exploitation of hydrogenases as electrocatalysts. Figure 7C shows a cell reported by Adams and co-workers for studying hydrogenases adsorbed onto a packed bed of graphite.[68] This configuration is useful for stationary electrodes because H_2 is bubbled through the high surface area graphite bed and this assists mass transport. A simple enzyme−catalyst fuel cell may be constructed by combining an electrode modified with an O_2-tolerant hydrogenase (the anode) with an electrode modified with an O_2-reducing enzyme such as fungal laccase (the cathode), as illustrated in Figure 7D. This setup not only tests the technological potential of enzyme catalysts but also reveals interesting details about the behavior of hydrogenases under demanding conditions of low H_2 in air, close to the levels experienced in biology (see section 8.2). Thus, fuel cell experiments not

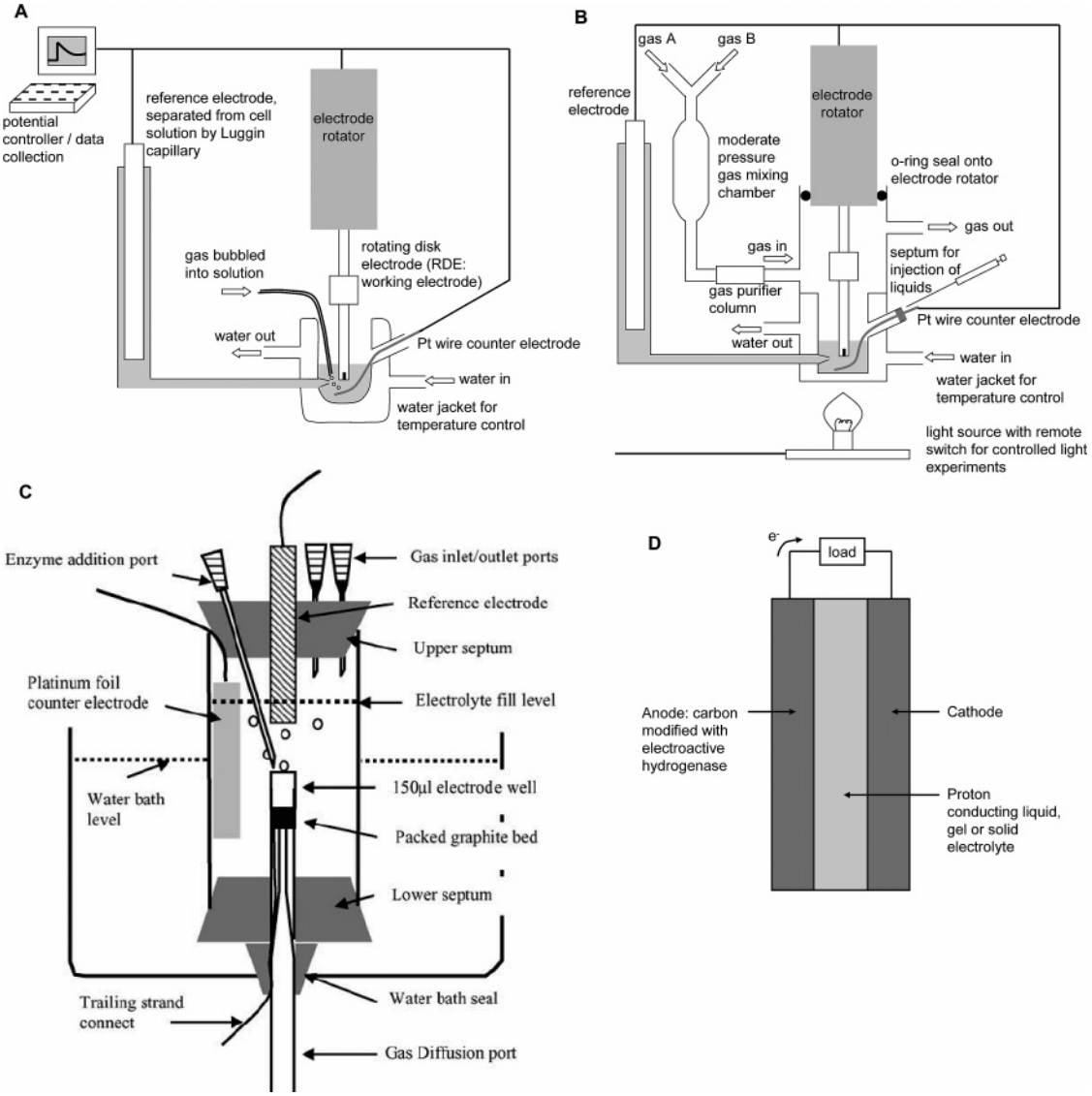

Figure 7. Various electrochemical cells for studying enzymes with gaseous substrates. The working electrode is rotated in cells A and B to provide efficient mass transport of substrate and product, and the reference electrode is housed in a side arm separated by a Luggin capilliary so that it is held at constant (atmospheric) temperature while the cell temperature is controlled by a thermostated water jacket. These cells are typically housed within an anaerobic glove box. Gases are bubbled through the cell solution in design A but flowed through the headspace in B after passage through a purifier column. Gas mixtures may be prepared in design B by introducing component gases into a mixing chamber at appropriate relative pressures (<100 bar) or mixing at ambient pressure using calibrated mass-flow controllers. For experiments requiring controlled light conditions, the walls of cell B are blacked-out and a light source is introduced below the solution. Panel B is adapted from Vincent, K. A., Cracknell, J. A., Parkin, A., & Armstrong, F. A. *Dalton Trans.* **2005**, 3397−3403 with permission of The Royal Society of Chemistry. Cell C was designed for trials of a fuel cell electrode consisting of a packed graphite bed modified with hydrogenase; gas bubbling assists substrate supply. In this design, the reference electrode is not held at constant temperature but is always at the cell temperature. Panel C is reprinted from *Enzyme Microb. Technol.*, Vol. 36, W. Johnston, M. Cooney, B.Y. Liaw, R. Sapra, M. W. W. Adams, "Design and characterization of redox enzyme electrodes: new perspectives on established techniques with application to an extremeophilic hydrogenase" 540−549, Copyright 2005, with permission from Elsevier. Panel D: a simple design for a membraneless fuel cell that exploits enzymes as catalysts for H_2 oxidation and O_2 reduction. A proton-conducting electrolyte (this can be a film of aqueous buffer) is all that is used to separate the anode (graphite modified with hydrogenase) from the cathode (graphite modified with an O_2-reducing enzyme such as fungal laccase).

only provide a route to exploiting enzymes in energy technologies but also tell us about how pairs of redox-coupled enzymes might function in living cells.

3.1.1. The Importance of Controlling Mass Transport

Hydrogenases generally have very high rates of turnover and low K_M values. This means that the electrocatalytic response (the current detected as a function of potential) of a hydrogenase at a standard-sized (usually >1 mm diameter) stationary electrode will often be limited by mass transport of the reactant (H_2). Consequently, the limiting current plateau attained as the driving force is raised really only reflects the rate at which H_2 arrives at the electrode. As we discuss further in section 4.2, this problem can be overcome or minimized by rapid rotation of the working electrode, the aim of which is to maintain the H_2 concentration at the electrode surface at (or close to) the level of that in the bulk. The waveform and current at a high rotation rate then report directly on the inherent catalytic properties of the enzyme (and the rate of interfacial electron transfer to the electrode) rather than merely reporting on the rate of transport of H_2 to the electrode. An alternative strategy is to make the

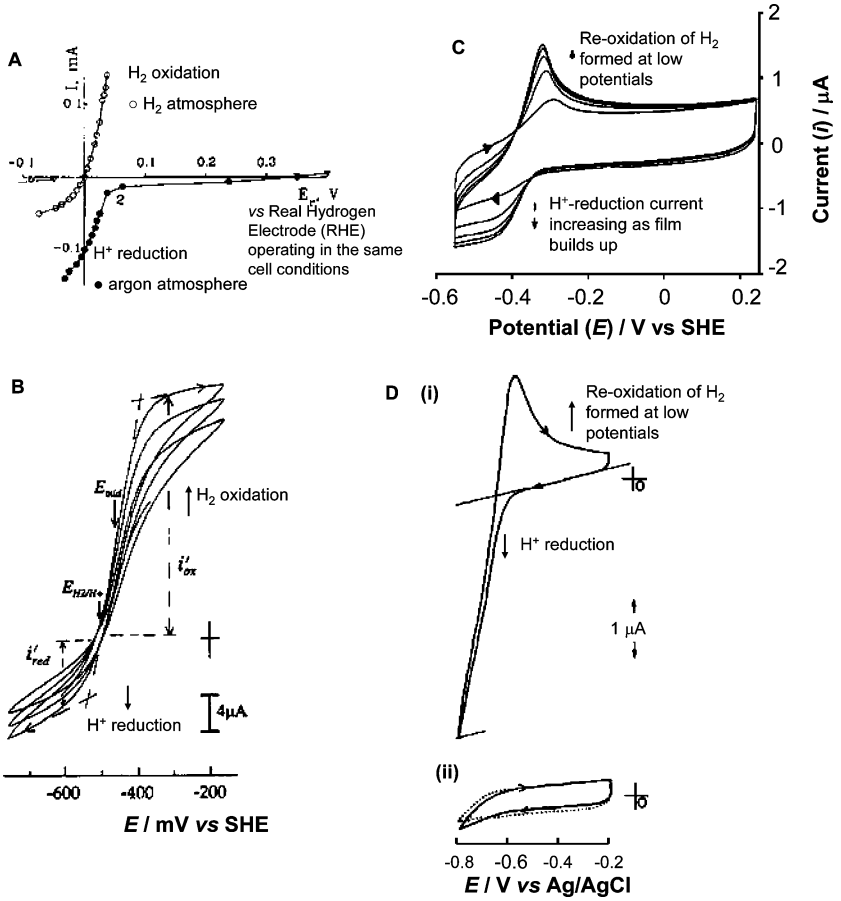

Figure 8. Various early observations of electrocatalysis by adsorbed hydrogenases. Panel A: Current vs potential plot for H_2 oxidation and H^+ reduction at a carbon black electrode with immobilized *T. roseopersicina* hydrogenase in enzyme-free phosphate buffer, pH 7.0, 30 °C. Reprinted with permission from *J. Biotechnol.*, Vol 27, S. D. Varfolomeyev, A. I. Yaropolov, A. A. Karyakin, "Bioelectrocatalysis: The electrochemical kinetics of hydrogenase action" 331−339, Copyright 1993, with permission from Elsevier. Panel B: Electrocatalytic reduction of H^+ (i'_{red}) and oxidation of H_2 (i'_{ox}) observed for a vitreous carbon electrode in contact with a drop of *M. elsdenii* [FeFe]-hydrogenase (2 μM) exposed to H_2. Other conditions: pH 8.6, 10 mV s^{-1}, 22 °C. Attenuation of the current response is observed during the three potential cycles. Reprinted from Butt, J. N.; Filipiak, M.; Hagen, W. R. Direct Electrochemistry of *Megasphaera elsdenii* iron hydrogenase. *Eur. J. Biochem.* **1997**, *245*, 116−122, with permission from Blackwell Publishing. Panel C: Cyclic voltammograms recorded at 50 mV s^{-1} during adsorption of *A. vinosum* [NiFe]-MBH from dilute solution (1 μM hydrogenase in mixed buffer, pH 6.0, 0.1 M NaCl) onto a freshly polished stationary PGE electrode under N_2 at 30 °C. The poly-cationic coadsorbate polymyxin B sulfate (0.2 mg mL^{-1}) is present in solution. H_2 that is produced at low potentials is reoxidized as the potential is scanned toward more positive values. Adapted from ref 75 with permission, Copyright 2004, American Chemical Society. Panel D: Cyclic voltammograms for a pyrolytic graphite electrode in contact with 9 nM *D. vulgaris* Hildenborough hydrogenase under N_2 (i) in the presence of 0.16 μM poly-L-lysine (MW 37,000) and (ii) without poly-L-lysine. Other conditions: 0.10 M Tris-HCl, pH 7.70, scan rate 5 mV s^{-1}. The blank electrode response is given by the dotted line in (ii). Reproduced and adapted from ref 77 by permission of ECS—The Electrochemical Society.

enzyme film less dense by polishing away some of the enzyme molecules so that it behaves like an array of microelectrodes, each with efficient radial substrate diffusion.[69] In section 5.1 we discuss voltammograms obtained for a very active film of hydrogenase, which show how difficult it can be to remove mass transport control, particularly at low H_2 levels that are depleted so easily.

3.1.2. Gas Supply and Gas Purity

The tiny quantities of sample addressed in protein film voltammetry experiments mean that the effects of even trace quantities of impurities in the gas supply can be detected. Highly O_2-sensitive hydrogenases, such as *Desulfovibrio gigas* [NiFe]-hydrogenase, may be susceptible to oxidative damage or inactivation even when exposed to high-purity H_2 that is certified to contain <1 ppm O_2 (e.g. Air Products Premier Grade H_2). For this reason, the gas inlet line should include a purifier column containing an O_2-scrubbing catalyst, for example, Varian Gas Clean Oxygen Filter (outlet <50 ppb O_2; Figure 7B).

3.1.3. Light Intensity

A number of hydrogenases show light-dependent reactivity, usually involving dissociation of photolabile carbonyl groups.[70,71] In order to explore photoactivity coupled to electrochemical reactions, a halogen lamp is included in the cell shown in Figure 7B. With the glass cell blacked out, the illumination level may then be varied during experiments. The use of a Reed switch permits the light to be controlled through the glove box window.

3.2. Methods for Preparing Hydrogenase Films on Electrodes

Hydrogenases only undergo direct electron transfer or electrocatalysis when adsorbed on an electrode surface. In early studies of hydrogenase electrochemistry in the 1970s, redox mediators were included in the electrolyte solution to facilitate electron transfer to hydrogenase molecules in solution or in poor contact with an electrode.[72] However, navigation through the many states of these enzymes (Figure

6) is difficult (if not impossible) if the enzyme is free in solution, because full potential control is lost. Direct electronic contact between the protein and the electrode (as shown in Figure 5C) provides much more precise control, and methods have since been established for preparation of highly electroactive films of hydrogenase, usually on graphite electrodes. Voltammetric studies of hydrogenases have been directed either (a) toward understanding the activity and reactivity of hydrogenases, usually on disk electrodes and requiring enzyme catalytic behavior that is not limited by mass transport of substrate or interfacial electron transfer, or (b) toward generating enzyme electrodes that are good electrocatalysts for H_2 oxidation or H_2 evolution, requiring robust films with activity that ideally approaches the expectation for a mass-transport limited current. As we show in later sections, these approaches actually go hand-in-hand, because a fundamental understanding of the potential-dependent behavior of hydrogenases and their reactions with small molecules is essential if they are to be exploited as catalysts in hydrogen-cycling technologies.

3.2.1. Direct Adsorption of Hydrogenase onto an Electrode

In the early 1990s, Varfolomeyev et al. showed that *Thiocapsa roseopersicina* [NiFe]-hydrogenase gave an electrocatalytic response when adsorbed on a carbon black electrode.[73] Under an argon atmosphere, negative currents were detected corresponding to H^+ reduction, whereas, under a H_2 atmosphere, the H^+ reduction was suppressed, and a large positive current was observed at higher potentials corresponding to H_2 oxidation (Figure 8A).[73] Because these measurements were made in enzyme-free buffer solution with no mediator, it was clear that the hydrogenase was exchanging electrons directly with the electrode.

In 1997, Butt and colleagues reported direct electrochemistry of *Megasphaera elsdenii* [FeFe]-hydrogenase at a glassy carbon electrode in contact with a drop of solution (Figure 8B).[74] The voltammetric response persisted after the electrode was rigorously rinsed and inserted into enzyme-free electrolyte, indicating again that the electroactive enzyme was adsorbed on the electrode surface. Direct adsorption onto a freshly polished pyrolytic graphite surface dipped in dilute protein is a straightforward method for preparation of highly electroactive films for many hydrogenases.[66,74−76] Pershad et al. reported in 1999 that this approach works well for the [NiFe]-MBH of *Allochromatium* (formerly *Chromatium*) *vinosum* on a pyrolytic graphite edge (PGE) electrode.[75] (A PGE electrode consists of a piece of pyrolytic graphite that is oriented so as to project the edges of the aromatic layers toward the electrolyte; see below.) Cycling the potential at a stationary electrode during adsorption of *A. vinosum* [NiFe]-MBH (from 1 μM solution) under a N_2 atmosphere provides a convenient means of monitoring growth of the film, as shown in Figure 8C. In these scans, H^+ is reduced by the enzyme at low potentials, giving rise to a negative current. The H_2 produced in this reaction (which remains in the vicinity of the enzyme because the electrode is not rotated) is reoxidized as soon as the potential is taken above about -0.4 V, giving rise to a positive current that drops off at higher potentials as the H_2 concentration close to the electrode becomes depleted. Any hydrogenase that can both evolve and oxidize H_2 rapidly will show a similar response as it adsorbs at a stationary electrode, and therefore, the voltammograms generated during film formation do not convey any specific information.

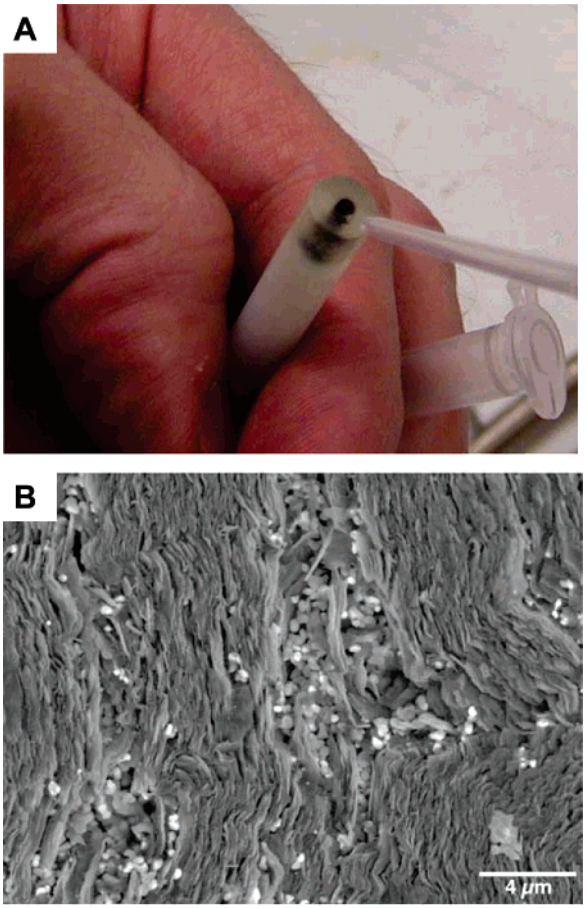

Figure 9. Panel A depicts how a film of protein is formed on a pyrolytic graphite "edge" electrode by spotting dilute protein onto the surface. Panel B is a scanning electron micrograph of the "edge" surface of pyrolytic graphite polished with 1 μm α-alumina, rinsed with water, and then sonicated for 10 s in water (from ref 78). Particles of alumina remain on the surface but are removed upon further sonication. Reprinted from *Journal of Solid-state Electrochemistry*, Vol. 10, 2006, p 830, "The pyrolytic graphite surface as an enzyme substrate: microscopic and spectroscopic studies" C. F. Blanford, F. A. Armstrong, Figure 5b, Springer-Verlag 2006, with kind permission of Springer Science and Business Media.

Addition of a poly-amine coadsorbate such as polymyxin B sulfate (0.2 mg mL^{-1}) to the enzyme solution improves adsorption of *A. vinosum* and *D. gigas* [NiFe]-hydrogenases and *Desulfovibrio desulfuricans* [FeFe]-hydrogenase on PGE. The coadsorbate also stabilizes the film when the electrode is transferred to enzyme-free solution. However, polymyxin appears to have little beneficial effect on adsorption of the *Ralstonia* membrane-bound hydrogenases, perhaps because of a different surface charge distribution. Films of *A. vinosum* [NiFe]-MBH with polymyxin on PGE are stable for several hours, enabling many experiments to be carried out on the same film. Bianco and Haladjian used poly-L-lysine to adsorb a hydrogenase from *Desulfovibrio vulgaris* Hildenborough on a pyrolytic graphite electrode.[77] Under a N_2 atmosphere, a solution of hydrogenase containing poly-L-lysine gave a strong H^+ reduction response, with H_2 reoxidized at higher potentials (Figure 8D). In the absence of the coadsorbate, the electrochemical response resembled that of the blank electrode. The requirement for poly-L-lysine suggests that the response is due to enzyme that is adsorbed on the electrode surface, although all experiments were conducted with hydrogenase present in the electrolyte.

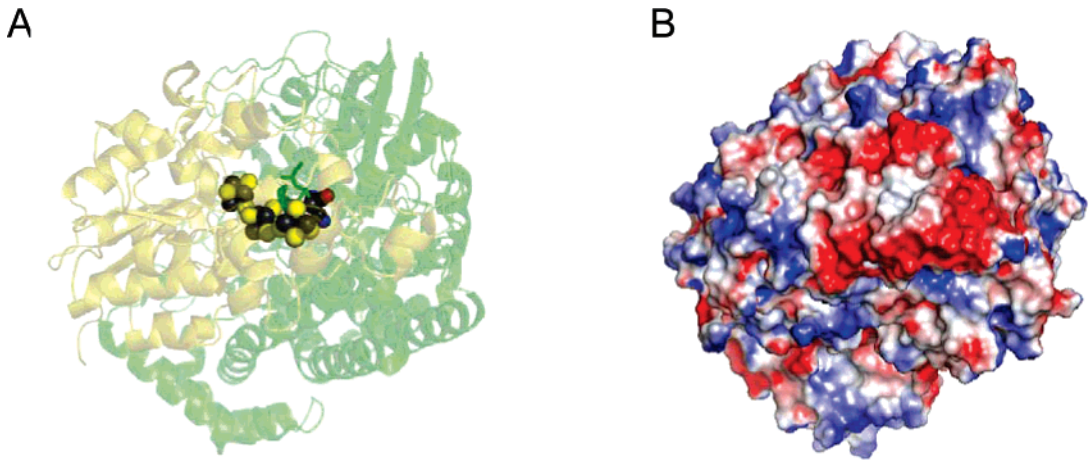

Figure 10. (A) A molecule of *D. gigas* [NiFe]-hydrogenase (PDB code: 1YQW)[39] viewed looking up the electron-transfer relay into the enzyme from the distal cluster that is the closest entry/exit point to the electrode surface. The large subunit is shown as a green ribbon, the small subunit is shown as a brown-yellow ribbon, and clusters are shown as spheres. (B) The same view but shown as an electrostatic surface, illustrating the complex charge distribution (red = negative; blue = positive) that is a footprint for interaction with the heterogeneous graphite surface. Representations constructed using Pymol.

Figure 9A depicts one of the ways a protein film can be formed on a PGE electrode.[78] The PGE surface is chemically heterogeneous in terms of having a variety of different oxidized carbon functionalities (such as C═O, C−OH, and COOH),[79] and polishing with alumina makes it extremely rough with deep cracks and defects, as shown in the scanning electron micrograph (Figure 9B).[78] These factors may be important in providing adsorption sites for a diverse range of proteins. The PGE electrode might indeed be regarded as providing a "combinatorial" surface for protein binding, usually offering at least some binding zones that will favor productive adsorption of a particular protein.

In Figure 10 we depict how a hydrogenase that is binding in a productive orientation, i.e., able to carry out fast interfacial electron transfer (because the entry/exit site can get close to the electrode), would appear to the underlying electrode. The electrostatic surface projection of *D. gigas* [NiFe]-hydrogenase (panel B) shows a ring of negative charge encircling the region close to the distal cluster: this suggests that productive binding will require a compensatory ring of positive charges on the electrode, and this may be why poly-cationic coadsorbates such as polymyxin are important in stabilizing a film.

Adsorption of hydrogenases onto pyrolytic graphite basal plane (PGB) electrodes sanded with a fine emery paper[57,77] probably reflects adsorption at "edge" defects that are created on the basal surface by abrasion, since it was noted that polishing with alumina does not result in enzyme adsorption. Adsorption at a small total area of defect sites may explain the very small current responses (on the order of 100 nA) reported at 65 °C for hydrogenase from the hyperthermophile *Aquifex aeolicus* on PGB.[57]

3.2.2. Strategies for Entrapment and Attachment of Hydrogenases at Electrodes

A freshly polished PGE disc electrode is excellent for studying hydrogenase reactions under controlled conditions,[6] but electrodes with a much larger surface area, possibly porous, are desirable for technological applications such as fuel cells. The importance of scaling up and achieving long-lived electrocatalysis requires the development of strategies for attaching the enzymes firmly to the electrode rather than relying on the weak, noncovalent interactions that are produced by coadsorbates such as polymyxin.

Morozov et al. have reported adsorption of *T. roseopersicina* and *D. fructosovorans* [NiFe]-hydrogenases onto bare carbon or carbon modified with a viologen-containing poly(pyrrole) derivative. This polymer is prepared by depositing the monomer *N*-methyl-*N*′-(12-pyrrol-1-yldodecyl)-4,4′-bipyridinium ditetrafluoroborate, in acetonitrile, onto a carbon support and then electropolymerizing by cycling the potential, which appears to enhance coverage and film stability. High currents, close to 1.4 mA/cm^2, are recorded at an overpotential of ca. 200 mV.[80−82] Johnston et al.[68] adsorbed the bifunctional H_2-oxidizing/sulfur reducing hydrogenase I from the extremophile *Pyrococcus furiosus* onto pyrolytic carbon paper or a packed graphite column (Figure 7C) in an attempt to form a robust enzyme electrode for fuel cell applications; however, they obtained small current responses.[68]

Bianco and co-workers carried out experiments in which small volumes (1−2 μL) of protein are trapped between a graphite electrode and a piece of dialysis membrane.[83,84] A *D. vulgaris* [FeFe]-hydrogenase solution (67 μM) examined in this configuration showed an electrocatalytic H^+ reduction current, but the membrane strategy did not enhance stability as the current was attenuated after the first electrode-potential cycle and restored only after the electrode was repolished and re-exposed to enzyme.[83] These studies are likely to be complicated by exchange of enzyme molecules between the electrode and the trapped solution layer, and thus, it is unclear whether the whole of the sample addressed electrochemically was subjected to the same regime of potential control. A similar membrane-electrode approach was used by Ikeda et al.,[55] and later by Bianco and co-workers,[85] to facilitate methyl viologen or cytochrome c_3-mediated H_2 production or uptake from whole cells of *D. vulgaris* Hildenborough trapped close to a glassy carbon electrode. Little information has been deduced from such experiments beyond the fact that currents > 50 μA cm^{-2} can be achieved for either H_2 uptake or production.[85] Lojou et al. have also demonstrated H_2 oxidation at electrodes modified with clay films that incorporate [FeFe]-hydrogenase from *D. vulgaris* Hildenborough and either its physiological redox partner (a polyheme cytochrome c_3) or methyl viologen.[57] Although they

attribute a single reversible, noncatalytic electron-transfer peak observed at about −0.3 V vs SHE in the absence of mediator, under H_2, to direct electron transfer between hydrogenase and the electrode,[57] it is difficult to see how nonturnover signals can be associated with intact, active hydrogenase if catalysis is not observed simultaneously.

Miyake and co-workers have described a method for preparing a Langmuir−Blodgett film of hydrogenase on an indium tin oxide electrode by compression of an enzyme layer at the interface of air and aqueous buffer.[86,87] The film of *T. roseopersicina* [NiFe]-hydrogenase showed electrochemical H_2 evolution at −0.55 V only in the presence of methyl viologen, which is presumably acting as a mediator.

In addition to physical entrapment, strategies are being sought for covalent attachment of hydrogenases to the electrode surface. Although there are numerous methods for attaching proteins to surfaces, it is important for electron-transport enzymes such as hydrogenases that the coupling establishes a close contact between the electrode surface and the electron entry/exit site: for a hydrogenase, this would involve attachment close to the "distal" FeS cluster, that furthest from the active site. A method for attachment of amine functionalities onto carbon electrodes reported earlier by Savéant and co-workers was adapted by De Lacey and co-workers for covalently attaching *D. gigas* [NiFe]-hydrogenase, probably via glutamic acid side chains, to 4-amino phenyl groups introduced onto the graphite electrode.[88] Stability was good (90% activity remaining after 1 week at 1 bar H_2 and room temperature) and probably better than would be observed for enzyme in solution under these conditions. As with direct adsorption of enzyme onto PGE electrodes, some enzyme molecules are probably orientated incorrectly for electron transfer and thus do not contribute to the electrochemical response. Further, hydroxylamine groups in the linker give redox peaks around 0 V vs SHE which convolute the high potential region of the voltammogram where interesting inactivation reactions of the enzyme occur (see section 6).

Strategies for covalent attachment of hydrogenases in electroactive conformations need to be developed further if hydrogenase-modified electrodes are to be employed as robust electrodes for fuel cells or H_2 production applications.

4. The Study of Enzymes by Protein Film Voltammetry

4.1. How Reactions Are Induced by the Electrode Potential

The direction of catalysis (i.e. whether H_2 is oxidized or evolved) is dictated by the electrode potential in accordance with the Nernst equation (eq 2B). The relative activities in either direction depend on the inherent bias of the enzyme itself, which may relate to the perceived physiological role of a particular hydrogenase with respect to H_2 oxidation (uptake) or H_2 evolution. At a finer level, the electrode potential is also an essential control factor in the transformations between the states of hydrogenase that are shown in Figure 6. The other factors are those familiar in conventional solution studies, i.e., pH, variations in gas atmosphere, temperature, introduction of inhibitors, and variations in light conditions. The electrode potential can be varied as a linear potential sweep, a modulated potential sweep, or one or more potential steps (measuring the current as a function of time at a constant potential is known as chronoamperometry). Although PGE is an excellent material for adsorbing proteins, it is not an ideal electrode for potential step experiments because the high charging currents with long time constants mask reactions that occur within time scales of about 5 s.[89−92]

The ability to achieve both potential and time resolution is crucial in the analysis of complex interconversions because it allows the detection of thermodynamically unstable states and key aspects in the determination of mechanism, including the order of events. An example is the well-known electrochemical concept of an "EC" reaction: this is a sequence in which a chemical (C) step is preceded by an electrochemical (E) step, and it is easily diagnosed by voltammetric methods.[93] Good examples of EC reactions are activation of Ready (section 6.2) and Unready (section 7.1.1) states of [NiFe]-hydrogenases.

4.2. What Does Protein Film Voltammetry Reveal?

The essence of protein film voltammetry in studies of electron-transport enzymes lies in the ability to control and measure catalytic electron flow simultaneously and to link this catalytic activity to different components and properties of the enzyme. Importantly, the current (usually denoted by a lower case *i*) is directly proportional to the rate of catalytic electron flow (usually given by a lower case *k*). By scanning or stepping the electrode potential, the rates and direction of electron flow can be changed, and specific sites in the enzyme can be interconverted between different redox states, not only modulating catalytic rates but also inducing activation, inactivation, or greater susceptibility to attack by inhibitors. It is normal practice in any kinetic study to test the effect of varying conditions (such as pH): in a voltammetry experiment, it is quite easy to distinguish between a change in catalytic rate that is due to an interesting kinetic factor and a change that is simply a consequence of varying the thermodynamic driving force.

Figure 11 shows a conceptual model for interpreting the protein film voltammetry of an enzyme.[5] In this model, catalytic electron flow is divided into three stages, analogous to a series of resistors Ω_E, Ω_{cat}, and Ω_{trans}, that express inherent barriers to interfacial electron transfer, enzyme catalysis, and substrate mass transport, respectively. The capability of the series for fast electron flow is better

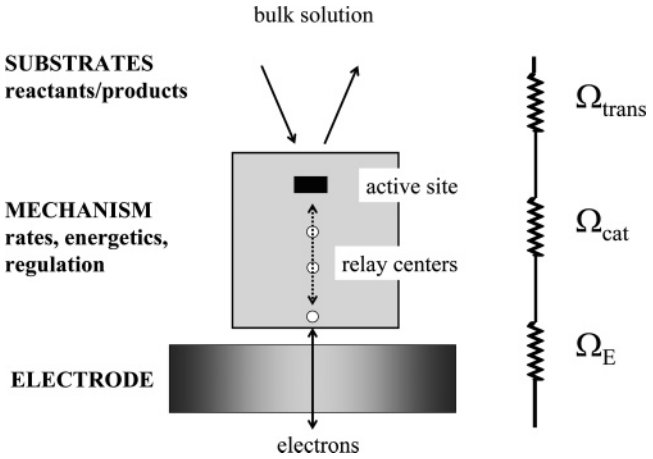

Figure 11. Catalytic electron flow through an enzyme on an electrode in which the possible rate-determining stages are represented by resistors in series. The electron entry/exit site is the lower one of the relay centers indicated as circles. Reprinted and adapted with permission from ref 5a. Copyright 2003 American Chemical Society.

represented in terms of the conductance ($\sigma = 1/\Omega$). The total conductance σ_{tot} is given by $1/\sigma_{tot} = 1/\sigma_E + 1/\sigma_{cat} + 1/\sigma_{trans}$, where, in the language of enzyme kinetics,[94] individual $1/\sigma$ values express the respective electron transit times for each stage. Ideally, the current−potential characteristics should reflect the inherent properties of the enzyme (σ_{cat}) and not interfacial (electrode−enzyme) electron transfer or mass transport of substrate; thus, σ_E and σ_{trans} should be as large as possible.

In the first instance, σ_E (reflecting the ease of interfacial electron transfer) is related to the standard electron *exchange* constant k_0, which depends on the location of electron relay centers in the enzyme and how effectively at least one of these centers (the electron entry/exit site) makes electronic contact with the electrode surface. For a hydrogenase, we would expect the electron entry/exit site to be the distal iron−sulfur cluster. The actual rate of interfacial electron transfer k_E is related to k_0, and for reasonably small potential ranges, k_E is expected to increase exponentially with overpotential (the electrochemical driving force $|E - E^{\circ\prime}|$) according to eqs 3A and 3B, which are for oxidation and reduction reactions, respectively.

$$k_E(\mathrm{ox}) = k_0 \exp\{\alpha nf(E - E^{\circ\prime})\} \quad (3A)$$

$$k_E(\mathrm{red}) = k_0 \exp\{-(1 - \alpha)nf(E - E^{\circ\prime})\} \quad (3B)$$

In these equations, $f = F/RT$ and α is known as the transfer coefficient (a typical value is 0.5). Ideally (but see later), k_0 is sufficiently large that fast interfacial electron transfer is achieved easily with a small driving force. Noting (see section 5, eq 7) that the current in either direction is directly related to the rate of electron flow by the expression $i = nFk\Gamma A$ (where A is the electrode surface area and Γ is the electroactive coverage of enzyme molecules), we obtain an equation for the net current (the Butler−Volmer equation) expected for any potential value E:

$$i_E = i_0[\exp\{\alpha nf(E - E^{\circ\prime})\} - \exp\{-(1 - \alpha)nf(E - E^{\circ\prime})\}] \quad (4)$$

The Butler−Volmer equation lies at the heart of electrochemical kinetics. It is analogous to the Marcus model provided the overpotential $|E - E^{\circ\prime}|$ is smaller than the reorganization energy for the redox reaction occurring.

For optimizing σ_{trans}, we exploit the fact that transport of substrate to the enzyme as well as product dispersion can be controlled hydrodynamically by rotating the electrode at high speeds. The current at a planar rotating disc electrode is given by the Levich equation (eq 5),

$$i_{(\omega)} = 0.62nFAD^{2/3}\nu^{-1/6}\omega^{1/2}C \quad (5)$$

where D is the diffusion coefficient of the substrate (note that D-values are very large for H_2 and H^+), ν is the kinematic viscosity of the solvent, ω is the electrode rotation rate, C is the concentration of the substrate, and other terms have already been defined. Quite simply, the current increases as the square root of the electrode rotation rate, and this is seen later in Figure 20B. Eventually, the conductance component σ_{trans} will cease to control the current. Depending on the activity of the enzyme, the linear relationship between the current and the square root of the electrode rotation rate ($\omega^{1/2}$) predicted by the Levich equation (eq 5) breaks down as ω continues to increase and control passes to the enzyme. The observed relationship between current and rotation rate is then given by the Koutecky−Levich equation (eq 6),

$$\frac{1}{i_{\mathrm{lim}(\omega)}} = \frac{1}{i_{\mathrm{lim}}} + \frac{1}{0.62nFAD^{2/3}\nu^{-1/6}\omega^{1/2}C} \quad (6)$$

where $i_{\mathrm{lim}(\omega)}$ is the limiting (plateau) current at rotation rate ω (see below; for example, Figure 15A), i_{lim} is the maximum limiting current achieved at infinite rotation rate, and the other terms have been defined earlier. Although i_{lim} is normally obtained from the intercept of a plot of $1/i_{\mathrm{lim}(\omega)}$ against $1/\omega^{1/2}$, it is often possible to obtain an approximation by using a rotation rate above which the current and waveform no longer change significantly when ω is increased. As mentioned earlier, mass transport control is removed entirely if a microelectrode (<1 μm diameter) is used or if the enzyme is present only at very dilute coverage on a normal macroelectrode (see section 3.1.1).

Even if σ_E and $\sigma_{trans} \gg \sigma_{cat}$, so that the current response is controlled by the enzyme, the sensitivity of the measurements and the quality of the information will depend on the activity of the enzyme because a high turnover rate translates directly into a large catalytic current. The signal-to-noise advantage for a highly electrocatalytically active enzyme is analogous to that achieved in spectrophotometric measurements of a protein possessing an intense chromophore. Both transient and steady-state experiments can be performed on the same sample, and the minuscule sample quantity presents a further opportunity, that of being able to see the enzyme responding to extremely low levels of an inhibitor.

4.3. Enzymes as Complex Electrocatalysts

In section 4.2 and Figure 11, we considered an adsorbed enzyme as one of a series of resistors. The enzyme itself can be thought of as a machine comprising a host of electronic components such as relays, switches, gates, resistors, capacitors, diodes, and feedback circuits. A voltammogram recorded in the presence of substrate reveals at least two properties of the enzyme. First, the *current* is a direct measure of the rate of catalytic electron flow through the enzyme and it reflects the turnover rate at specific electrode potentials. If the electroactive coverage of enzyme is known, the current can be converted into a turnover frequency analogous to values obtained by conventional steady-state kinetics (see below). Second, the *potential* at which catalysis occurs—usually the steepest part of the climb in activity—reflects the identity of the electrochemical "control center". The electrochemical control center is unique to voltammetric experiments with enzymes as opposed to simple electron-transfer proteins. The control center is the redox site up to which there is fast and reversible electron exchange with the electrode (Figure 12).

For most enzymes, intramolecular electron transfer is rapid, so that the control center is the catalytic site; but cases may arise where the rate-determining step is an intramolecular electron transfer. This could occur when a conformational change is required to facilitate long-range electron transfer.[95] The control center is then one of the relay sites (such as a heme or Fe−S cluster), so that details of the catalytic action further up the line are not revealed.[5] When interfacial electron transfer is rate determining, the voltammogram may not reveal a clearly defined potential for the control center, and this is frequently the case for hydrogenases because they have particularly high activity.

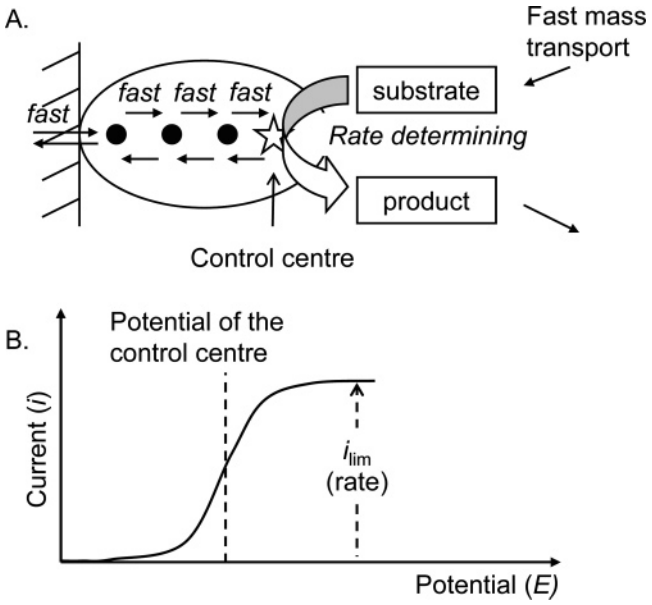

Figure 12. Concept of the electrochemical control center in an enzyme. (A) The control center is the last site up to which electron transfers from the electrode are fast and reversible; in this case it is the active site. Note that the rate-determining step occurs downstream of the control center. (B) An ideal voltammogram in which the half-wave potential is defined by the electrochemical properties of the control center and the limiting current is proportional to the rate of the rate-determining step, as given by eq 7.

The advantage of being able to observe the catalytic rate directly is that any change in activity is immediately observable. The rate at which this change occurs in response to a stimulus such as a potential step or injection of an inhibitor (i.e. the kinetics of the transformation) is directly obtained from the current−time trace. This is illustrated in Figure 13, which compares how a change in catalytic turnover rate following a perturbation is observed in a conventional experiment as opposed to an electrochemical experiment. In the latter case, the two levels of activity are clearly distinguished and the kinetics of interconversion are easily measured.

4.4. Differences between Characteristic Potential Values Measured by Potentiometry and by Catalytic Voltammetry

Should we expect voltammetric and potentiometric methods to give the same values for a reduction potential? There are different ways of looking at this issue. First, consider an electron-transport enzyme which contains (i) a redox active catalytic site, at which the substrate is bound and transformed, and (ii) one or more relay centers to mediate long-range electron transfer between the protein surface and the catalytic site. The redox properties of centers in these enzymes have traditionally been measured by potentiometric methods, but whereas the relay centers have simple redox chemistry (they cycle between two states simply differing by one electron), the catalytic site cycles through complex states, including those with bound substrate and short-lived intermediates. Therefore, it is important to question the meaning of a reduction potential for such a catalytic site that is measured by potentiometry, usually in the absence of the substrate. It is obvious that if the enzyme is active, the substrate will be transformed, and no equilibrium can be established. This is probably not true for electron relay

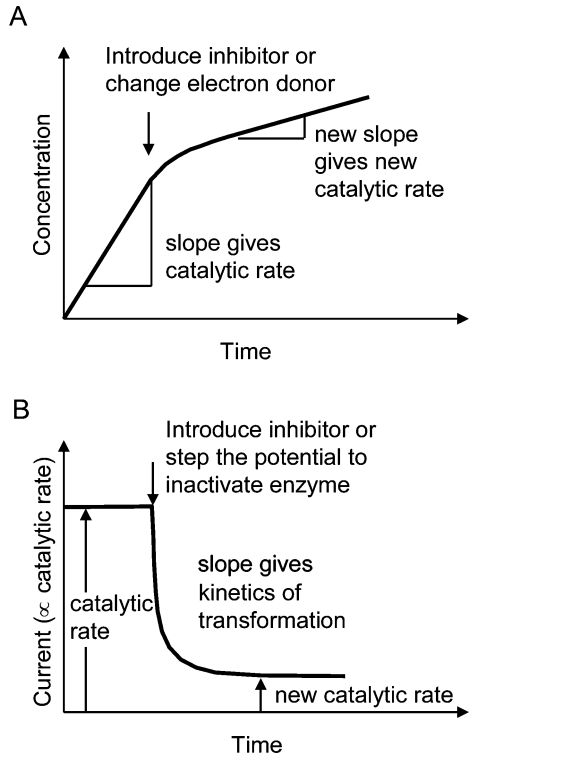

Figure 13. Comparison of how catalytic rate and changes in catalytic rate are displayed in (A) conventional solution assays and (B) voltammetric measurements.

centers such as Fe−S clusters for which titrations with and without substrate may yield the same values. Potentiometric titrations of hydrogenases are particularly problematic because H_2O is the source of substrate: application of sufficiently negative potentials should thus result in catalytic turnover, and equilibrium cannot be achieved. In other words, an enzyme that is active in H_2 production cannot be titrated below the potential at which H_2 should be formed—any results contradicting this are likely to have stemmed from inactive or damaged enzyme. Consider also the activation of a hydrogenase measured by reductive potentiometric titration. If H_2 binds rapidly but only to a reduced active state, then the potential at which the site is reduced must be raised, and when no H_2 is present, the value must be different.

5. Electrocatalytic Activity of Hydrogenases

We now consider PFV applied to hydrogenases, focusing on studies that have revealed details of catalytic constants, activity, inactivation/reactivation, inhibition, or applications. Few hydrogenases have been isolated and purified, and the [NiFe]-enzymes from *Allochromatium vinosum* (MBH), *Desulfovibrio fructosovorans*, and *D. vulgaris* and the *D. desulfuricans* [FeFe]-hydrogenase have become particularly important test systems for the reactions of hydrogenases as determined through electrochemical measurements. The active and inactive states depicted in Figure 6 apply to these systems, and also the crystallographically characterized *D. gigas* [NiFe]-hydrogenase and *Clostridium pasteurianum* [FeFe]-hydrogenase I. In the following sections, we describe how the interconversions of these hydrogenases are revealed in electrochemical experiments and what has been learnt through PFV studies on hydrogenases that are not yet structurally characterized.

In defining the electroactivity of hydrogenases, it is helpful to distinguish between the *inherent* activity of the active site

and the *overall* activity of the enzyme-modified electrode, which depends additionally on the rate of electron transfer to and from the redox partner, which in this case is the electrode. First, it is essential to ensure that mass transport of the substrate to the electrode is not rate determining (see Figure 12), and this question can usually be answered by using a rotating disk electrode. The inherent activity is related directly to the *maximum* catalytic current obtained in an experiment at saturating substrate concentration, according to eq 7.

$$k_{cat} = i_{lim}/nFA\Gamma \quad (7)$$

where k_{cat} is the turnover frequency of the enzyme, i_{lim} is the maximum catalytic current attainable in an experiment (i.e. when mass transport is not limiting), Γ is the coverage of electroactive enzyme, and other terms have been defined previously.

In order to determine k_{cat}, it is necessary to determine Γ, and this depends on the ability to detect *nonturnover* signals by performing cyclic voltammetry experiments under conditions where no catalysis is occurring. The early electrochemical studies of hydrogenases discussed in section 3.2.1 showed that these enzymes have high electroactivity and bidirectional catalytic activity, but they provided no detailed information beyond this.[72,74,77] It was difficult to know how many enzyme molecules are actually involved in the catalysis, and this emphasizes the need to distinguish between gross coverage (which is usually based on how much enzyme was applied to a surface) and electroactive coverage, which is a measure of how many enzyme molecules are in good electronic contact with the electrode.

In principle, any redox sites in hydrogenases that are capable of reversible electron transfer should give rise to reversible electrochemical signals (an oxidation peak and a reduction peak) centered at the reduction potential of the site, which do not alter upon electrode rotation. Observation of these nonturnover signals allows the electroactive coverage of a protein to be estimated (from the areas under oxidation and reduction peaks), and this value (Γ) can then be used to determine the turnover frequency of the enzyme from the catalytic current using eq 7. Nonturnover signals are observed quite easily for small electron-transfer proteins, such as ferredoxins, that give high electroactive coverages, but enzymes are more difficult because their larger size limits the electroactive coverage and signals from individual sites may be lost among a broad envelope due to the other sites. However, nonturnover signals have been determined for several enzymes, including cytochrome *c* peroxidase and two fumarate reductases for which consistent values for the turnover frequency have been obtained.[96−98] Nonturnover signals from hydrogenases have been difficult to detect, and a rare example is the [NiFe]-hydrogenase from *A. vinosum*.[75] By using a low temperature (0 °C) to enhance adsorption, and inhibiting catalytic electron flow with CO, reversible signals appear at the potentials (expected from earlier potentiometric studies) for the two [4Fe-4S] clusters (at approximately −0.3 V) and at higher potential for the single [3Fe-4S] cluster (Figure 14A). The data are refined by substracting the baseline, using a program that fits a cubic spline function to the baseline in regions sufficiently far from the peak (Figure 14B). The limit of detection of such signals is about 1−2 pmol cm^{-2}. It is from this lower detection limit that the extremely high activity of some hydrogenases is estimated.

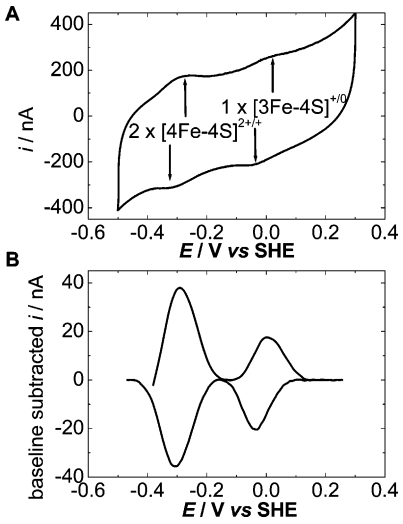

Figure 14. Non-turnover signals for a film of *A. vinosum* [NiFe]-MBH on a PGE electrode (0.03 cm^2) under a N_2 atmosphere: (A) raw data; (B) baseline-subtracted data. Conditions: 0 °C, CO-saturated buffer, pH 7, scan rate = 0.1 V s^{-1}. Recent data (ref 99) based on experiments reported in ref 75.

We should emphasize here that although Γ is required in order to calculate "per enzyme" activities (k_{cat}) using eq 7, it is unnecessary for interpreting most aspects of the electrocatalytic properties of enzymes on electrodes. The high activity of hydrogenases means that most measurements of electrocatalytic behavior can be carried out with electrodes

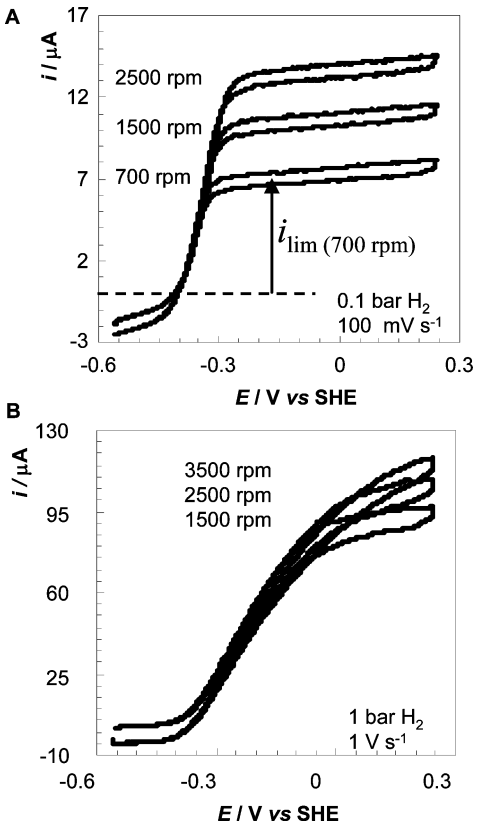

Figure 15. Electrode rotation rate dependence of the H_2 oxidation current recorded for a film of *A. vinosum* [NiFe]-MBH on a pyrolytic graphite "edge" (PGE) electrode at (A) 0.1 bar H_2 and (B) 1 bar H_2. Other conditions: 45 °C, pH 7. Reproduced and adapted from ref 100, by permission of The Royal Society of Chemistry.

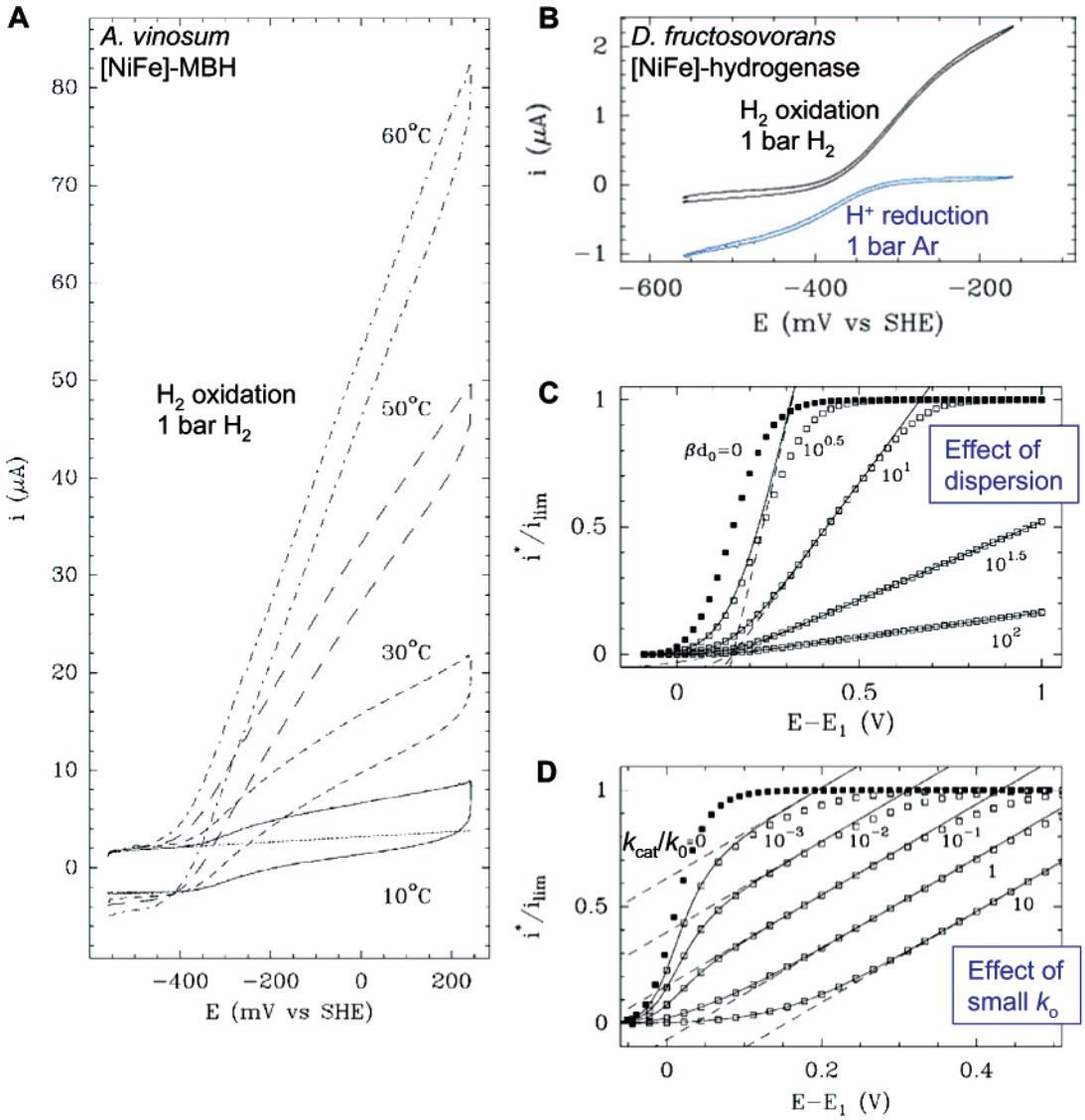

Figure 16. Examples of the appearance of the linear waveform in enzyme catalytic voltammetry. Panel A: Cyclic voltammograms showing catalytic H_2 oxidation by *A. vinosum* [NiFe]-MBH adsorbed at a PGE electrode at pH 7.0 under 1 bar H_2, 1 V s^{-1}, electrode rotation = 2500 rpm, over a range of temperatures 10−60 °C. Panel B: Cyclic voltammograms showing catalytic H_2 oxidation under 1 bar H_2, and H^+ reduction under 1 bar Ar for *D. fructosovorans* [NiFe]-hydrogenase at a PGE electrode at pH 7.0, 10 mV s^{-1}, electrode rotation = 1000 rpm, 40 °C. Calculated waveforms according to eq 10 for variations in βd_0 (which expresses the dispersion of electron-transfer rates) and on the ratio k_{cat}/k_0 are shown in panels C and D, respectively. Panels A, C, and D are reprinted with permission from ref 101. Copyright 2002 American Chemical Society. Panel B is reprinted with permission from ref 102. Copyright 2006 American Chemical Society.

containing too few enzyme molecules to be detected through nonturnover signals, i.e. <1−2 pmol cm^{-2}.

5.1. Ensuring the Electrochemistry Is Not Controlled by Transport of Substrate

The wave shape of a cyclic voltammogram recorded when substrate is present is generally the first provider of information on the electrocatalytic properties of the adsorbed hydrogenase. Here we are interested to see if the electrocatalytic wave shape provides information complementary to and exceeding that obtained by conventional kinetics. As outlined in section 4.2, it is important to be able to rotate the electrode at high speed because hydrogenases are usually highly active and the current and wave shape will otherwise be controlled by mass transport of H_2 to and from the electrode. In the event of extremely high activity, the current increases with electrode rotation rate ω, and the reciprocal plot according to the Koutecky−Levich equation (eq 6) produces a good approximation for the current that would be obtained if substrate mass transfer were not limiting (effectively at "infinite" rotation rate).

This fact is demonstrated in experiments on a very active film of *A. vinosum* [NiFe]-MBH on a PGE electrode at 45 °C (Figure 15). Experiments in Figure 15A were conducted under 0.1 bar H_2 and show sigmoidal voltammograms, each reaching a current plateau ($i_{lim(\omega)}$) that increases strongly as the rotation rate is increased. Note that the potential at which the plateau is reached also increases with rotation rate. The latter feature becomes more marked under 1 bar H_2 (Figure 15B). The current still increases with rotation rate, but electron-transfer limitations now become apparent in the wave shape. As discussed in section 4.2, mass-transport control is undesirable when trying to elucidate details of mechanisms, but it can be alleviated by abrading the electrode with cotton wool *after* forming the enzyme film to lower the coverage. A sparse population of enzyme

molecules on an electrode behaves as a microelectrode array.[69] This may be particularly important when studying hydrogenases at very low levels of H_2, where mass transport control is otherwise dominant.

5.2. Effects of Interfacial Electron Transfer on the Electrocatalytic Wave Shape

Even when substrate mass transport is not a limiting factor, the wave shape can be difficult to interpret, and some models are required. In 2002, we published a paper that proposed an explanation for the unusual wave shape often observed for electrocatalysis by adsorbed enzymes, and particularly for hydrogenases.[101] It had been often observed that instead of the catalytic current reaching a constant value at a reasonably high overpotential, it continues to increase in a linear manner, so the current displays a "residual slope". Some results obtained for *A. vinosum* [NiFe]-MBH on a PGE electrode are shown in Figure 16A, and similar effects are seen for H_2 oxidation and H^+ reduction catalyzed by the *D. fructosovorans* [NiFe]-hydrogenase (Figure 16B).[102]

The experiments on *A. vinosum* [NiFe]-MBH shown in Figure 16A were carried out with an electrode that had been abraded with cotton wool after forming the enzyme film. This treatment lowers the coverage and alleviates mass-transport control. As the temperature is raised from 10 to 60 °C, the catalytic activity increases dramatically, as expected: more significantly though, the wave shape changes from sigmoidal to one that resembles an Ohmic dependence, almost throughout the entire potential range! Yet this is not an Ohmic dependence—the problem is not one of there being a resistance to electron flow (one possibility, that ion transfer is rate-limiting, is unlikely because variations in the ionic composition of the electrolyte do not change the result). The linear voltammogram was explained in terms of the presence at the electrode of enzyme molecules having high catalytic activity but adsorbed *inhomogeneously*, with interfacial electron-transfer efficacy varying from facile to sluggish.

The explanation embodies the essence of the series resistor model described earlier (Figure 11), in that the electrocatalytic current due to an adsorbed enzyme having an inherently high catalytic turnover frequency will usually be limited by either mass transport of substrate (equivalent to a resistance, Ω_{trans}) or interfacial electron transfer (equivalent to a resistance, Ω_E), but the latter is now subject to a dispersion of values and a spread of electron-transfer rates k_0 is obtained. A summary of the model is now presented.

Scheme 1. Model for a Two-Electron Catalytic Oxidation Reaction in Which the Active Site Interconverts between Three Consecutive Oxidation Levels, O, I, and R, Each Capable of Coupled Chemical Reactions Such as Protonation. Reprinted and Adapted with Permission from Ref 104. Copyright 2002 American Chemical Society

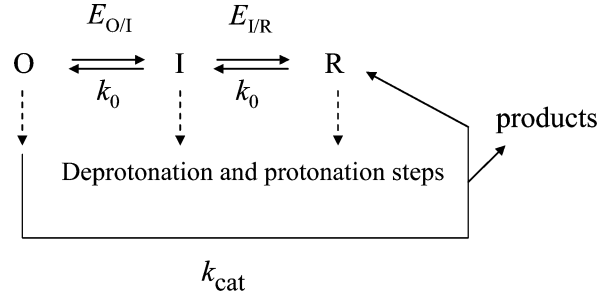

Provided mass transport is not limiting, the ideal wave shape for electrocatalysis by an adsorbed enzyme can be predicted starting from the simple model shown in Scheme 1, in which a two-electron catalytic reaction occurring at the active site with a rate constant k_{cat} is preceded by two one-electron transfers, each with a rate that is governed by an interfacial electrochemical electron exchange rate constant k_0 and potentials $E_{I/R}$ and $E_{O/I}$ respectively. More realistically, these interconversions are complicated by coupled chemical reactions such as acid−base equilibria, but these can be ignored here in the interest of simplicity.

As mentioned earlier, the Butler−Volmer relationship predicts an exponential climb in rate constant with driving force. Equation 8, derived for a catalytic oxidation reaction, is based upon the Butler−Volmer relationship,

$$\frac{i_{lim}}{i} - 1 = e_{O/I}^{-1}(1 + e_{I/R}^{-1}) + \frac{k_{cat}}{k_0}\{e_{I/R}^{-1/2} + e_{O/I}^{-1/2}(1 + e_{I/R}^{-1})\} \quad (8)$$

where $e_{O/I} = \exp[f(E - E_{O/I})]$ and $e_{I/R} = \exp[f(E - E_{I/R})]$ with $f = F/RT$.[101] The current in such a case should increase exponentially with potential and reach a maximum value i_{lim} that is related to k_{cat} as given in eq 7.

Equation 9 depicts the exponential decrease of the interfacial rate constant k_0 with distance d, where k_0^{max} is the value at closest contact (d is at its minimum value d_{min}) between the electrode and the relay site closest to the protein surface (the entry/exit site for electrons in the enzyme).

$$k_0(d) = k_0^{max} \exp(-\beta d) \quad (9)$$

The observation that a limit is not reached, at least within the potential range of the experiment, is considered by introducing the idea that the population of enzyme molecules is not homogeneously coupled to the electrode. The revised model assumes that intramolecular electron transfer along the FeS clusters is very fast, and the rate of interfacial electron transfer depends exponentially on the tunneling distance between the electrode and the electron entry/exit site.

The inhomogeneity is introduced by allowing d to have a range of values d_{min} to d_{max} ($d_{max} = d_{min} + d_0$, where d_0 is the spread of distances), all of which occur with the same probability. For an oxidation, the corrected catalytic current (i^*) in normalized form is then given by eq 10.

$$\frac{i^*}{i_{lim}} = \frac{1}{a^{ox}}\left(1 + \frac{1}{\beta d_0} \ln \frac{a^{ox} + b_2^{ox}}{a^{ox} + b_1^{ox}}\right) \quad (10)$$

where a^{ox} and b_2^{ox} are given by

$$a^{ox} = 1 + e_{O/I}^{-1}(1 + e_{I/R}^{-1}) \quad (10A)$$

and

$$b_2^{ox} = \frac{k_{cat}}{k_0^{max}}[e_{I/R}^{-1/2} + e_{O/I}^{-1/2}(1 + e_{I/R}^{-1})] \quad (10B)$$

and

$$b_1^{ox} = b_2^{ox} \exp(-\beta d_0) \quad (10C)$$

Figure 16C and D show, respectively, how the waveform depends on the function βd_0 (which expresses the dispersion of electron-transfer rates) and on the ratio k_{cat}/k_0. The dependences on βd_0 are computed with $k_{cat}/k_0 = 10$, and dependences on k_{cat}/k_0 are computed with $\beta d_0 = 10$.

With some simplifying assumptions, including $E_{O/I} = E_{I/R}$, the wave shape in the linear part of the voltammogram is approximated by eq 11:

$$\frac{i^*}{i_{lim}} = \frac{1}{\beta d_0}\left(\frac{f}{2}(E - E_1) - \ln\frac{2k_{cat}}{k_0^{max}}\right) \quad (11)$$

and the slope in this region is

$$\frac{\partial i^*}{\partial E} = \frac{i_{lim}}{\beta d_0}\frac{F}{2RT} \quad (12)$$

Analogous equations can be derived for an electrocatalytic reduction. The model thus predicts that a "classical" sigmoidal waveform will be expected when k_{cat}/k_0 is small (i.e., interfacial electron transfer is fast compared to turnover frequency and there is no dispersion ($\beta d_0 = 0$)). The "Ohmic" behavior results from electrocatalysis by enzyme molecules that have low values for k_0 relative to turnover frequency, so that they contribute only when the driving force is raised to compensate for this. The "residual" slope is a function only of the dispersion (Figure 16C).

The residual slope is more significant than might be expected. Although the limiting current value cannot be measured directly, eq 12 predicts that it is proportional to the slope multiplied by the temperature. The slope is thus a measure of the inherent activity of the enzyme; indeed, a graph of log $\partial i/\partial E \times T$ against $1/T$ is equivalent to an Arrhenius plot in which the slope is equal to $-E_a/R$ (where E_a is the activation energy). (Note that Figure 16C does not convey this fact easily because the current is normalized with respect to a constant value of i_{lim}.) Processing the data shown in Figure 16A in this way gave an activation energy of approximately 50 kJ mol^{-1} for electrocatalytic H_2 oxidation by *A. vinosum* [NiFe]-MBH.[101] It is important to note also that the unconventional shape of the voltammogram (reflecting a dispersion of the response of enzyme molecules in their overall rates of catalytic H_2 oxidation or production) does not seriously limit the usefulness of the electrochemical approach.

There are other variations in wave shape. One common observation is that, instead of reaching a limiting plateau as the potential is scanned, the catalytic current reaches a peak and then decreases.[76,92,103] By rotating the electrode, it can be shown that this peak is not due to substrate depletion. This kind of behavior can arise in several situations relevant to unraveling the complex interconversions of hydrogenases (Figure 6). One situation is that the enzyme converts to an inactive form as the potential is changed (see section 6). Another scenario is that the enzyme has an optimal operating potential, so that applying too large a driving force results in lower activity. This can arise when the catalytic mechanism involves a particular oxidation level of the active site that must survive for a sufficient period of time to allow an essential event to occur, such as substrate binding (note here that this also means that the rate of electron flow along an intramolecular relay can be *too fast* and evolution could have adjusted the potentials of the relay centers in order to synchronize the rates of electron flow and active site processes). Sometimes the potential sweep will reveal a second increase in current (a boost) after the original activity has appeared to reach a limiting value.[97] Another situation that may arise is that the population of adsorbed enzymes is inhomogeneous with regard to inherent catalytic properties such as characteristic reduction potentials of active sites. Unlike inhomogeneity in interfacial electron-transfer rates, an inherent inhomogeneity in the entire sample of enzyme can be detected spectroscopically.

5.3. Catalytic Constants

Two criticisms can be directed toward catalytic cycles that have been proposed for hydrogenases. The first of these is that, understandably, the species presented are predominantly, and often exclusively, those that live long enough to be characterized. However, from kinetic studies, it is clear that hydrogenases are extremely active enzymes, with k_{cat} values ranging from hundreds s^{-1} to upward of 10,000 s^{-1}.[75,100] As a consequence, true intermediates will be difficult to detect because even the most stable species will have lifetimes $\ll 1$ ms. The second criticism is that the mechanism for H_2 evolution is usually written as the reverse of H_2 oxidation. The principle of microscopic reversibility will apply between each pair of states on a cycle, but *different* cycles could be accessed for each direction of catalysis because in an electrochemical experiment, as in a living cell, energy is provided to drive the reactions. As an example, an electrode can enforce a specific distribution of oxidation states so that the enzyme follows a different reaction pathway according to the potential applied.[5b] Consequently, instead of a single cycle involving the detected active species shown in Figure 6, a more appropriate model for H_2 evolution and H_2 oxidation could involve separate catalytic cycles, each with transient intermediate species that are likely to escape direct spectroscopic detection. An important factor in enzyme active-site structures, and hydrogenases in particular, is that H-atoms are not located by X-rays and have only been pinpointed when their nuclear spin has become involved with an unpaired electron (see Review by W. Lubitz in this Issue). Thus, H_2 or H^+/H^- could be bound in certain states of the enzyme without this being apparent from structural or spectroscopic studies, but their participation can be inferred from voltammetric experiments through the changes in characteristic potentials with pH and $\rho(H_2)$.

The Michaelis−Menten equation as it applies to solution assays is expressed in eq 13, in which $[E]_0$ is the total enzyme concentration and [S] is the substrate concentration. The catalytic rate at saturating substrate concentration, $V_{max} = [E]_0 k_{cat}$.

$$\nu = \frac{[S][E]_0 k_{cat}}{K_M + [S]} \quad (13)$$

The basic catalytic constants K_M and k_{cat} are not easy to measure for hydrogenases either by conventional solution assays or by electrochemistry. It is important to note that rates may be controlled by substrate binding and a Briggs−Haldane model may be more appropriate.[94] Nonetheless, the Michaelis−Menten equation has at least empirical value. Values of K_M for hydrogenases tend to be low, and the very high activities of the enzymes may mean that a true "initial rate" (ν) prior to depletion of substrate is difficult to measure in solution assays and a true limiting current (at "infinite" rotation rate) is difficult to measure electrochemi-

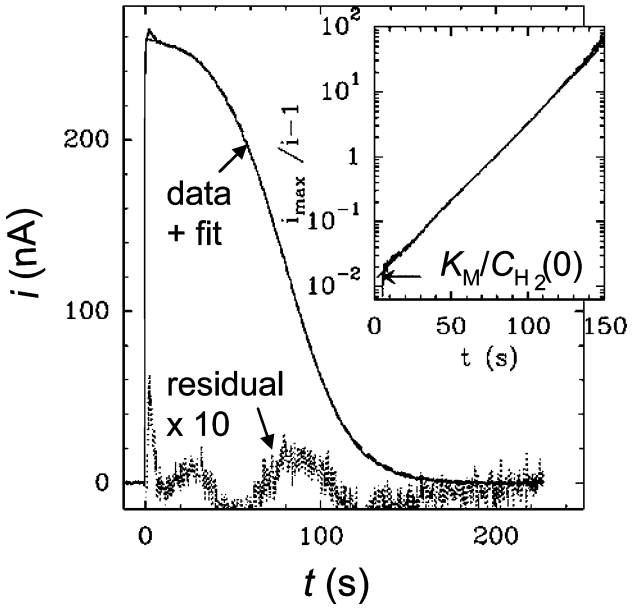

Figure 17. Catalytic, sigmoidal transient current for H_2 oxidation by *D. fructosovorans* [NiFe]-hydrogenase following injection of an aliquot of H_2-saturated solution to give approximately 0.64 mM in the electrochemical cell solution that is continually flushed with Ar. Other conditions: pH 6.1, $E = -160$ mV, 40 °C, rotation rate = 2000 rpm, $\tau = 18$ s. Dotted line: residual, enlarged ×10, after the data were fitted to eq 14 (dashed line). Inset: the log transform of the transient, fitted to a straight line according to eq 14A. Reprinted with permission from ref 66. Copyright 2004 American Chemical Society.

cally. Equally, as we have just discussed, determining k_{cat} requires knowledge of the electroactive coverage of the enzyme, which may be too low to detect. The activities of hydrogenases can approach diffusion control, and K_M values may be much larger than K_S, the true dissociation constant for the enzyme−substrate complex.[94]

Léger and co-workers have reported a novel method to measure the Michaelis and inhibition constants of hydrogenases for H_2 and other gaseous reactants. The electrochemical cell is open to the glovebox atmosphere, and the solution is sparged with a carrier gas (an inert gas such as N_2 or Ar, or H_2 in certain cases) (Figure 7A). A small amount of reactive gas is introduced, typically by injecting an aliquot of solution of known concentration, and the gas is then flushed out in the stream of carrier gas. The principle of the experiment is that this efflux provides a continuous range of concentrations of the reactive gas over which to measure the catalytic current. The system was checked by monitoring the reduction of O_2 at a bare PGE electrode, from which it was confirmed, by measurements of current as a function of time, that the concentration of introduced gas (O_2) decreases exponentially with a reproducible time constant (τ), provided the rate of gas flow and the electrode rotation rate are kept constant.

Figure 17 shows an experiment designed to measure K_M for the [NiFe]-hydrogenase from *D. fructosovorans*. The enzyme is adsorbed on a PGE electrode which is placed in the electrochemical cell containing buffer at pH 6.1 and rotated at 2000 rpm.[66] The electrode potential was set at −160 mV, and then H_2 was injected and the oxidation current was monitored as the H_2 was flushed from the solution with a flow of Ar. The trace is sigmoidal because at early times the level of H_2 is well above the concentration required to saturate the enzyme ($\gg K_M$) and removal of H_2 does not initially attenuate the current. Only once the level has dropped to approach K_M does the current start to decrease, finally leveling off as the H_2 is removed completely. As it is flushed out of solution, the H_2 concentration passes through levels that would be physiologically relevant.

The sigmoidal plot is analyzed according to eq 14, derived from the Michaelis−Menten equation (eq 13), and its log form (eq 14A). Here, $i(t)$ is the current at time t, analogous to v for any given substrate concentration, and i_{max} is the current at saturating substrate concentration, analogous to V_{max}. The concentration of H_2 at time t, $C_{H_2}(t)$, is given by $C_{H_2}(0)\exp(-t/\tau)$, where $C_{H_2}(0)$ is the initial concentration of H_2 introduced into the cell solution, and τ is the time constant for removal of H_2 in the Ar flow. Whereas determination of K_M from solution assays relies upon measurement of initial rates (v) before more than a few percent of substrate has been transformed, this condition is maintained in an electrochemical experiment by rotating the electrode rapidly. In practice, this experiment will still be difficult for hydrogenases having a low K_M, since it may not be possible to rotate rapidly enough at low H_2 concentrations to avoid the limitation from H_2 mass transport.

$$i(t) = \frac{i_{max}}{1 + \frac{K_M}{C_{H_2}(0)}\exp(t/\tau)} \quad (14)$$

$$\log_{10}\left(\frac{i_{max}}{i(t)} - 1\right) = \log_{10}\left(\frac{K_M}{C_{H_2}(0)}\right) + \frac{t}{2.3\tau} \quad (14A)$$

The value of K_M is determined from the y-intercept of the log transform. From several experiments (these could be carried out consecutively on the same enzyme film), Léger obtained $K_M = (6.5 \pm 3) \times 10^{-3}$ bar (approximately 5 μM) for *D. fructosovorans* [NiFe]-hydrogenase. From conventional methods, K_M values for [NiFe]-hydrogenases lie in the broad range 0.07−11 μM.

Reference to Figure 1 shows that the $E(H^+/H_2)$ potential shifts 90 mV more positive when the concentration of H_2 is lowered from 1 mM to 1 μM. For an experiment at fixed electrode potential or solution redox potential, this corresponds to a lowering of the driving force for H_2 oxidation by 90 mV. This would be important in experiments carried out at a low overpotential but not in cases where the driving force is always enough to ensure that the current remains on a plateau.

An alternative, but more laborious, method for determining K_M is to calculate i_{lim} (from a Koutecky−Levich plot, requiring current data at a number of different rotation rates) over a range of constant H_2 concentrations. Film loss from the electrode during the extended time taken for the series of rotation rate steps and gas exchanges may render this approach impractical.

5.4. Dependence of Activity on pH

Conventional kinetic assay methods using a chemical electron acceptor such as methyl viologen or methylene blue show that H_2 oxidation is faster at high pH, and it might be assumed that this reflects an inherent property of the enzyme. This notion in fact dates back from early days of hydrogenase research. That this is not always the case and may indeed be a deception is shown in an electrochemical study of how the rates of H_2 evolution and oxidation by *A. vinosum* [NiFe]-

MBH depend on pH.[104] Protein film voltammetry experiments allow the potential (thermodynamic) dependence of activity and the maximum activity (at the current plateau) to be measured simultaneously. Another way of looking at this is that a variation in catalytic rate due to an interesting kinetic factor can be resolved from the effects of changing the thermodynamic driving force. Figure 18A shows H_2 oxidation voltammograms recorded in a simple experiment for a hydrogenase-modified electrode that is transferred back and forth between two solutions of different pH, with the point to note being that the voltammetric wave shifts in potential but the limiting current is the same in either case. (Transferring the electrode back and forth between solutions ensures that any film loss is compensated for in the comparison.) A similar result was reported later for the [NiFe]-hydrogenase from *D. fructosovorans* (Figure 18B).[66] In both these cases, the voltammogram for H^+ reduction showed not only a shift in potential but also an increase in limiting current reflecting the higher concentration of H^+.

The useful potential ranges of methyl viologen and methylene blue as oxidants[105] are indicated in Figure 18A. Their inclusion emphasizes the point that the lower H_2 oxidation activity at lower pH observed for the [NiFe]-hydrogenases reflects only the additional driving force that is required. Thermodynamically, H_2 is oxidized more easily at high pH. However, the H_2 oxidation activity of the [FeFe]-hydrogenase from *D. desulfuricans* clearly increases with pH (Figure 18C).[71] The unusual shape of the voltammograms for the [FeFe]-hydrogenase at higher potentials is due to very rapid and reversible inactivation of the enzyme as the potential is raised—we return to this in section 6.

The results of a detailed analysis of the pH dependence of the catalytic activity of H_2 oxidation and H^+ reduction by *A. vinosum* [NiFe]-MBH are compiled in Figure 19.[104] The plot shows rotation-rate-optimized currents ($\omega = \infty$) that are normalized with respect to values (=1.0) at pH 6.6, $E = -560$ mV (H^+ reduction) and at pH 7.3, $E = 240$ mV (H_2 oxidation). The lack of dependence of oxidation activity on pH has already been mentioned; data for H^+ reduction activity were analyzed in terms of a model involving three protonated reduced states, two of which (with $2H^+$ and $3H^+$) are able to undergo catalysis.

Scheme 2 shows how the oxidative and reductive catalytic cycles suggested from these results could be aligned. In this scheme, H_2 evolution and H_2 oxidation involve different species and different catalytic cycles. They differ in that oxidation of H_2 always involves species in which there is always at least one extra H present. Note that $O:H_2$ is equivalent to $R:2H^+$.

Evolution of H_2 by *A. vinosum* [NiFe]-MBH is inhibited by H_2, and this is also evident from the rotation rate dependence of the H^+ reduction current (data not shown).[104] The current increases as the rotation rate is increased due to removal of H_2 from the electrode surface.

Analysis of the data shows that the potentials $E_{O/I}$ and $E_{I/R}$ are not sensitive to the presence of H_2, and this leads to the proposal that all the species involved in H_2 oxidation bind an H_2 molecule in all oxidation states.[104] The two-cycle scheme predicts that H^+ reduction activity is suppressed when H_2 binds to the active site because the enzyme switches to H_2 oxidation, although this suggestion is not obviously correlated with the simple proposal given in Figure 6A, in which only three active states—Ni-SI, Ni-C, and Ni-R—are included. A tentative assignment is that "$I:H_2$" is likely to

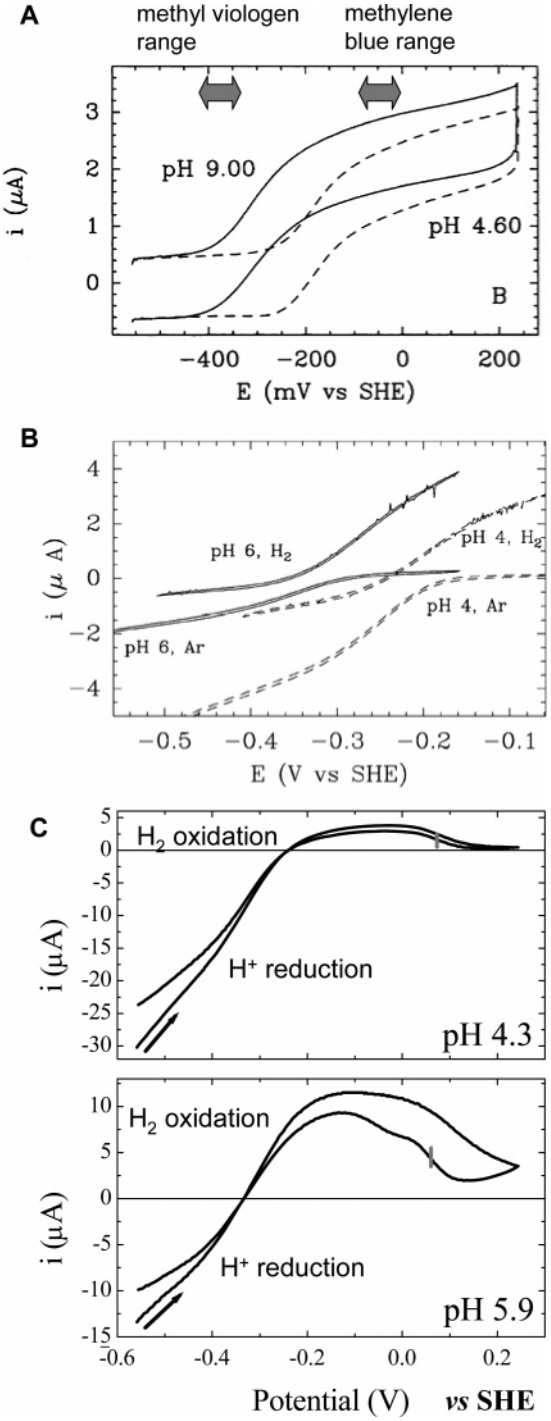

Figure 18. Effect of pH on the activity of hydrogenases. Panel A: voltammograms recorded at 200 mV s^{-1}, 1 bar H_2, and 5 °C for a film of *A. vinosum* [NiFe]-MBH transferred between pH 9 (solid line) and pH 4.6 (dashed line) buffer, each containing 0.1 M NaCl and 20 μg mL^{-1} polymyxin. Reprinted with permission from ref 104. Copyright 2002 American Chemical Society. Panel B: voltammograms recorded at 20 mV s^{-1} and 40 °C for a film of *D. fructosovorans* [NiFe]-hydrogenase transferred between pH 6 (solid lines) and 4.1 (dashed lines) buffer flushed with either H_2 or Ar as indicated. Reprinted with permission from ref 66. Copyright 2004 American Chemical Society. Panel C: voltammograms for *D. desulfuricans* [FeFe]-hydrogenase recorded at 10 mV s^{-1}, under 1 bar H_2, 10 °C. In each case, the enzyme is adsorbed on a PGE electrode that is rotated at 2000−2500 rpm. Reprinted with permission from ref 71. Copyright 2006 American Chemical Society. For reference, panel A shows the useful ranges of oxidizing potential achieved with methyl viologen (−446 to −326 mV) and methylene blue (11−131 mV).[105]

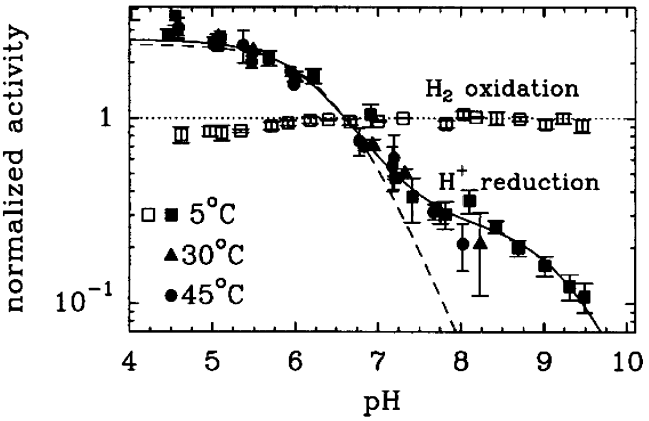

Figure 19. Relative pH dependences of the rates of H^+ reduction (solid symbols) and H_2 oxidation (open symbols) by *A. vinosum* [NiFe]-MBH adsorbed on a PGE electrode. The H_2 oxidation rate is essentially independent of pH, and activity is fixed at 1.0 at E = 240 mV, pH = 7.3. The line through the H^+ reduction data is a fit to equations derived for the model shown in Scheme 2, in which H_2 is released from species R:2H$^+$ or R:3H$^+$, and activity is normalized to the value obtained at pH 6.6, E = −560 mV. Reprinted with permission from ref 104. Copyright 2002 American Chemical Society.

Scheme 2. Scheme of Reactions Involved in *Separate* Cycles for H_2 Production and H_2 Oxidation by a [NiFe]-hydrogenase. Reprinted with Permission from Ref 104. Copyright 2002 American Chemical Society

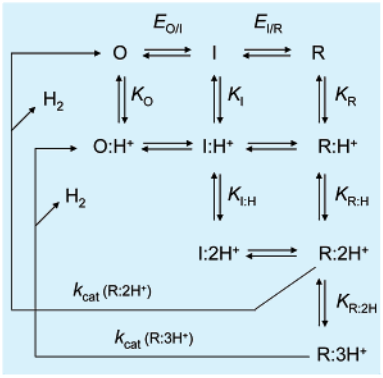

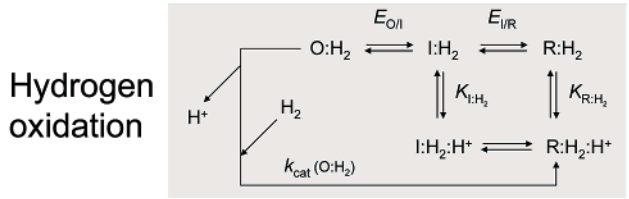

be at the oxidation level of Ni-C; however, there is strong evidence (from EPR) that only Ni-C and Ni-R are in rapid equilibrium with each other.[36] The results suggest how difficult it is to assign oxidation levels where species may differ not only in protonation state but also in having an elusive H_2 bound or not bound.

5.5. Activity Comparison of Hydrogenases with Pt

Activation of H_2 on precious metal (M) surfaces involves homolytic cleavage of the H−H bond and formation of neighboring M−H bonds.[106] Platinum catalysts used in proton exchange membrane (PEM) fuel cells usually operate in a humidified gaseous environment rather than in solution, at temperatures close to 100 °C,[107] whereas hydrogenases function in an ambient aqueous medium and are therefore limited by the solubility of H_2 (ca. 1 mM).

An investigation to compare the oxidation activities of a [NiFe]-hydrogenase and a Pt electrode under ambient conditions was published in 2002.[100] The experiment involved forming a high-coverage film of *A. vinosum* [NiFe]-MBH on a PGE electrode and comparing the limiting current with that obtained for a Pt electrode prepared by treating either the same PGE electrode or a gold electrode of the same size, with H_2PtCl_6. The limiting currents were of the same magnitude and diffusion-controlled up to 2500 rpm in all cases. The main difference was that raising the H_2 level resulted in the hydrogenase electrode requiring a larger overpotential than the Pt electrode in order to achieve the limiting current. The interpretation of this is based on the earlier discussion of the wave shape and its link with dispersion of interfacial rate constants: the active site of the hydrogenase is extremely active, but its maximum turnover frequency is ultimately limited by interfacial electron transfer (section 5.2). Attaining the highest current requires contributions from enzyme molecules that are not well coupled to the electrode, and therefore, an increasingly higher driving force is required to engage them. A similar result was obtained in 2005 by Karyakin and co-workers, who compared

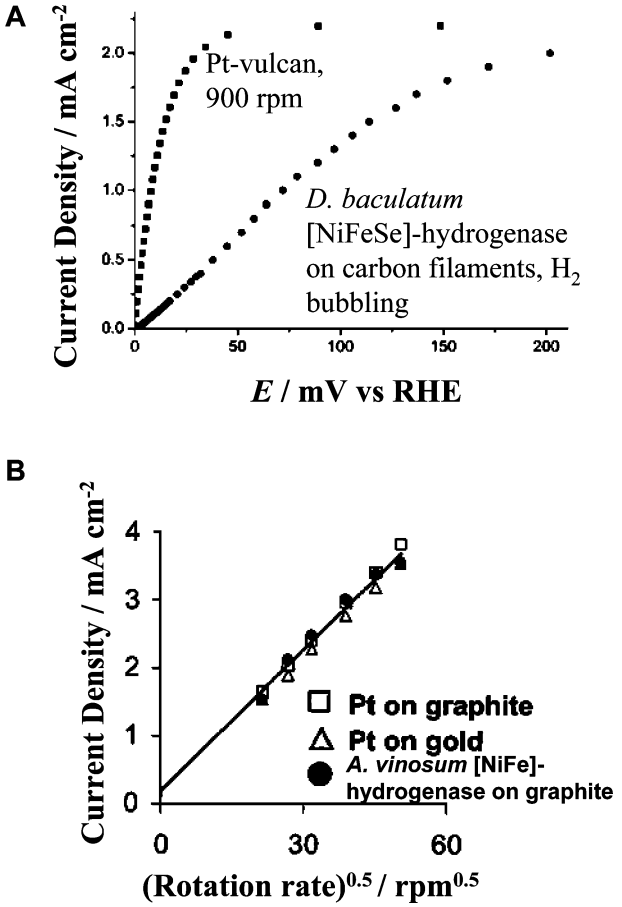

Figure 20. Comparing the H_2 oxidation electroactivity of Pt and hydrogenase modified electrodes. Panel A: Quantifying the maximal current density for Pt/Vulcan (electrode rotation rate: 900 rpm) vs a carbon filament electrode modified with *Desulfomicrobium baculatum* [NiFeSe]-hydrogenase (stationary, but with H_2 bubbling to assist mass transport), showing the electrode potential (driving force) required to attain maximum activity. Reproduced with permission from ref 82. Copyright the Biochemical Society. Panel B: Levich plot (see eq 5) comparing the limiting currents ($i_{lim(\omega)}$) achieved for 1 bar H_2, 45 °C, pH 7, at platinized graphite, platinized gold, or a PGE electrode modified with *A. vinosum* [NiFe]-MBH. Reproduced from ref 100 by permission of The Royal Society of Chemistry.

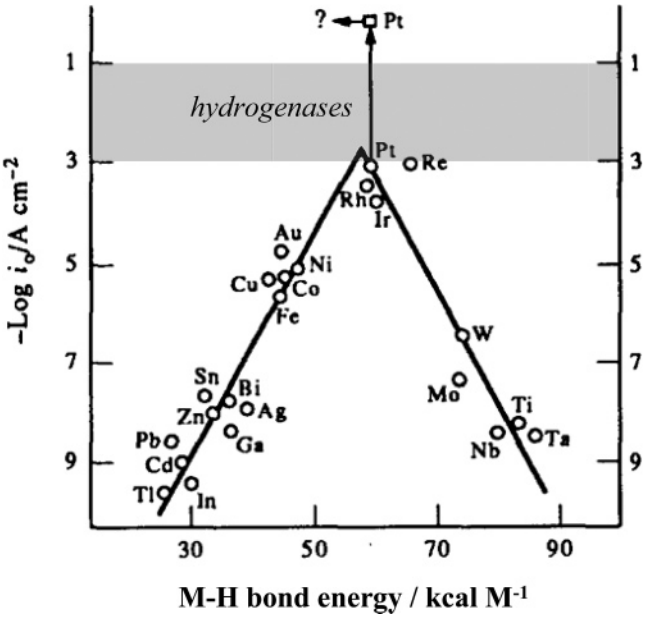

Figure 21. Volcano plot of the exchange current density (shown as log i_0) obtained for H_2/H^+ interconversion at various transition metals as a function of the metal−hydrogen atom (M−H) bond strength (○). The exchange current density for Pt is likely to be an underestimate, and this is indicated by the vertical arrow and the uppermost point marked □. The activity of hydrogenase active sites is represented by the broad gray area. Adapted with permission from *Electrochim. Acta*, Vol. 39, O. A. Petrii, G. A. Tsirlina, "Electrocatalytic Activity Prediction For Hydrogen Electrode Reaction: Intuition, Art, Science" 1739−1747, Copyright 1994, with permission from Elsevier.

the current density obtained for a carbon filament electrode on which was adsorbed *Desulfomicrobium baculatum* [NiFeSe]-hydrogenase (with H_2 bubbling through the solution) with the current density reported for a rotating disc Pt/vulcan electrode.[82] These results are included in Figure 20.

A practical comparison based on activity per electrode area is unreasonable, because the footprint of a hydrogenase molecule on a surface is several orders of magnitude larger than the area of a pair of Pt atoms, and in any case, the currents are usually diffusion controlled. From a fundamental viewpoint, it is therefore more informative to compare site-for-site activities. The catalytic activities of transition metals are often represented by Volcano Plots (Figure 21).[108,109] For H_2 oxidation at an electrode, the exchange current density (the rate of flow of electrons back and forth at the reversible potential) is plotted against the energy of the M−H bond. The principle here is that the rate of oxidation of H_2 depends on the thermodynamic ease of formation of an M−H bond that is not so strong as to become a stable product rather than an intermediate. The apex is occupied by Pt and Re, each with exchange current densities of about 10^{-3} A cm^{-2}, although a recent appraisal has suggested that this value could be as high as about 1 A cm^{-2}.[109,110] A "lean", efficient (economically speaking) Pt electrode has a coverage of <0.1 mg cm^{-2},[107] equivalent to 10^{-8} mol atom Pt per cm^2, and we thus arrive at a range of about 0.1−100 s^{-1} for the turnover frequency of a Pt "active site". The equivalent quantity for the enzyme is not easy to estimate, but one option is to consider the rate of H_2/D^+ exchange catalyzed at the active site, as measured by mass spectrometry: values > 100 s^{-1} are obtained.[111] A second way of comparing is to consider maximum currents for Pt and hydrogenase electrodes typically achieved under comparable conditions. For Pt, typical current densities are 1−10 A cm^{-2} at overpotentials of around 0.4 V. By comparison, a PGE electrode modified with *A. vinosum* [NiFe]-MBH can produce about 3−4 mA cm^{-2} at 45 °C at an overpotential ranging from 0.4 to 0.6 V. For a hydrogenase coverage of 10^{-12} mol cm^{-2}, this means that the activity per active site lies in the same range as that of the equivalent PtPt site, as included in Figure 21.

5.6. Catalytic Bias: H_2 Oxidation vs H^+ Reduction

Protein film voltammetry provides quantitative information on the inherent bias of a redox enzyme to function in a particular direction because the electrode potential can be varied continuously over the widest possible range either side of the formal potential for the substrate. The cyclic voltammograms shown in Figure 22 illustrate different aspects of the catalytic bias of hydrogenases that can be deduced from electrochemical experiments performed at 1 bar H_2 under anaerobic conditions.[76] The [FeFe]-hydrogenase from *D. desulfuricans* is an active catalyst for both H_2 production and oxidation under a 1 bar H_2 atmosphere, although as noted earlier and as will be discussed in section 6, it inactivates rapidly at high potential, producing a complex waveform. The value of the potential of zero net current (averaged for the forward and reverse scans) corresponds to the formal reduction potential of the H^+/H_2 couple expected under these

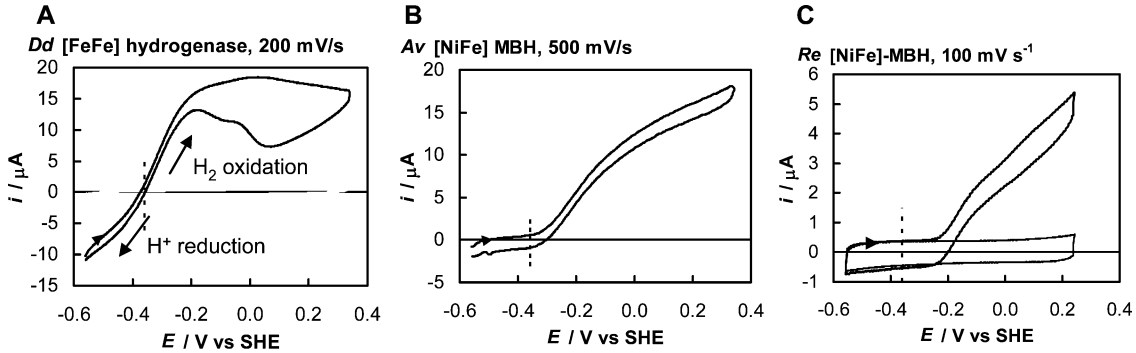

Figure 22. Cyclic voltammograms for a PGE electrode modified with (A) *D. desulfuricans* (*Dd*) [FeFe]-hydrogenase, (B) *A. vinosum* (*Av*) [NiFe]-MBH, and (C) *Ralstonia eutropha* (*Re*) [NiFe]-MBH (black lines). Blank electrode scans are shown in gray. Scan rates are indicated on each panel. Other conditions: pH 6.0, 30 °C, electrode rotation 2500 rpm. Dashed lines indicate the potential of the H^+/H_2 couple under these conditions. Reprinted with permission from ref 76. Copyright 2005 American Chemical Society.

conditions (−360 mV at pH 6, 30 °C, 1 bar H_2, marked by a dashed vertical line in Figure 22).

In contrast to *D. desulfuricans* [FeFe]-hydrogenase, the results depicted for the [NiFe] enzymes show very low or zero H^+ reduction activity under H_2. This is mainly due to inhibition of this reaction by H_2: significant H^+ reduction currents are observed under an inert N_2 atmosphere for the *D. fructosovorans* [NiFe]-hydrogenase (Figure 18B) and the *A. vinosum* [NiFe]-MBH, and a small current is observed for the *Ralstonia eutropha* [NiFe]-MBH. Electrode rotation is particularly important here in removing the product (H_2) from the solution close to the electrode in order to relieve product inhibition. Studies of H^+ reduction by *A. vinosum* [NiFe]-MBH under N_2 showed clearly that the catalytic current increases as the rotation rate is increased and, further, that this effect was not altered by increasing the buffer concentration (arguing against an interpretation that the current increase is due to relief of H^+ depletion).[104] Léger et al. have estimated the constant, K_I, for H_2 inhibition of H^+ reduction by *D. fructosovorans* [NiFe]-hydrogenase as approximately 0.2 bar (i.e. approximately 0.2 mM) (at −660 mV, pH 6, 40 °C).[66] Note how high this is compared to K_M for H_2 oxidation by the same enzyme: $6.5 \pm 3 \times 10^{-3}$ bar, measured at −160 mV, pH 6, 40 °C.[66] Rapid rotation of the electrode to maintain the substrate and product concentrations at levels close to the bulk solution level is essential if measured potentials are to have any thermodynamic relevance.

The catalytic bias of some hydrogenases is also evident in the onset potential for H_2 oxidation under 1 bar H_2. The voltammogram for *A. vinosum* [NiFe]-MBH reveals an onset potential for electrocatalytic H_2 oxidation close to $E(H^+/H_2)$, whereas, for *R. eutropha* [NiFe]-MBH, the onset of H_2 oxidation is shifted about 80 mV more positive.[76] This subtle effect would not be clear at all from solution assays using soluble redox mediators. Protein film voltammetry thus provides a simple means to assess and quantify the bias and potential profile for the activity of hydrogenases.

5.7. Rate-Determining Steps

As mentioned above, the high activity of hydrogenases makes it very difficult to establish rate-determining steps in catalysis of H_2 oxidation or H^+ reduction. There is good evidence that conventional assays are probably limited by the rate of reaction with the small-molecule redox partner. For example, values of the turnover frequency for H_2 oxidation by [NiFe]-hydrogenases are hundreds per second when measured with methylene blue[2] but several thousand per second when estimated by PFV.[75]

5.7.1. H^+/D_2 Exchange Experiments

A first stage in pinpointing a rate-determining step is the H/D isotope effect, which has been reported to be very small for H_2 oxidation or proton reduction but quite sizable for the H^+/D_2 exchange reaction. Alterations of catalytic oxidation current between exchanges of H_2 and D_2 in the cell headspace were measured for *A. vinosum* [NiFe]-MBH adsorbed on a PGE electrode over a range of temperatures (Figure 23).[112]

This method allowed investigation of the isotope effect on the same sample of enzyme. While a small kinetic isotope effect is evident at higher temperatures ($H_2/D_2 = 1.15$ at 45 °C), as the temperature is lowered, the isotope effect becomes more pronounced ($H_2/D_2 = 1.55$ at 10 °C).[112] This is explained by a change in the rate-determining step as the temperature is varied. At higher temperature, the catalytic current is controlled by interfacial electron transfer (as discussed in section 5.2 and shown in Figure 16), which is not expected to show an isotope effect. As the temperature is lowered, the H−H cleavage reaction (which *is* expected to show an isotope effect) becomes increasingly rate-limiting. An analogous rate limitation (slow interfacial electron transfer) might apply in conventional solution reactions when a small electron acceptor is used. Therefore, H_2 oxidation does show an isotope effect, but this effect is obscured under conditions in which intermolecular or interfacial electron transfer is rate-limiting.

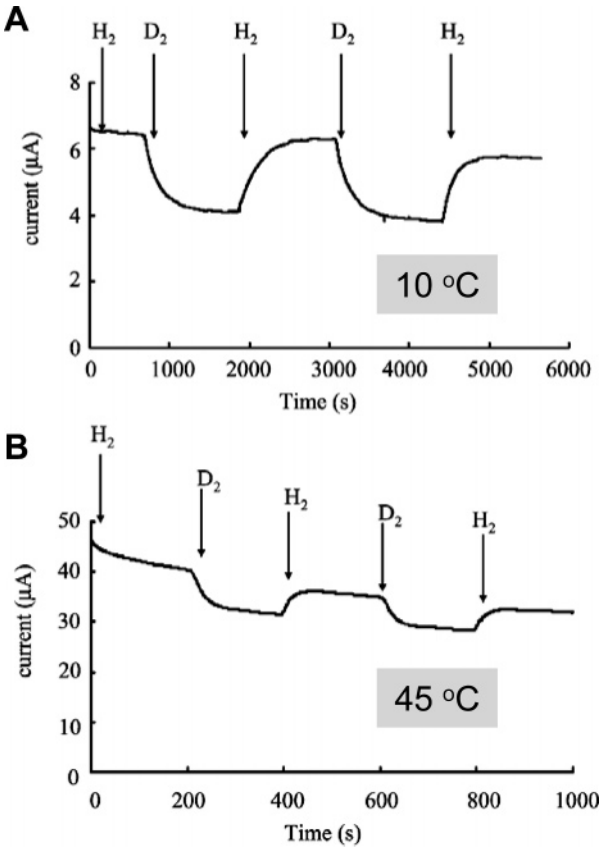

Figure 23. Controlled potential experiment for a film of *A. vinosum* [NiFe]-MBH on a PGE electrode. The gas atmosphere above the cell solution is interchanged between H_2 and D_2 at a total pressure of 1 bar. Panel A: At 10 °C, a kinetic isotope effect of 1.55 is observed. Panel B: at 45 °C, a kinetic isotope effect of 1.15 is observed. Other conditions: electrode potential is 242 mV, mixed buffer solution at pH 6.0, and electrode rotation rate 2500 rpm. Reproduced from ref 112 by permission of The Royal Society of Chemistry.

5.7.2. Intramolecular Electron-Transfer Limitations?

This section considers conditions under which *intramolecular* electron transfer could become rate-limiting. A common feature of [NiFe]-hydrogenases is that the medial [3Fe-4S] cluster has a much higher reduction potential than the two [4Fe-4S] clusters,[8,75,113] which makes it behave as an electron trap (Figure 24). In 1998, Rousset et al. described experiments on the *D. fructosovorans* [NiFe]-hydrogenase in which the medial [3Fe-4S] cluster was mutated to a [4Fe-4S] cluster.[114]

The mutation produced a medial cluster with a much more negative reduction potential, allowing the authors to test the

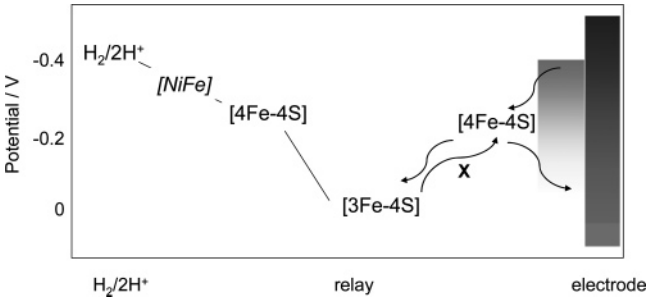

Figure 24. Energetics of electron flow along the Fe−S cluster relay for a [NiFe]-hydrogenase on an electrode. The rate-determining uphill electron-transfer step during H_2 oxidation (k_{cat}^{ox}) detected for the H184G mutation repaired by imidazole[102] is indicated as X.

influence of cluster reduction potentials on the catalytic activity. Using conventional kinetic assays, the activity of this enzyme in either direction was little changed compared to the wild type enzyme. The authors suggested that intramolecular electron transfer must be so fast that the rate-determining step is one of the reactions occurring at the active site. However, as discussed above, two further observations need to be considered. The first of these is that studies using protein film voltammetry showed that the rate of electrocatalytic H_2 oxidation by a [NiFe]-hydrogenase (*A. vinosum*) is much higher than that measured using chemical electron acceptors, suggesting that the rate-determining step in conventional solution kinetics could actually be intermolecular electron transfer to the acceptors.[75] Second, further electrochemical experiments on the *A. vinosum* [NiFe]-MBH suggested that interfacial electron transfer could be rate-limiting for many of the enzyme molecules adsorbed on a graphite electrode surface.[101] The situation can also be viewed from the perspective of the voltammograms shown in Figure 15, section 5.2. When H_2 mass transport is rate-limiting, as it appears to be under 0.1 bar H_2 and at rotation rates below 2500 rpm (Figure 15A), the current plateau is reached at a potential of approximately −0.3 V, which is far below that of the [3Fe-4S] cluster, at approximately −30 mV. The [3Fe-4S] cluster thus maintains an adequate rate of electron flow that allows diffusion-controlled oxidation of 0.1 bar H_2 even when the electrode potential driving the reaction is nearly 0.3 V more negative.

To help resolve this issue, Léger and co-workers carried out experiments with mutant forms of *D. fructosovorans* [NiFe]-hydrogenase in which the ligands to the distal [4Fe-4S] cluster were altered to perturb the thermodynamics and kinetics of electron-transfer reactions.[102] This cluster is close to the surface, and it is coordinated by three cysteine-S ligands and a histidine-N (Figure 25).

Histidine is an unusual ligand for [4Fe-4S] clusters, so the question also arises as to why it is required in this enzyme. When the histidine (H184) was mutated to glycine or cysteine, a [4Fe-4S] cluster still formed, as did the other clusters and the active site which appears unchanged (as shown by EPR).[102] Also, the reduction potentials of the new clusters were not greatly different from the wild-type enzyme. The H^+/D_2 isotope exchange rate was not significantly altered for either of the mutants, H184G or H184C, but these variants had lost nearly all of their ability (3 and 1.7% remaining, respectively) to catalyze H_2 oxidation when methyl viologen or methylene blue was used as the electron acceptor. When the H_2 oxidation experiment with H184G was carried out in the presence of imidazole or 1-methyl imidazole, the activity

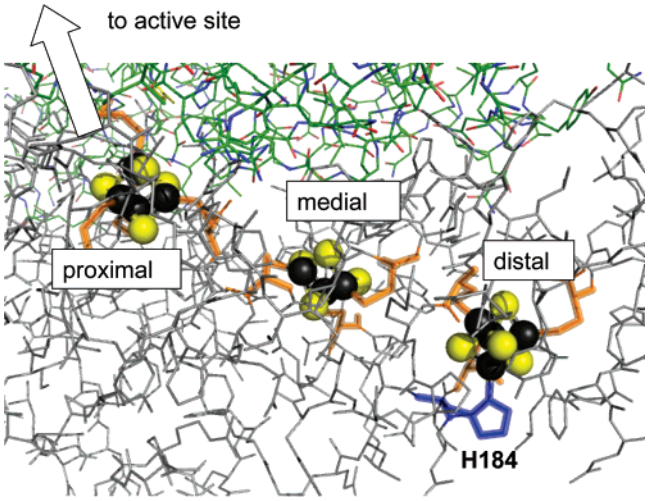

Figure 25. Representation of the structural environment of the Fe−S clusters in the electron relay system in [NiFe]-hydrogenases. The data are taken from the *D. gigas* structure (PDB code: 1YQW).[39] In the very similar hydrogenase from *D. fructosovorans*, mutation of histidine 184 to cysteine or alanine inactivates the enzyme. Addition of exogenous imidazole or 1-methyl imidazole to H184G repairs the connection.[102]

recovered to about 25% of its normal value. This recovery was attributed to imidazole being able to bind in the cavity created by the histidine-glycine mutation, forming a coordinate bond to the cluster and thus mimicking the actual presence of histidine.

Léger and co-workers used PFV to investigate the effects of the distal cluster alterations on intra- and interfacial electron transfer.[102] As shown in Figure 26, the enzyme's activity was severely affected by both H184G and H184C mutations, and this is significant because it provides a very convincing demonstration that the distal cluster is the electron entry/exit point. The H184G mutant showed very little electrocatalytic activity at all, either for H_2 oxidation or for H^+ reduction under Ar (dashed lines, Figure 26A), but addition of imidazole to the cell solution resulted in the immediate appearance of activities in both directions (solid lines) which increased as imidazole was titrated in, in accordance with the results obtained in conventional assays. The H184C mutation showed severely retarded interfacial electron transfer in both directions, as can be seen from the appearance of the voltammograms (Figure 26B) for oxidation of H_2 and for H^+ reduction. Thus, at pH 6, the onset of catalytic oxidation current occurs around 0 V instead of −0.3 V as observed for native enzyme, whereas H^+ reduction commences at −0.5 V instead of −0.3 V; thus, there is a large window of potential in which the enzyme is inactive. Figure 26C shows that the effect of imidazole in activating H184G is reversed by adding a thiol, mercaptopropanol, which mimics the cysteine ligation in H184C.

Further studies established an interesting difference in the way that imidazole repairs the enzyme depending upon whether H_2 oxidation or H^+ reduction is being addressed.[102] The experiments are shown in Figure 27. First, as imidazole is titrated into the electrochemical cell and voltammograms are recorded for H^+ reduction under Ar, the potential at which catalysis commences becomes more positive (i.e. the required overpotential becomes more positive) and the current magnitude increases with no change in the residual slope. As discussed in section 5.2, this is indicative of an increase in the rate of interfacial electron transfer (k_0) without any change

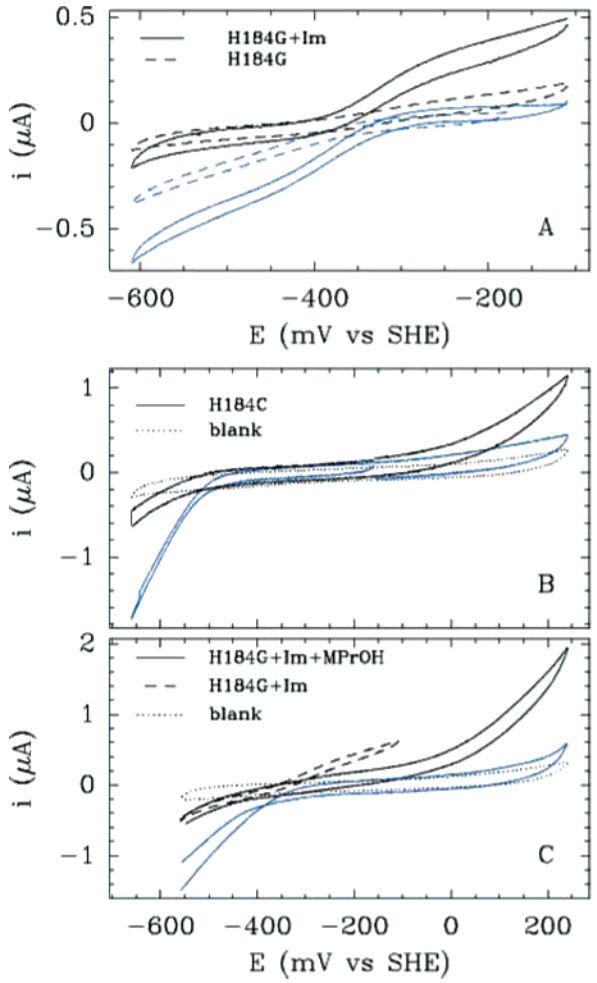

Figure 26. Voltammograms for *D. fructosovorans* [NiFe]-hydrogenase variants adsorbed at a PGE electrode, under an atmosphere of H_2 (black lines) or Ar (blue lines). Panel A: H184G mutant at pH 7, before (dashed lines) and after the addition of 20 mM imidazole. Panel B: H184C enzyme, at pH 6. Panel C: H184G mutant, at pH 6, in the presence of 10 mM imidazole, before (dashed line) and after the addition of 2 mM mercaptopropanol (MPrOH). Scan rate = 10 mV s^{-1}, electrode rotation = 1000 rpm (Panel A) or scan rate = 20 mV s^{-1}, electrode rotation = 2000 rpm (Panels B and C). The temperature is 40 °C in all cases. Reprinted with permission from ref 102. Copyright 2006 American Chemical Society.

in k_{cat}^{red} (the turnover frequency for H^+ reduction). In contrast, for H_2 oxidation (Figure 27B), raising the imidazole concentration causes the current to increase and there is a gradual increase in the residual slope. This is indicative of both k_0 and k_{cat}^{ox} increasing as imidazole binds to the enzyme. From the variation of residual slope with imidazole concentration, 1:1 complexation was established for imidazole binding, and the dissociation constant was estimated as 12 mM (40 °C, pH 7), i.e. binding is weak. Since the active site and the other two Fe−S clusters are unaffected by the mutation, the increase in turnover frequency k_{cat}^{ox} must be due to an increase in the rate of intramolecular electron transfer from the medial [3Fe-4S] cluster to the distal [4Fe-4S] cluster, which is an uphill process. During H^+ reduction, the direction of electron flow is reversed, but any increase in the rate of *downhill* electron transfer from the distal [4Fe-4S] to the medial [3Fe-4S] cluster is unimportant, as this was already sufficient to maintain the catalytic rate.

Given that the distal [4Fe-4S] cluster must be the electron entry/exit site, the k_0 results establish that the unusual

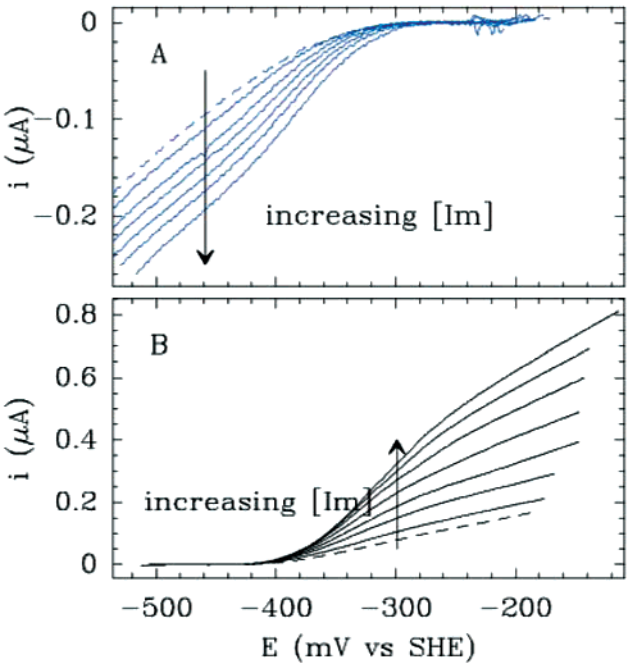

Figure 27. Effect of exogenous imidazole (Im) on the activity of *D. fructosovorans* H184G [NiFe]-hydrogenase adsorbed at a PGE electrode. Panel A: H^+-reduction under 1 bar Ar. Panel B: H_2-oxidation under 1 bar H_2. Conditions: pH 7, 40 °C, scan rate = 10 mV s^{-1}, electrode rotation = 2000 rpm. Reprinted with permission from ref 102. Copyright 2006 American Chemical Society.

histidine ligation of the distal [4Fe-4S] cluster in [NiFe]-hydrogenases confers the ability for fast interfacial electron transfer in either direction. It follows that histidine is also essential for intermolecular electron transfer in homogeneous kinetic measurements and presumably also in physiological function. This effect results from an inherent change in kinetic capability rather than any change in reduction potential. Histidine ligation might somehow lower the reorganization energy as well as provide greater electron coupling (delocalization of the [4Fe-4S] wave function) to the protein surface (the imidazole ring is surface exposed, Figure 25). In assessing these factors, it is significant that k_{cat}^{ox} but not k_{cat}^{red} is dependent on imidazole coordination, because a lowering of the reorganization energy would be particularly beneficial for an uphill reaction rather than a downhill reaction.

5.8. Outlook

Although the experiments described in this section have only been performed on a small number of hydrogenases, they outline a direct electrochemical approach that could easily be employed to screen and to compare the activity characteristics of a very wide range of hydrogenases. As different behaviors are categorized, a library of recognizable voltammetric responses is established, making it possible to assess, for example, catalytic bias toward H_2 production vs oxidation, suitability for fast interfacial electron transfer at an electrode, or affinity for H_2 at trace levels. In subsequent sections we discuss how PFV can be used to diagnose and interpret inactivation/activation reactions of hydrogenases and their reactions with small molecule inhibitors. Finally, we consider how all of this information can be used for rational selection of enzymes for novel fuel cell applications, including a device operating on low level H_2 in air.

6. Reversible Inactivation of Hydrogenases under Anaerobic Conditions

6.1. Characteristic Potentials of Anaerobic Active/Inactive Interconversions

Both [NiFe]- and [FeFe]-hydrogenases undergo reversible oxidative inactivation under anaerobic conditions (see Figure 6). For the [NiFe]-enzymes, anaerobic oxidation generates the "Ni-B" or "Ready" state, and for [FeFe]-hydrogenases, it generates H_{ox}^{inact}. For the [NiFe]-enzymes, the oxidized inactive forms are assigned as Ni(III)−Fe(II) and the active site incorporates an atom in a bridging position between the Ni and the Fe. In Ni-B, this is a hydroxide or oxide, but other atoms such as S can be incorporated under special conditions (see section 7.3). Definitive structural assignments for [FeFe]-hydrogenases have yet to be established. In the [FeFe]-enzymes studied so far, the oxidized inactive state is an even-spin system: since an active site in which CO ligands are coordinated to Fe(III) is doubtful, it follows that H_{ox}^{inact} is more likely to be Fe(II)Fe(II) than Fe(III)(III). A complicating factor in [FeFe]-hydrogenases is the [4Fe-4S] cluster which shares a bridging cysteine with one of the active site Fe atoms (Figure 4B) and is likely also to share electrons. In conventional experiments, it has been proposed that this Fe−S cluster remains in the oxidized level (2+), but it is possible that an electron is delocalized onto it or that it accepts an electron in a transitory manner.

The anaerobic oxidative inactivation and reductive reactivation reactions, summarized in Figure 6, can be investigated by PFV to determine the order of the steps involved and other details of the mechanisms.[76] Figure 28 shows oxidative inactivation as it is observed in cyclic voltammograms of *Allochromatium vinosum* [NiFe]-MBH oxidizing H_2 and recorded at a slow scan rate.[92] In this experiment the electrode is rotated at 2500 rpm, so the decrease in current as the potential is scanned to positive values is due to inactivation of the enzyme rather than depletion of substrate. On the return scan, the electrocatalytic current recovers as the enzyme reactivates at lower potentials. The potential at which activity returns is highly sensitive to the conditions of the experiment, and a characteristic quantity, E_{switch}, is defined as the potential of maximum slope in the reductive activation direction, determined from a derivative plot, as shown in Figure 28B. From experiments on *A. vinosum* [NiFe]-MBH it was concluded that E_{switch} is a robust parameter to which can be attached thermodynamic significance at high pH and at least an empirical significance at lower pH values.

Many of the characteristics of the active−inactive interconversion for *A. vinosum* [NiFe]-MBH are seen at a glance in Figure 29. The shapes of the voltammograms show that the rate and extent of inactivation depend on pH, temperature, and partial pressure of H_2. In general, the inactivation that is observed during the sweep toward positive potentials is much slower than the reactivation that is observed on the return sweep. For *A. vinosum* [NiFe]-MBH, this hysteresis is particularly evident at low pH and low temperature.

The values for E_{switch} marked in Figure 29A and B move to higher potential with decreasing pH or increasing temperature, and we return to this below. Panel C shows that decreasing the H_2 pressure 100-fold, from 1 to 0.01 bar at 25 °C, increases the rate of inactivation but hardly alters E_{switch} or the sharp nature of the reactivation peak. Dihydrogen thus impedes anaerobic inactivation, but it appears not to be involved in a rate-determining or potential-dependent step during reactivation. Studies at much lower H_2 pressures, comparable to physiological conditions, are highly desirable.

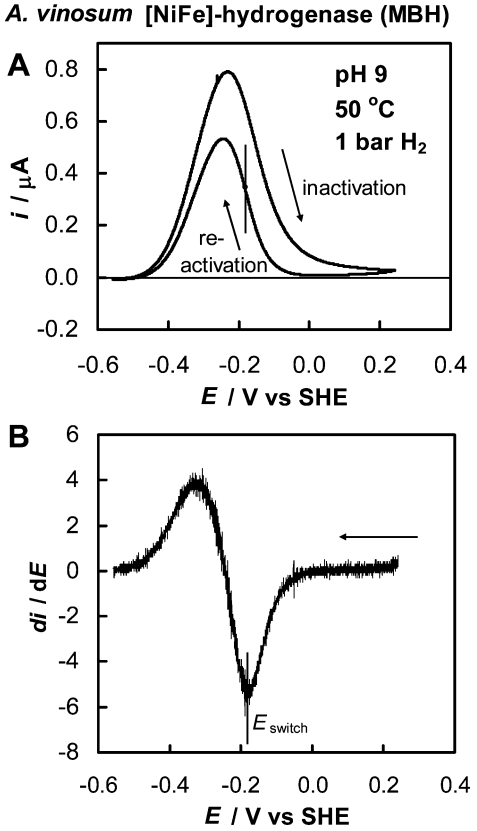

Figure 28. (A) Anaerobic inactivation and reactivation observed in a slow cyclic voltammogram (0.3 mV s^{-1}) for a PGE electrode modified with *A. vinosum* [NiFe]-MBH at pH 9, 50 °C, and 1 bar H_2. The electrode was rotated at 2500 rpm, so the decrease in current as the potential is scanned toward more positive values is due to reversible inactivation rather than substrate depletion. (B) Derivative plot (d*i*/d*E* vs *E*) for the reactivation sweep (toward more negative potentials) of the voltammogram shown in A, showing how E_{switch} is determined. Reprinted and adapted with permission from ref 92. Copyright 2003 American Chemical Society.

It has been reported that *Desulfovibrio gigas* [NiFe]-hydrogenase is not inactivated in the presence of H_2,[115] but this is clearly not the case for *A. vinosum* [NiFe]-MBH when studied by PFV. In fact, extensive studies show that anaerobic oxidative inactivation is a common feature of both the [NiFe]- and [FeFe]-hydrogenases, and further examples are shown in Figure 30. Conditions facilitating fast inactivation have been chosen in order to demonstrate the effect more clearly, but in all hydrogenases studied so far, reactivation is faster than inactivation. Values of E_{switch} for *Ralstonia eutropha* [NiFe]-MBH and *Desulfovibrio desulfuricans* [FeFe]-hydrogenase are 115 and 75 mV, respectively, compared with −95 and −110 mV for *A. vinosum* and *D. gigas* [NiFe]-hydrogenases (data not shown) under identical conditions: pH 6.0, 30 °C, and 1 bar H_2. Although the *R. eutropha* and *D. desulfuricans* enzymes inactivate faster, the high E_{switch} potentials confer a greater potential window for activity, bounded at low potential by the onset of H_2 oxidation (see section 5.6 and Figure 30C). Generalizations are still difficult: for the *D. desulfuricans* [FeFe]-hydrogenase, oxidative inactivation is faster at lower pH,[71] for *A. vinosum* [NiFe]-MBH, it is faster at high pH,[92] whereas, for the *D. gigas* [NiFe]-hydrogenase, there is little effect of pH

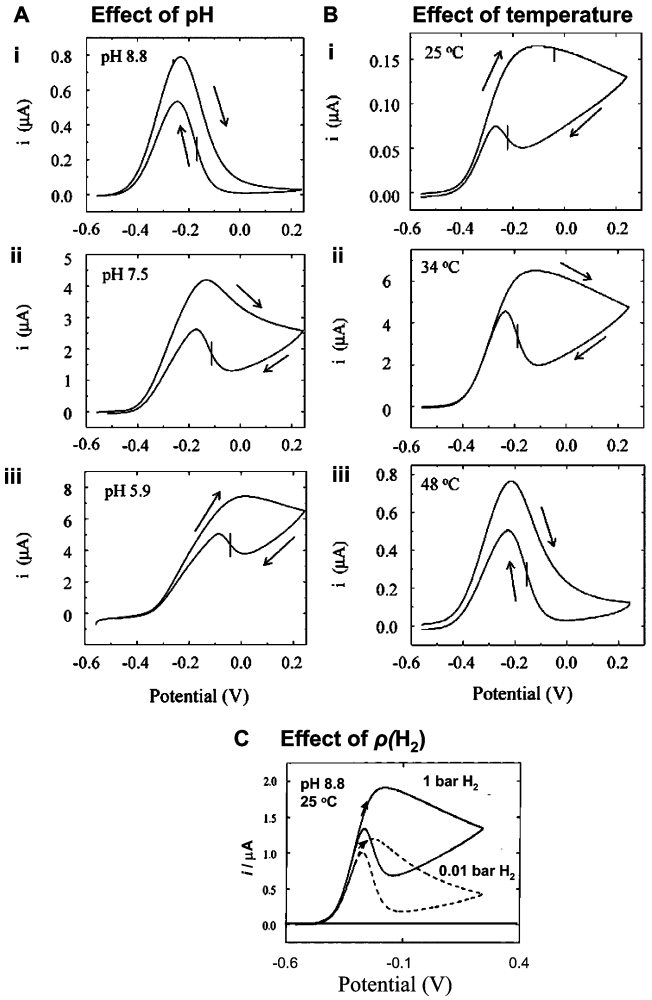

Figure 29. Cyclic voltammograms for a film of *A. vinosum* [NiFe]-MBH on a PGE electrode recorded at 0.3 mV s^{-1} to investigate anaerobic inactivation and reactivation. Arrows indicate the direction of the potential cycle. Voltammograms in A were all recorded at 45 °C and 1 bar H_2 and show the effect of varying pH as indicated. Voltammograms in B were all recorded at pH 8.8 and 1 bar H_2 and show how varying the temperature alters the waveform. The voltammogram recorded at 48 °C was for a film of much lower coverage, hence the low catalytic current. The vertical bar on each curve indicates the position of E_{switch} (see text). Both voltammograms in C were recorded at 25 °C and pH 8.8, and they show the effect of varying $\rho(H_2)$. In all cases, the electrode was rotated at 2500 rpm and potentials are quoted vs SHE. Reprinted and adapted with permission from ref 92. Copyright 2003 American Chemical Society.

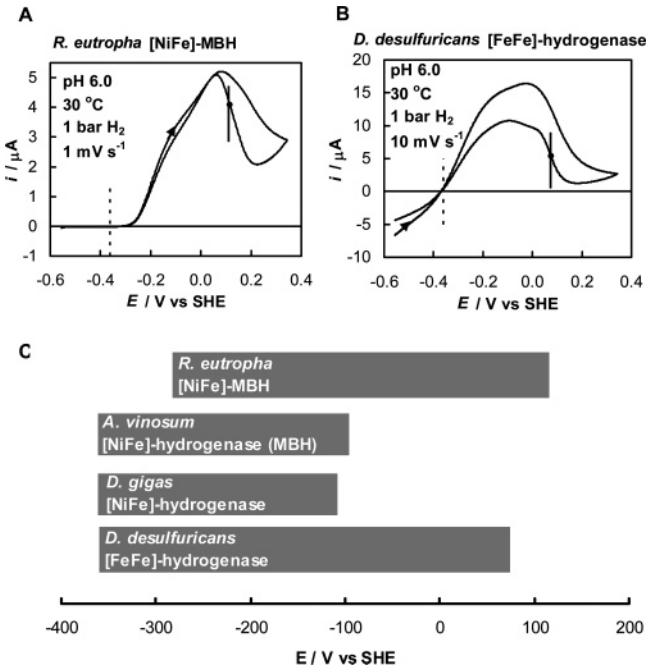

Figure 30. (A and B) Cyclic voltammograms showing anaerobic inactivation of *R. eutropha* [NiFe]-MBH (an O_2-tolerant hydrogenase; see later) and *D. desulfuricans* [FeFe]-hydrogenase under the conditions indicated. In each case, the enzyme is adsorbed directly on a PGE electrode that is rotated at 2500 rpm. The direction of scan is indicated by an arrowhead in each case, and E_{switch} is marked by a vertical line. Panel C shows the potential window for H_2-oxidation activity for four different hydrogenases, defined at low potential by the onset of H_2 oxidation and at high potential by E_{switch}. Reprinted and adapted with permission from ref 76. Copyright 2005 American Chemical Society.

on the rate.[12] Anaerobic interconversions appear to be reversible, although experiments are often plagued by film loss during the slow scans required to observe significant inactivation.

Figure 31 shows plots of E_{switch} against pH for *A. vinosum* [NiFe]-MBH and *D. desulfuricans* [FeFe]-hydrogenase, along with the corresponding "Pourbaix diagrams" that represent the potential and pH domains in an analogous manner to a phase diagram. The pH dependences are classical and show strongly coupled proton−electron transfer ($1H^+/e^-$); thus, it is most likely that the proton binds close to the electron.

In the Pourbaix diagrams, upper zones represent the conditions under which the enzyme is inactive, and vertical lines separate species differing in protonation state. The active states are not distinguished from one another, and all that is known for certain in each case is that the enzyme is *active*, so any of the active states depicted in the green boxes in Figure 6A (or more) are likely to be represented. The [NiFe]-MBH from *A. vinosum* shows a p*K* (7.6) in an active form: below pH 7.6 the activation process involves uptake of one proton per electron whereas above pH 7.6 there is no *net* transfer of protons. Taking into consideration the spectroscopic and X-ray data, this is consistent (see Figure 6A) with Ni-B binding a single OH^- ligand: reduction causes this ligand to be released in a rapid reaction that includes protonation at pH < 7.6.

The temperature dependence of E_{switch} gives the entropy of reaction ΔS, and ΔH can be calculated from $\Delta G = \Delta H - T\Delta S$. The ΔS and ΔH values are given in the footnote of Table 1, which compares various data pertaining to the transition between inactive and active states for different hydrogenases obtained by protein film voltammetry and values measured by spectroscopically monitored potentiometric titrations, although coincident data are limited. The large, positive entropies and enthalpies for the activation process are as expected if reductive activation involves removal of a tightly bound ligand.

Studies of the [FeFe]-hydrogenase from *D. desulfuricans* show (Figure 31) that the anaerobically oxidized enzyme exists in two pH-interconvertible inactive states (p*K* 5.9) and there is also evidence for a deprotonation in an active state ($pK_{red} = 8.9$).[71] There is a further complication in that the voltammogram (Figure 30) has an unusual shape in the H_2 oxidation region that could signal the presence of sample inhomogeneity,[76] but this remains to be clarified by spectroscopy. The Pourbaix diagram in Figure 31 shows that, below pH 5.9 and above pH 8.9, the activation process

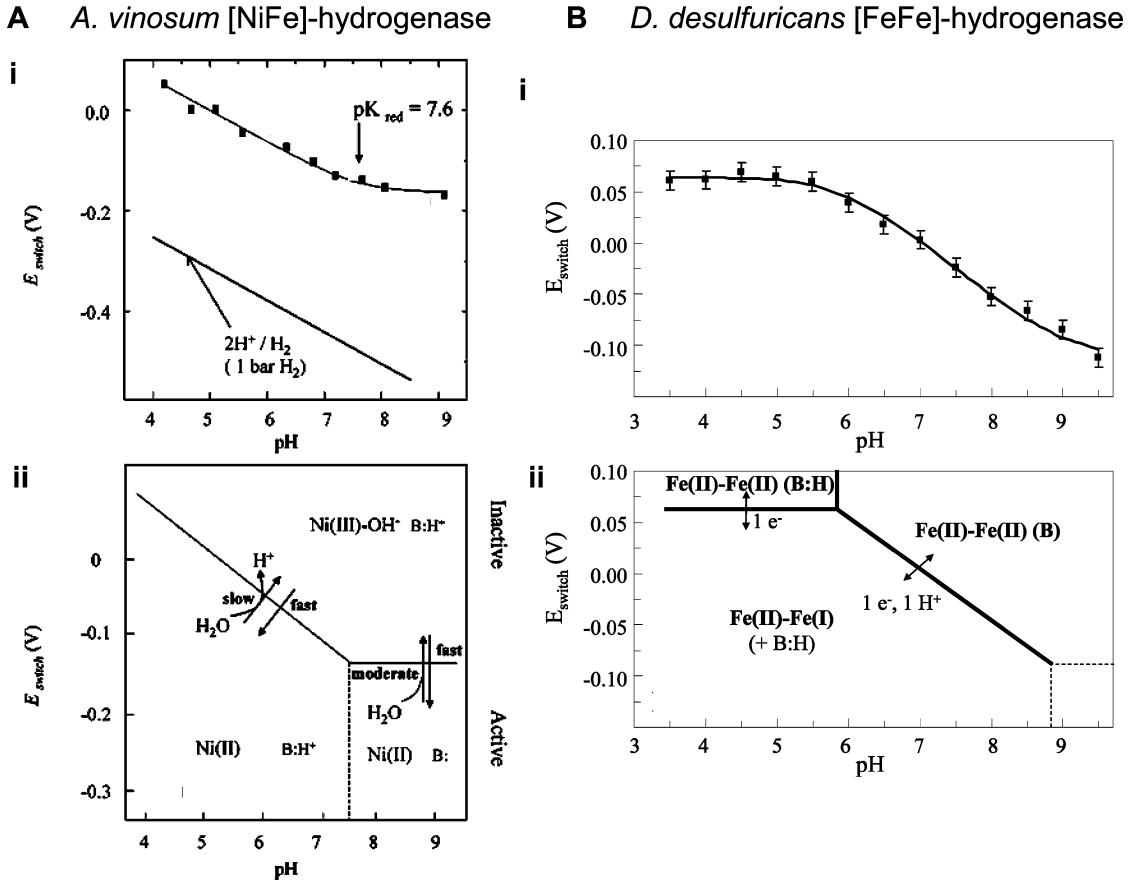

Figure 31. The pH dependence of E_{switch} associated with anaerobic inactivation for two hydrogenases. In each case, the panel marked (i) shows E_{switch} data obtained from slow cyclic voltammetry experiments for the enzyme-modified PGE electrode in solutions of different pH plus a fit to the experimental data based on transfer of $1H^+/1e^-$, while (ii) represents the corresponding Pourbaix diagram showing species and reactions that are consistent with these results. Panel A: Data for *A. vinosum* [NiFe]-MBH on a PGE electrode obtained from voltammograms recorded at 0.3 mV s^{-1} at 45 °C. The pH dependence of the H^+/H_2 couple at 1 bar H_2 is also shown. Reprinted with permission from ref 92. Copyright 2003 American Chemical Society. Panel B: Data for *D. desulfuricans* [FeFe]-hydogenase on a PGE electrode obtained from voltammograms recorded at 10 mV s^{-1} at 10 °C. Reprinted with permission from ref 71. Copyright 2006 American Chemical Society. Other conditions: 1 bar H_2, electrode rotation rate = 2500 rpm.

Table 1. Reduction Potentials for Activation of Anaerobically Oxidized Hydrogenases Obtained from PFV Experiments, and Corresponding Reduction Potentials for the Active Site as Measured by Spectroscopic Techniques

enzyme	E_{switch} (PFV)	rate of anaerobic inactivation (PFV, IR)	rate of activation after anaerobic inactivation (PFV, IR)	*E* (EPR)	*E* (IR)
D. gigas [NiFe]-hydrogenase	−110 mV (pH 6.0, 30 °C)[76]	slow[12,76]	fast[12,76]	−140 mV (pH 8.0)[116] −210 mV (pH 8.3)[115]	−150 mV (pH 8.0)[117]
A. vinosum [NiFe]-MBH[a]	−95 mV (pH 6.0, 30 °C)[76] −162 mV (pH > 7.6)[92]	slow[76,92]	fast[76,92]	−115 mV (pH 8.0)[118a]	
R. eutropha [NiFe]-MBH	+115 mV (pH 6.0, 30 °C)[76]	fast[76]	fast[76]		
D. desulfuricans [FeFe]-hydrogenase	69 mV (pH < 5.9, 10 °C); −50 mV (pH 8.0, 10 °C)[71] 75 mV (pH 6.0, 30 °C)[76]	fast[76]	fast[76]	−270 mV (pH 7.0)[119]	−75 mV (pH 7.0); −92 mV (pH 8.0)[120]

[a] The ΔS, ΔH (PFV) values for *A. vinosum* [NiFe]-MBH are as follows: 193 ± 39 J K^{-1} mol^{-1}, 78 ± 11 kJ mol^{-1} (pH 8.8); 261 ± 53 J K^{-1} mol^{-1}, 95 ± 15 kJ mol^{-1} (pH 7.5); 290 ± 48 J K^{-1} mol^{-1}, 96 ± 15 kJ mol^{-1} (pH 6.0) [92]

involves no net transfer of protons whereas, between pH 5.8 and 8.9, activation involves net transfer of one proton per electron.[71] The p*K* of 5.9 suggests that samples of oxidized inactive *D. desulfuricans* [FeFe]-hydrogenase prepared at pH values close to 6 should display heterogeneity. It is interesting to note that the structure of *Clostridium pasteurianum* [FeFe]-hydrogenase I, obtained at pH 5.1 by Peters and co-workers[121] and thought to be in the anaerobically oxidized state, H_{ox}^{inact},[122] should be predominantly in the acid form (assuming the *D. desulfuricans* [FeFe]-hydrogenase data are applicable to this enzyme). There are two obvious options for the protonation site: (1) the central atom X of the bridging ligand or (2) at a coordinated OH^-/H_2O (as suggested by the *C. pasteurianum* hydrogenase I crystal structure[121]). It may be that the anaerobic oxidized states should be regarded as "resting states" that are protected against the more aggressive actions of O_2 (see below). Albracht and co-workers have recently argued, on the basis of IR-monitored potentiometric titrations with *D. desulfuricans* [FeFe]-hydrogenase, that the conversion of H_{ox}^{inact} into

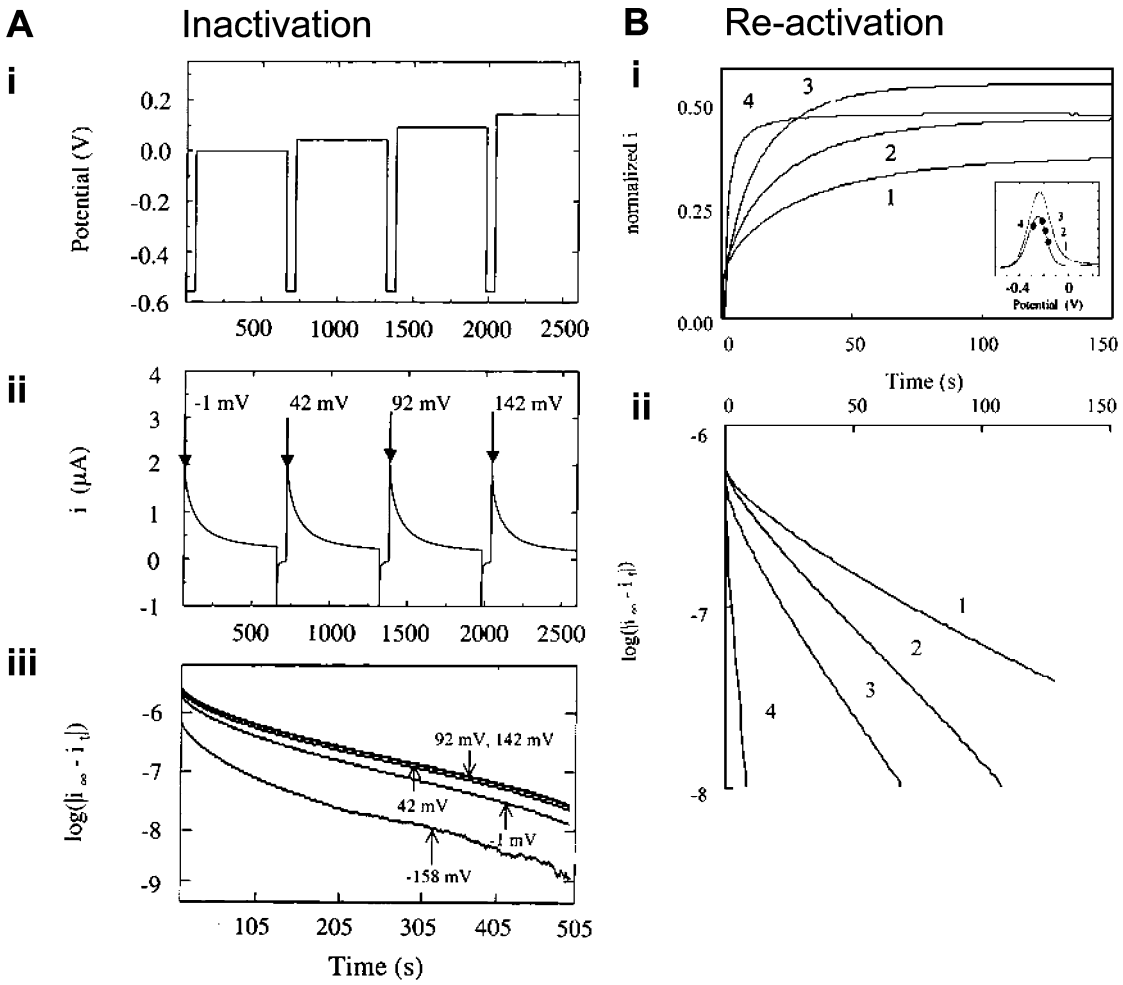

Figure 32. Potential-step kinetic experiments to measure rates of (A) inactivation and (B) reactivation of *A. vinosum* [NiFe]-MBH on a PGE electrode under 1 bar H_2. Panel A(i) shows the potential steps used to repeatedly inactivate and then reactivate the enzyme, using different oxidizing potentials in each case. The temperature is 45 °C, and the pH is 8.8. Panel A(ii) shows the resulting kinetic traces—the decreases in H_2 oxidation activity are triggered by each potential step. This trace is shown from time = 60 s after the commencement of the experiment. Panel A(iii) shows semilog plots of the oxidative inactivation traces and reveals how the kinetics are slow, complex, and independent of potential over a range of about 0.3 V. Panel B(i) shows the kinetics of reactivation following steps to the potentials indicated in the voltammogram shown in the inset. The temperature is 45 °C, and the pH is 8.8. Panel B(ii) shows the corresponding semilogarithmic plots, which reveal simple, first-order kinetics that vary greatly with potential (the fast phase in the first 10 s is due to electrode charging). Reprinted with permission from ref 92. Copyright 2003 American Chemical Society.

H_{ox} (see Figure 6B) requires three electrons:[120] they propose that a one-electron transfer (at −75 mV, pH 7.0; see Table 1) produces an intermediate H_{trans} that is converted to H_{ox} by a further two-electron transfer at much lower potential. The second reaction is not evident in the PFV experiments,[71] possibly due to the presence of H_2, which could immediately provide the two electrons that are required, so that H_{trans} is not detected.

6.2. Kinetics of Anaerobic Active/Inactive Interconversions

The kinetics of the inactivation and reactivation processes have been studied using potential-step experiments (chronoamperometry). As outlined earlier (see Figure 13), the current−time trace from a potential-step experiment provides a direct measurement of the reaction kinetics. A set of experiments carried out on *A. vinosum* [NiFe]-MBH at pH 8.8 is shown in Figure 32.[92] The high-temperature (45 °C) is employed to increase the rate of the reactions, particularly oxidative inactivation. Experiments at this temperature are possible because directly adsorbed films of *A. vinosum* [NiFe]-MBH with polymyxin coadsorbate are fairly stable, but PFV experiments above ambient temperature are not successful for some hydrogenases due to film instability.

In the experiments shown in Figure 32A, the electrode potential is stepped from a value at which the enzyme is fully active to a more positive value at which the enzyme inactivates.[92] Likewise, in Figure 32B, reductive activation is studied by stepping the electrode potential from a value at which the enzyme is inactive (Ni-B in Figure 6A) to a value that induces reactivation (a potential more negative than E_{switch}). The kinetics in each direction are obtained from the respective current−time traces, and because the catalytic activity of hydrogenases is usually very high, the traces have a very good signal-to-noise ratio. The results show that oxidative inactivation is slow, with rates that increase as the pH is increased but do not vary with potential. The inactivation is complex (the first-order plots show curvature) whereas reductive reactivation is fast and shows clean first-order kinetics, allowing a marked potential dependence on rates to be observed (although the faster reactions are lost in the electrode charging "dead time"; see section 4.1). In

Scheme 3. Reaction Sequence for Anaerobic Oxidative Inactivation and Reductive Reactivation of *A. vinosum* [NiFe]-MBH

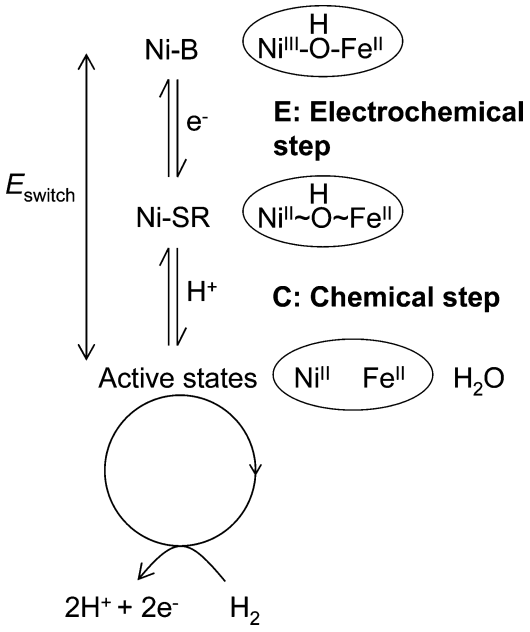

electrochemical terms, anaerobic oxidative inactivation is a "CE" process; that is, it requires a slow chemical step prior to electron loss, which traps the product as Ni(III), whereas reactivation is a faster EC process, in which removal of an electron is followed by a rapid chemical step, which is probably loss of the blocking oxygen ligand (Scheme 3).

The *D. desulfuricans* [FeFe]-hydrogenase has been studied briefly in the same way, and the main similarity with *A. vinosum* [NiFe]-MBH is that inactivation (which takes from tens of seconds to minutes, depending on pH and temperature) is also much slower than activation (which is complete within seconds and merged with the charging time of the graphite electrode).[71,76] But in contrast to *A. vinosum* [NiFe]-MBH, inactivation is faster at lower pH (<pH 6). It may indeed be the case that anaerobic interconversions between active and inactive states of hydrogenases are faster when the reaction does not involve net transfer of a proton (or OH^-).

7. Reactions of Hydrogenases with Small Neutral Molecules

7.1. O_2—Inhibitor and/or Substrate?

7.1.1. O_2-Sensitive [NiFe]-hydrogenases

As shown in Figure 6A, [NiFe]-hydrogenases react with O_2 to give at least two distinct inactive species, known as Ni-A (Unready) and Ni-B (Ready).[123] Most of the information on these reactions stems from spectroscopic (IR and EPR), X-ray structural, and electrochemical studies of the [NiFe]-MBH from *A. vinosum* and the similar, soluble periplasmic [NiFe]-hydrogenases from *Desulfovibrio*.[2]

Protein film voltammetry experiments to investigate the reactions of hydrogenases with O_2 involve injection of an aliquot of O_2-saturated buffer into the cell solution, while the potential of the electrode, modified with a film of the hydrogenase, is scanned or kept at a constant potential. Usually, O_2 is added during electrocatalysis of H_2 oxidation, so that the effect is observed immediately as a decrease in catalytic current. An experiment carried out with *A. vinosum* [NiFe]-MBH is shown in Figure 33. To avoid its direct reduction at the electrode, the aliquot of O_2 is added when the electrode potential is just above 0 V (Figure 33A): this action results in immediate loss of activity, following which the cell is flushed with H_2 to remove the O_2 while the potential cycle is continued. Even when the O_2 has been removed completely, there is no recovery of activity as long as the electrode potential remains above about 0 V, but below 0 V, the current increases as activity is restored. A very slow scan toward more negative potentials after introduction of O_2 at +242 mV (Figure 33B) indicates −70 mV as the E_{switch} potential associated with reductive activation, a value that is very close to E_{switch} determined for reactivation after anaerobic oxidative inactivation.

To elucidate further details of this reaction, experiments have been carried out in which O_2 additions are made at fixed potentials and reactions are induced by potential steps. In the experiment shown in Figure 34A, an aliquot of O_2-saturated buffer is injected to inactivate *A. vinosum* [NiFe]-MBH that is oxidizing H_2 at 1 bar and a high potential (242 mV). After flushing out O_2, reductive activation is monitored following a potential step (to −108 mV), and this reaction

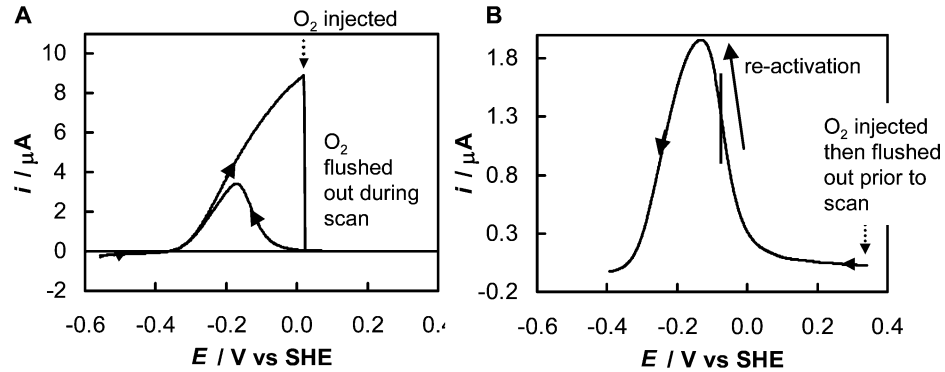

Figure 33. Effect of O_2 on *A. vinosum* [NiFe]-MBH adsorbed on a rotating PGE electrode. (A) Cyclic voltammogram recorded at 1 mV s^{-1}, showing that an injection of O_2-saturated buffer at ca. +50 mV on the forward scan (injection indicated by a dotted arrow) causes complete and rapid loss of activity. (B) The "switch" potential associated with reductive reactivation on the return scan (after O_2 has been flushed out of the solution) is determined from a very slow scan (0.1 mV s^{-1}) and is indicated by a vertical line. Other conditions: 1 bar H_2, pH 6, 30 °C, electrode rotation rate = 2500 rpm. Reprinted and adapted with permission from ref 76. Copyright 2005 American Chemical Society.

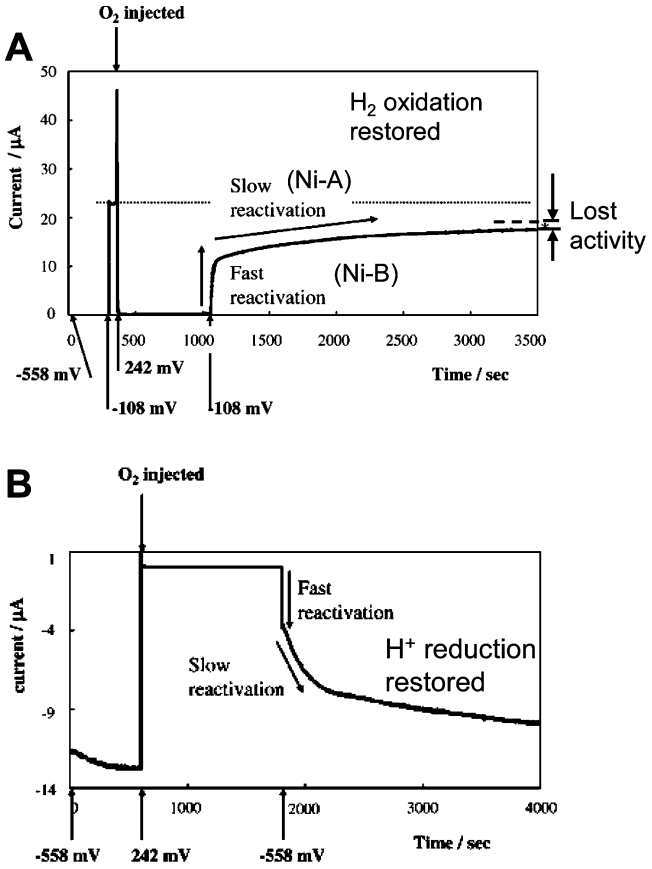

Figure 34. Current vs time traces for potential-step experiments monitoring recovery of H_2 oxidation or H^+ reduction activities for *A. vinosum* [NiFe]-MBH on a PGE electrode after inactivation by O_2. Panel A: The film of hydrogenase is subjected to a sequence of potential steps under 1 bar H_2. The potential was initially held at −558 mV for 300 s to fully activate the enzyme before a step to −108 mV for 60 s to check the initial activity at this potential. A step was then made to 242 mV (a potential at which O_2 is not reduced at the bare electrode), and 0.10 mL of O_2-saturated buffer was injected. The headspace was then flushed with H_2 for 600 s to remove O_2 from the solution, and the potential was then stepped back to −108 mV to initiate reductive activation. The dashed line shows the level to which the current returned in a control experiment involving the same potential step sequence carried out under anaerobic conditions (to account for film loss). The small difference (un-recovered activity, indicating "dead" enzyme) is indicated by a solid arrow. Panel B: A similar experiment under 1 bar N_2, in which the film of hydrogenase is again exposed to O_2 at high potential (242 mV) but recovery of activity (after flushing out O_2) is now monitored at a low potential (−558 mV) at which the hydrogenase is able to catalyze H^+ reduction. In both cases, the other experimental conditions were as follows: pH 6.0, 45 °C, electrode rotation rate = 2500 rpm. Reprinted with permission from ref 123. Copyright 2004 American Chemical Society.

proceeds in two phases. The first phase is over in a few seconds, but the second phase shows clean first-order kinetics with a half-life of about 5 min (280 s at 45 °C). The clear distinction in rates suggests that these phases correlate with activation of Ready (Ni-B) and Unready (Ni-A) states, respectively, as depicted in Figure 6A.[8,123] Although both states result in diminished catalytic current and therefore similarly appear as "inactive" in electrochemical measurements, they can be distinguished on the basis of their reactivation kinetics. Film loss from the electrode gives rise to a gradual loss of current during such long experiments, but this is taken into account when the final current level is compared to that attained when the same potential step sequence is carried out under anaerobic conditions (dashed line at 3200−3500 s in Figure 34A). It is thus evident that a fraction of the enzyme activity (indicated by an asterisk) fails to recover from exposure to O_2. We refer to this fraction of the enzyme as "dead" in Figure 6A, and it may reflect permanent damage by O_2 resulting from oxidation of Cys sulfur atoms in the active site region.[43,124] The reactivation process can also be studied by monitoring H^+ reduction at low potentials. In Figure 34B, the enzyme is reactivated at −558 mV under N_2 after exposure to O_2 at 242 mV. Two phases are again clearly evident in the (negative) current response as the activity toward H^+ reduction recovers, and there is also evidence of a third phase.

The experiments shown in Figure 35 were designed to establish conditions that favor formation of either Ni-A or Ni-B in *A. vinosum* [NiFe]-MBH, and they illustrate, once again, the importance of potential control. First (panel A), the effect of pH was investigated, using two sequences similar to those employed in Figure 34A, during which O_2 is injected while the electrode potential is held at 242 mV. The reactivation traces show that reaction with O_2 at higher pH (pH 8.8) results in a greater fraction of fast phase and "dead" enzyme than reaction at pH 7.0. Measurements could also be carried out to investigate the effect of injecting O_2 under a N_2 atmosphere, although, in this case, there is no H_2 oxidation current and the rapid inactivation by O_2 is not detected. The results shown in Figure 35B show that the fraction of slow phase (Ni-A) relative to fast phase (Ni-B) increases when O_2 is injected under N_2 instead of H_2 and when the electrode potential is increased.

The interpretation of these results is summarized in Scheme 4. If a molecule of O_2 enounters an active site that is furnished with an abundant supply of electrons in the presence of H_2, it is quickly reduced by four electrons (including one from the Ni^{II}) to give two molecules of water, one of which may remain trapped as the OH^- ligand that is found in Ni-B. On the other hand, when few electrons are available and H_2 is absent, the O_2 molecule is not fully reduced and reactive oxygen species ([O]) such as peroxide or a modified sulfur are trapped or retained in the active site. In connection with this study, Fontecilla-Camps and co-workers refined a structure of *D. gigas* hydrogenase in the Ni-A state and concluded that the bridging group was not a single atom, as observed for Ni-B, but had elongated electron density indicative of a diatomic ligand, which might be a peroxide.[39] The presence of a hydroperoxide (HO_2^-) in Ni-A could explain the observation that the value of E_{switch} observed when the enzyme has been inactivated with O_2 is very close to that observed for anaerobically inactivated samples that contain only Ni-B, with the argument being that HO_2^- and HO^- should exert similar electrostatic influences.

Léger and co-workers studied the electrochemical kinetics of the reaction of *Desulfovibrio fructosovorans* [NiFe]-hydrogenase with O_2.[66] The rates of inactivation were measured by recording the decrease in H_2 oxidation current following injection of O_2 shortly after stepping the electrode potential to a sufficiently high potential (190 mV) to avoid direct reduction of O_2 at the electrode. The experiments were carried out at 40 °C, over the pH range 5−7.8. An open cell was used, and after injection, the O_2 was flushed from the solution by a stream of H_2. The results were analyzed by considering that the rate of loss of H_2 oxidation activity depends on two processes. One is the O_2-independent

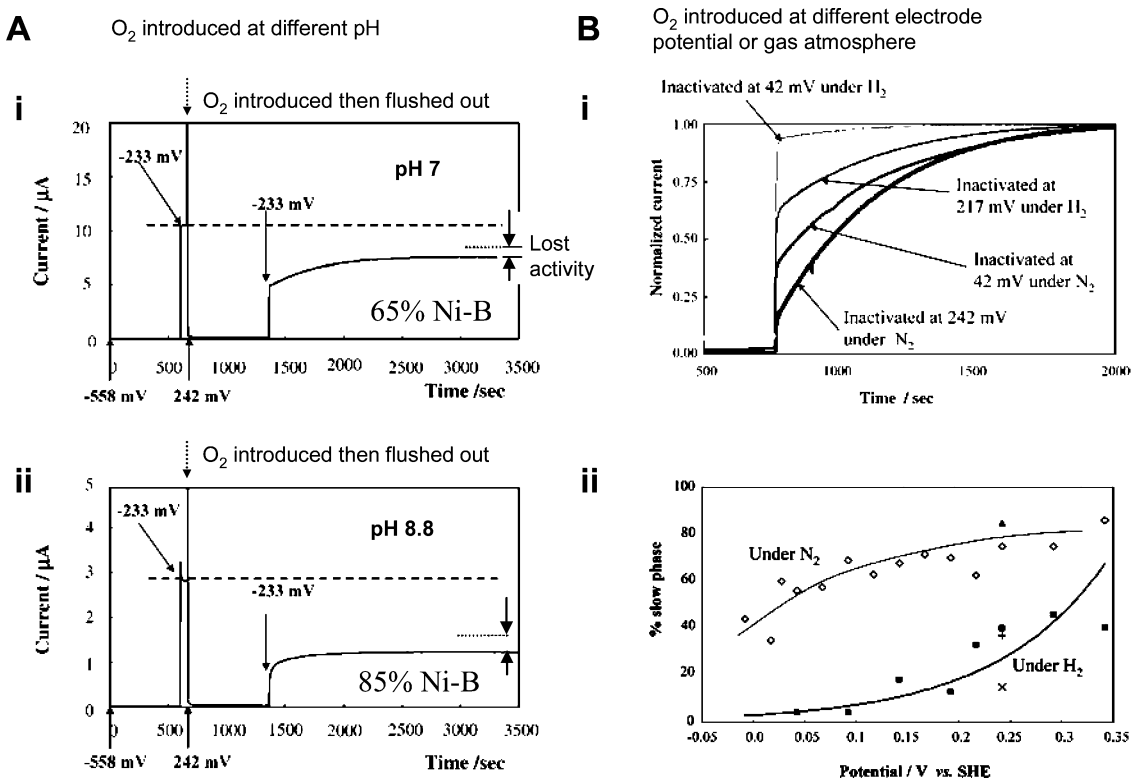

Figure 35. Experiments with *A. vinosum* [NiFe]-MBH on a PGE electrode, designed to examine the effect of pH, gas atmosphere, and electrode potential on the products of reaction with O_2. Panel A: the effect of pH. In each case the potential was initially held at −558 mV to fully activate the enzyme for 600 s before being stepped to −233 mV for 60 s (this reports on the initial activity at this potential prior to O_2-exposure). The potential was then stepped to 242 mV, and 250 μL of O_2-saturated buffer was injected into the cell solution (indicated by dotted arrow). H_2 (1 bar) was immediately flushed through the headspace for 600 s to remove O_2 before the potential was stepped back to −233 mV to initiate reactivation. The horizontal dotted lines indicate the amount of film recovery achieved in control experiments carried out without introducing O_2, and the solid arrows indicate unrecovered activity (dead enzyme) following O_2 inactivation. Panel B: the effect of electrode potential and gas atmosphere. Plot i shows reactivation after addition of O_2 under a variety of potential and gas atmosphere conditions as indicated. In each case the reactivation is monitored at 1 bar H_2, pH 6.0, −158 mV. Plot ii summarizes the results for a number of these experiments, showing the percentage of "slow phase" observed in the reactivation following O_2-exposure under different conditions. Other experimental conditions: 45 °C, electrode rotation rate 2500 rpm. Reprinted and adapted with permission from ref 125. Copyright 2005 American Chemical Society.

Scheme 4. Summary of Limiting Cases for the Reactions of Active [NiFe]-hydrogenase with O_2. Reprinted and Adapted with Permission from Ref 125. Copyright 2005 American Chemical Society

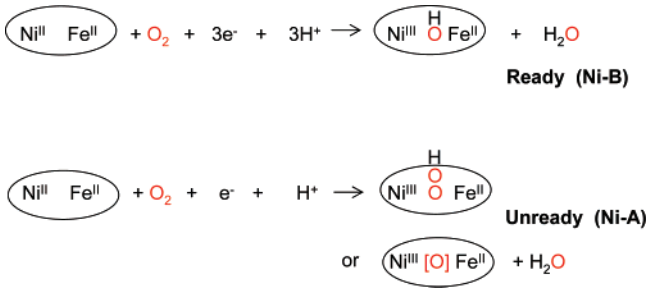

anaerobic conversion of active enzyme to Ni-B (a first-order process, rate constant k_b, was assumed) and an O_2-dependent process having a rate constant $k_a C_{O_2}(t)$, where $C_{O_2}(t)$ is the concentration at time t as O_2 is flushed from the cell. This experiment could be repeated many times, simply by stepping the potential back to −560 mV to reactivate the enzyme when the reaction is complete. About 50% of the activity was lost each time, but much of this was regained when the reductive poise was extended for longer times. This is consistent with formation of both Ni-B and Ni-A, as just discussed, in addition to some permanent loss of activity due to film loss or formation of "dead" enzyme. The kinetics were analyzed using eq 15,

$$\frac{d(\ln i)}{dt} = -(k_b + k_a)C_{O_2}(0)\exp(t/\tau) \qquad (15)$$

where $d(\ln i)/dt$ is the rate of inactivation by O_2, which depends upon the concentration of O_2 at time t, as it is flushed out of the cell with time constant τ. Results are shown in Figure 36, in which the top panels show the traces obtained at 1 bar H_2 and 0.1 bar H_2, and the lower traces show the respective logarithmic transforms with fits to eq 15. Note that film loss has occurred between experiments and the initial current magnitude is therefore different in each case, but this does not affect the kinetics of reaction with O_2. Attack by O_2 is partly competitive with H_2 (lowering the pressure from 1 to 0.1 bar only results in a 3-fold increase in rate of reaction with O_2). The rate constants obtained at pH 7 and 40 °C were 38 s^{-1} (bar O_2)$^{-1}$ at 1 bar H_2 and 105 s^{-1} (bar O_2)$^{-1}$ at 0.1 bar. Thus, H_2 affords only partial protection against O_2, suggesting perhaps that the two gas molecules favor different oxidation levels of the active site. Further experiments showed, however, that the kinetics of O_2 inactivation are independent of potential over a wide range (40−500 mV at pH 7) and independent of pH (5−7.8). Again, data at very low levels of H_2, closer to physiological

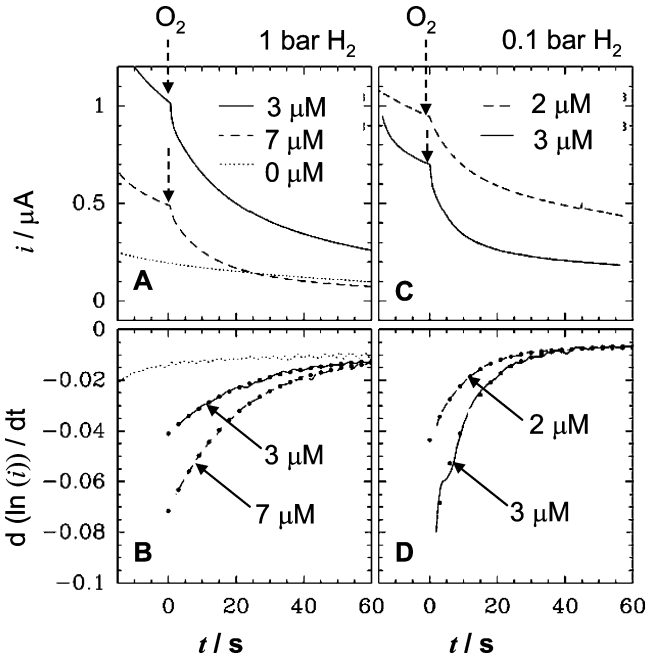

Figure 36. Decreases in the rates (catalytic currents) for H_2 oxidation by *D. fructosovorans* [NiFe]-hydrogenase after injection of small aliquots of O_2-saturated buffer (at time, $t = 0$). Approximate initial concentrations of O_2 in the cell solution after each injection are indicated. Panel A: 1 bar H_2, time constant for flushing out O_2 from the cell, $\tau = 24$ s. Panel C: 0.1 bar H_2, $\tau = 10$ s. Panels B and D show corresponding plots of d(ln *i*)/d*t* at 1 bar H_2 and 0.1 bar H_2, respectively, against time and fits to eq 15 (•). Reprinted and adapted with permission from ref 66. Copyright 2004 American Chemical Society.

levels, would be useful to show how the enzyme might cope with O_2 in nature.

The mechanism of reactivation of Unready [NiFe]-hydrogenase (Ni-A) was investigated using a sequence of potential step experiments and gas injections, Figure 37.[125] First, a maximum amount of Ni-A was generated on the PGE electrode by poising the electrode potential at high potential under N_2 and then injecting O_2; the head gas was then changed to H_2, and after allowing all the O_2 to be flushed out, the enzyme was reactivated by a potential step. Experiments were carried out using a range of reactivation potentials, and the rate constant was measured in each case. Figure 37A shows that stepping to lower potentials increases the rate of reactivation until it reaches a maximum value (there is no difference between rates measured at −209 and −158 mV).

In each case, the rate constant was determined from a semilogarithmic plot of $\log(i_{max} - i_t)$ vs t. The results for two pH values, 6.0 and 6.8, are summarized in Figure 37B. The role of H_2 in the reactivation process was investigated in experiments in which the reactivation step potential was applied to enzyme under N_2 instead of H_2 (not shown).[125] The same period of incubation is employed in each case before switching the head gas to H_2 to measure the activity recovered. Far less enzyme was activated in the N_2 phase than expected. Importantly, under N_2, a potential step *back* to the initial potential even reversed the process of activation (data not shown). It was proposed that three distinct steps are involved—a rapid redox pre-equilibrium in which an electron is added; a slow, rate-determining (and reversible) step that alters or repositions the [O]-species without releasing it (thus implicating multiple forms); and a final

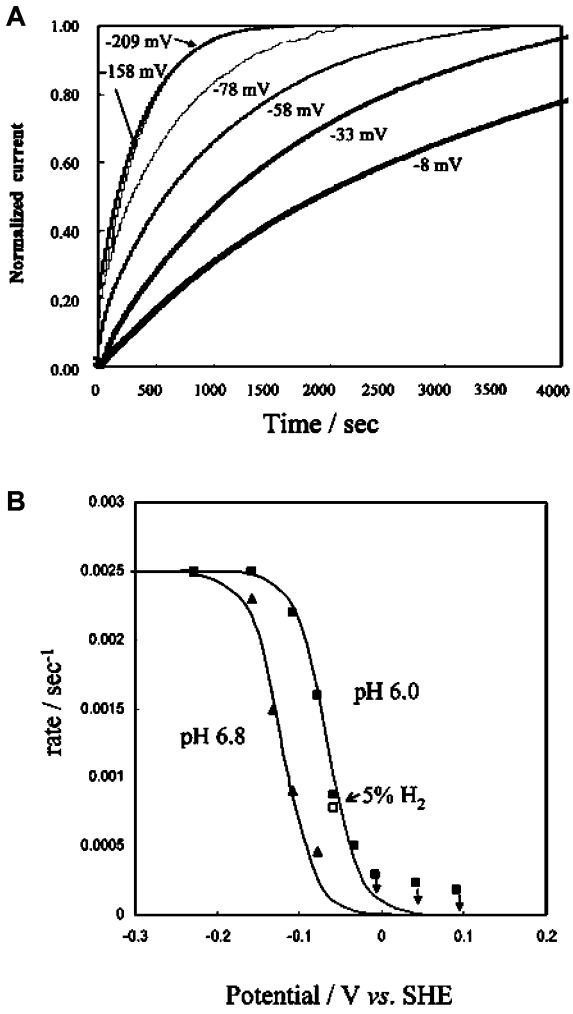

Figure 37. (A) Activation of the Unready (Ni-A) state of *A. vinosum* [NiFe]-MBH on a PGE electrode under 1 bar H_2 initiated by stepping the electrode potential down to different values. After incubating under N_2 and then injecting O_2 at 242 mV, H_2 was used to flush out the remaining O_2 for 600 s before the potential was stepped to various reducing potentials (−8, −33, −58, −78, and −158 mV), and the increase in activity was monitored. Other experimental conditions include the following: pH 6.0, 45 °C, and electrode rotation rate = 2500 rpm. B: Dependence of the rate of activation of Unready (Ni-A) enzyme on electrode potential and pH, measured at 45 °C. Data are derived from experiments shown in part A and others carried out at pH 6.8. Apart from the datum point indicated by an arrow (open square), all experiments were carried out under 1 bar H_2. Lines represent fits using eq 17A. Reprinted with permission from ref 125. Copyright 2005 American Chemical Society.

stage, requiring H_2, that commits the entire sequence to produce active enzyme. In the language of electrochemical kinetics, this is an "$EC_{rev}C_{irrev}$" sequence.

These stages are written

$$\underset{\mathbf{E}}{O} \underset{k_{-1}}{\overset{k_1}{\rightleftharpoons}} \underset{\mathbf{C_{rev}}}{R} \underset{k_{-2}}{\overset{k_2}{\rightleftharpoons}} \underset{\mathbf{C_{irrev}}}{P} \xrightarrow{k_3} \text{active enzyme} \qquad (16)$$

for which the steady-state equation is

$$\text{rate} = \frac{K_1 k_2 k_3}{K_1(k_{-2} + k_3 + k_2) + k_{-2} + k_3 + (k_2 k_3 / k_{-1})} \qquad (17)$$

where $K_1 = k_1/k_{-1}$. Because the first stage is a rapid electrochemical equilibrium, the rate equation can be expressed to include the potential dependence.

$$\text{rate} = \frac{k_2 k_3 \exp\{nF(E^\circ - E)/RT\}}{k_{-2} + k_3 + (k_2 k_3/k_{-1}) + \exp\{nF(E^\circ - E)/RT\}(k_{-2} + k_3 + k_2)} \quad (17A)$$

The role of H_2 in activating Ni-A is to render the reductively activated transformation *irreversible*, although exactly how this occurs remains unresolved. Support for this proposal was obtained in experiments in which reduction of Ni-A was carried out under CO. In this case, all that was required was to replace CO by H_2 and the enzyme reactivated as soon as the gas exchange occurred (data not shown). Thus, like H_2, CO also acts by rendering the reductive transformation irreversible, and this suggests that the final stage is a displacement process. There is ample evidence that exogenous CO binds to the Ni atom,[70] but in order to do this, any ligand that remains close to the Ni would probably be moved. In this way, we might envisage the final departure of the [O]-species, perhaps as a peroxide. In terms of the interconversions shown in Figure 6A, species R, the product of the fast and reversible electron-transfer step should correspond to species Ni-SU, but the subsequent slow step does not produce Ni-SI because a step to high potential regenerates Ni-A not Ni-B. Thus species P, which "remembers" that it originated from Ni-A and presumably still carries the inhibitory group (as mentioned earlier, this is likely to be a peroxide), is not defined in Figure 6A but can only proceed to active enzyme by adding H_2 (or CO).

7.1.2. O_2-Tolerant [NiFe]-hydrogenases?

In the hydrogenase literature, an enzyme that retains catalytic activity (assayed under *anaerobic* conditions) after a period of exposure to O_2 is frequently deemed "O_2-tolerant"; see, for example, refs 67, 126, and 127 (see "wireless H_2", section 8.2). Measurement of activity under aerobic conditions is difficult, since conventional assays rely upon reduced mediators either to supply electrons for H^+ reduction or to activate hydrogenases prior to H_2 oxidation, and these reductants are readily oxidized by O_2. Maness and co-workers recognized the importance of characterizing hydrogenase activity *in air* rather than *following exposure to air*, and they measured an H/D exchange rate for partially purified *Rubrivivax gelatinosus* hydrogenase in D_2O under mixtures of H_2 and air.[127] Protein film voltammetry provides a simple and direct means of measuring H_2 oxidation activity under *aerobic* conditions and of precisely defining the bounds of tolerance to O_2.[76,128] Measurement of H^+ reduction activity in air is not so straightforward: O_2 is reduced directly at bare regions of a graphite electrode at the low potentials required for H^+ reduction, giving rise to a large negative current that masks enzyme activity.

Figure 38A−C shows the effect of increasing O_2 partial pressure, $\rho(O_2)$, on the activity of three [NiFe]-hydrogenases.[128] These experiments were carried out at pH 5.6, 30 °C, and 142 mV, and no direct O_2 reduction at bare regions of the graphite working electrode is observed at this potential. Just 5 mbar O_2 is sufficient to completely remove the activity of the *A. vinosum* enzyme (Figure 38A). Karyakin and co-workers reported that a carbon fiber electrode modified with *Thiocapsa roseopersicina* [NiFe]-hydrogenase retains >90% of the activity observed under 0.82 bar H_2 in argon at the same level of H_2 in air.[81] This result is surprising given the sequence similarity of this enzyme to *A. vinosum* MBH (82% identity for the large subunits based on ClustalW alignment).[129,130] This result hints at how O_2 tolerance may be determined by extremely subtle structural factors.

The *Ralstonia* enzymes studied in Figure 38B and C are derived from Knallgas bacteria, facultative aerobes that are specialized in exploiting traces of H_2 that escape into O_2-rich soil or aquatic environments as discussed in section 1. Films of these hydrogenases are less stable on the electrode than those of the robust *A. vinosum* [NiFe]-MBH, but because film loss is reasonably consistent between experiments for a given enzyme sample, it is still possible to obtain valuable information on their reactivities with small molecules by performing control experiments solely under H_2. Introduction of 5 mbar O_2 leads to only a small drop in activity of *Ralstonia* enzymes: at ambient levels of O_2 (ca. 200 mbar), *R. eutropha* [NiFe]-MBH retains ca. 20% of the activity measured under anaerobic conditions, and better still, *R. metallidurans* CH34 [NiFe]-MBH retains at least 40% activity. The differences in O_2 tolerance between the highly similar *Ralstonia* [NiFe]-MBH enzymes (large subunit sequence identity 81% based on ClustalW alignment) must reflect subtle electronic or structural changes. Further, *R. eutropha* MBH shows the same pattern of dominant active site IR (CO) and (CN) bands as the [NiFe]-hydrogenases from *D. gigas* and *A. vinosum*, indicating that the active site coordination is similar in all cases.[128]

When O_2 is flushed out of the cell, the activity of the *Ralstonia* hydrogenases recovers rapidly and completely (taking into account some film loss that has occurred during the course of the experiment in each case). There is no evidence here for formation of a fraction of "dead" enzyme upon exposure to O_2 as occurs for the *A. vinosum* [NiFe]-MBH (section 7.1.1). In all of these experiments, the H_2 content is high (close to 1 bar, orders of magnitude above K_M), and further experiments at physiologically relevant levels of H_2 and O_2 are needed to determine the responses of hydrogenases to air under the low levels of H_2 that are experienced *in vivo*. In the fuel cell experiments discussed in section 8.2, we explore further what it means for a hydrogenase to actually *function* in air at low levels of H_2.

Figure 38D shows the potential dependence of reactivation of *R. eutropha* MBH under 1 bar H_2 following rapid inactivation by O_2 at high potential and subsequent removal of O_2 from the cell.[128] The rate of recovery clearly increases at more negative potentials, suggesting that O_2 binds at a redox center in the protein, rather than simply plugging a gas channel and blocking H_2 access to the active site. Having defined O_2-tolerance in terms of the ability to *function* in air, there remains the question of how this tolerance is provided. It is first of all unlikely that attack on FeS clusters would allow catalytic activity to be maintained for any length of time because O_2 damage to FeS clusters is not easily reversible.[131−133] The other target for attack is the active site, and we envisage two limiting cases: (a) that O_2 is prevented from reacting with the active site, either because it cannot approach or because it cannot bind, and (b) that it reacts at the active site to produce harmless products that escape rapidly. The latter situation is equivalent to formation of a state that reactivates on a time scale that is comparable with fast turnover. This issue is raised again in

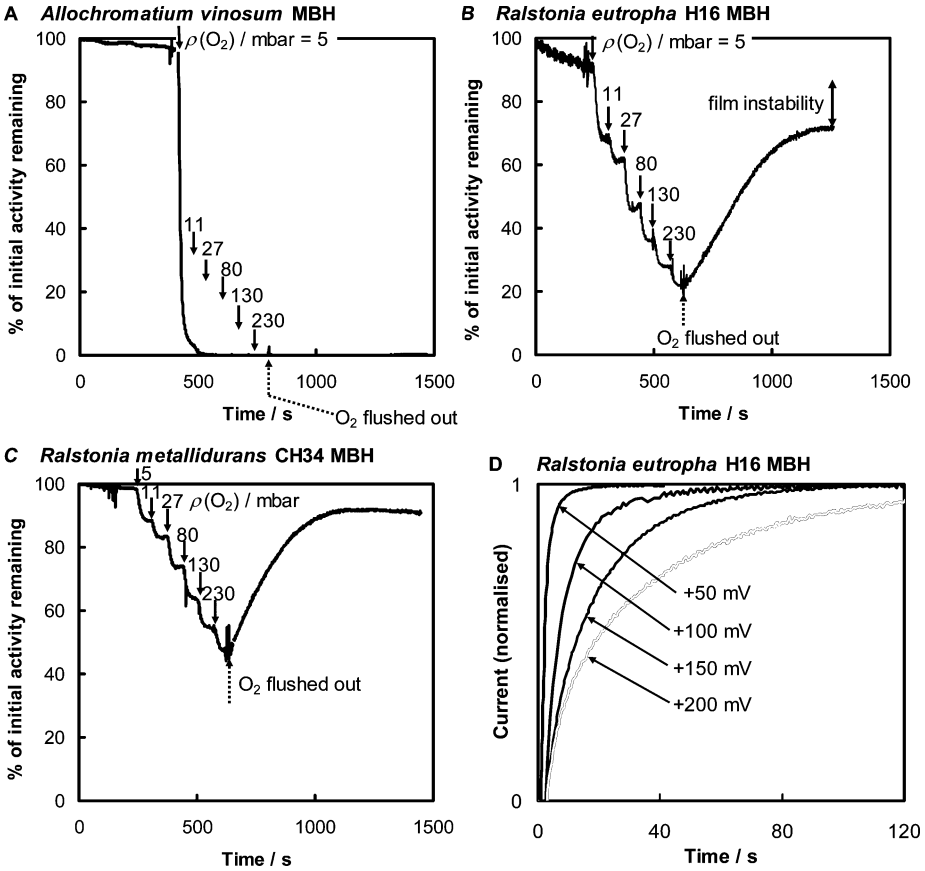

Figure 38. (A−C) Effect of stepwise additions of O_2 on the H_2 oxidation activity for a PGE electrode poised at +142 mV and modified with (A) *A. vinosum* [NiFe]-MBH, (B) *R. eutropha* H16 [NiFe]-MBH, and (C) *R. metallidurans* CH34 [NiFe]-MBH. In each case the electrochemical cell was initially flushed with H_2. At the time indicated, O_2 gas was injected into the headspace of the cell to give $\rho(O_2)$ = 5 mbar, and further injections of O_2 were made as shown. At the points indicated by the dotted arrow, H_2 was flushed through the cell to remove O_2, restoring anaerobic conditions. (D) Chronoamperometry experiments designed to measure the rate of recovery of the *R. eutropha* [NiFe]-MBH at different potentials under an anaerobic H_2 atmosphere after inactivation by O_2 at a high potential (+342 mV). Other conditions: pH 5.6, 30 °C, electrode rotation rate = 2,000 rpm. Panels A, B, and D are reprinted with permission from ref 128. Copyright 2005 National Academy of Sciences, U.S.A. Panel C: K. A. Vincent, J. A. Cracknell, M. Ludwig, O. Lenz, B. Friedrich, F. A. Armstrong, Unpublished data.

section 7.2.1, where we describe the interesting result obtained when CO is introduced.

7.1.3. [FeFe]-hydrogenases: Inactive States Protect against O_2 Damage

The [FeFe]-hydrogenases from *Megasphaera elsdenii* and *Clostridium pasteurianum* are purified under strictly anaerobic conditions and are very sensitive to O_2.[134] The enzymes from *Desulfovibrio vulgaris* and *D. desulfuricans* can be purified aerobically in an inactive form known as H_{ox}^{inact} (Figure 6B).[135,136] The inactive enzyme is activated by reduction (analogous to Ni-A and Ni-B for the [NiFe]-hydrogenases), and once activated, it is susceptible to irreversible O_2 damage. From early work on the *D. vulgaris* enzyme, it was thought that after reductive activation it was not possible to regenerate the O_2-stable oxidized state, but van Dijk et al. used the high-potential oxidant 2,6-dichlorophenol-indophenol (DCIP, E_{m7} = 217 mV[8]) to convert the enzyme anaerobically back to H_{ox}^{inact}.[137] This observation suggested that anaerobic inactivation protects the active site against destruction by O_2.

Figure 39 shows how PFV can be used to test the protective effect of anaerobic inactivation. In the cyclic voltammograms for *D. desulfuricans* [FeFe]-hydrogenase on a PGE electrode shown in panel A, O_2 is injected at different electrode potentials in order to compare its effect on enzyme that has been inactivated anaerobically as opposed to enzyme that is almost fully active. As discussed in section 6.1 and compared in Table 1 the "switch" potential for anaerobic inactivation of *D. desulfuricans* [FeFe]-hydrogenase is 75 mV (pH 6, 30 °C, 1 bar H_2), and so the enzyme is almost fully active at 42 mV prior to injection of O_2 (red line). In contrast, a substantial portion of the sample has already converted to the oxidized, inactive form when O_2 is injected at 242 mV (blue line). In each case, the electrode was poised at the vertex potential, 342 mV, for 300 s to allow complete removal of O_2 from solution. For comparison, an anaerobic cycle recorded under the same conditions is also shown (green line). The current drops essentially to zero upon injection of O_2 at 42 mV, and almost no recovery of activity is observed on the return scan (red line). When O_2 is injected at 242 mV, the current drops quickly to zero, but some reductive reactivation is now observed on the return scan (blue line) although there is still less recovery than observed in the anaerobic experiment (green line). (Note that, even in the anaerobic case, the current decreases during the voltammogram due to the instability of hydrogenase on the electrode.) These experiments lend strong support to the proposal that an [FeFe]-hydrogenase that has been oxidized anaerobically (in this case subjected to a weakly oxidizing electrode potential) is protected against damage by O_2. The high switch potential associated with H_{ox}^{inact} means that a

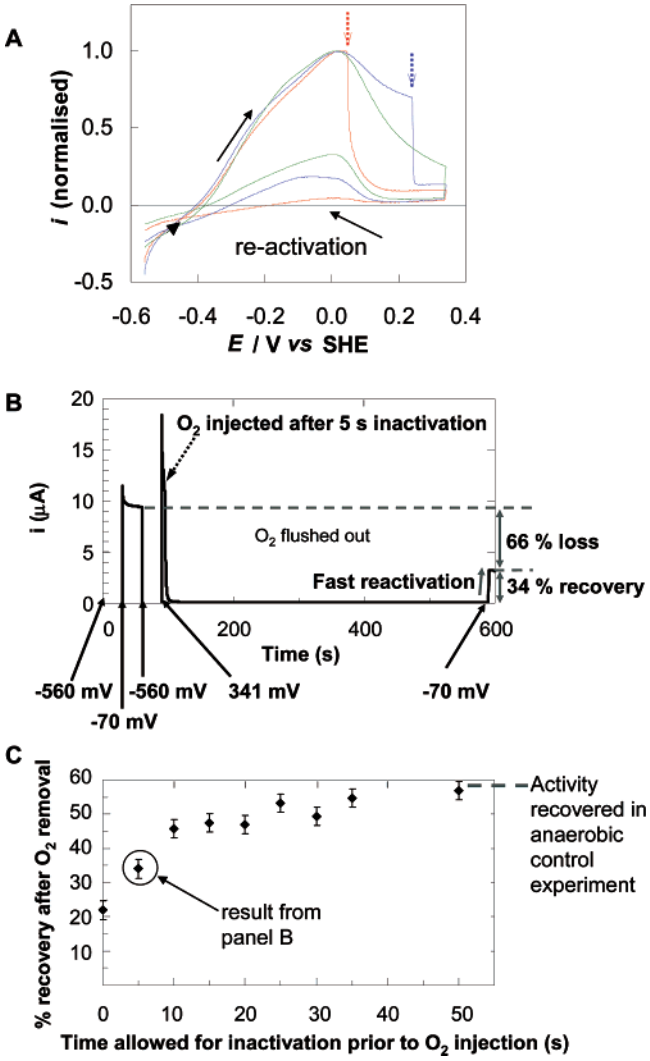

Figure 39. Experiments designed to explore the protection against O_2 afforded by the anaerobic, oxidized inactive state of *D. desulfuricans* [FeFe]-hydrogenase on a PGE electrode. Panel A: Cyclic voltammograms recorded at 10 mV s^{-1}, 30 °C, with a 300 s pause at 342 mV before the return sweep (toward more negative potentials). Red line: O_2 injected at 42 mV. Blue line: O_2 injected at 242 mV. Green line: anaerobic cycle. Black arrows indicate the direction of the scan. Reprinted with permission from ref 76. Copyright 2005 American Chemical Society. Panel B: Current vs time trace for an experiment at 10 °C in which the electrode potential is stepped to 341 mV at 100 s (a potential at which the enzyme can be inactivated anaerobically) and then O_2 is introduced after 5 s. The extent of recovery after flushing out O_2 is measured by comparing the activity after a reactivation period at −70 mV with the value from an initial control period at this potential (see gray dashed lines). Panel C: summary of a series of chronoamperometric experiments run as shown in panel B, but with different time periods for inactivation at +341 mV prior to introduction of O_2. In all experiments, 200 μL of O_2-saturated buffer was injected into a 2 mL cell solution, yielding approximately 90 μM O_2 in the cell solution. Other conditions: electrode rotation rate = 2500 rpm, pH 6.0, 1 bar H_2. Panels B and C are reprinted with permission from ref 71. Copyright 2006 American Chemical Society.

high potential oxidant would be required to generate this state in conventional solution studies, suggesting a reason for the difficulty in regenerating the O_2-stable state in early work on the [FeFe]-enzymes, and the success with DCIP as oxidant.

Chronoamperometry experiments shown in Figure 39B and C quantify exactly how much the *D. desulfuricans* [FeFe]-hydrogenase is protected by oxidative inactivation. Panel B shows a current vs time trace recorded at 10 °C (films of this enzyme on PGE are much more stable at lower temperatures). First, the enzyme is fully activated at −560 mV. Next, the potential is stepped to −70 mV to measure the initial H_2 oxidation activity, and then it is stepped back to −560 mV and then to 341 mV, a potential at which the hydrogenase inactivates anaerobically. After 5 s at 341 mV, before too much enzyme has inactivated, O_2 is introduced, and then the cell is flushed with H_2 for about 500 s before the potential is stepped to −70 mV to cause reactivation. The extent of recovery is gauged by comparing the current with that measured in an anaerobic control experiment at −70 mV. Panel C summarizes results for a series of similar experiments in which the potential is held at 341 mV for increasing lengths of time prior to O_2 injection. The recovered activity increases as the inactivation period is lengthened.

The experiment in Panel B shows that formation of the H_{ox}^{inact} state is so fast at pH 6.0 that even a 5 s period at 341 mV enables substantial inactivation before O_2 is added. In this case, 34% of the initial activity level measured at −70 mV is restored. A 60 s inactivation period prior to O_2 injection results in recovery of almost 60% of activity, a level similar to that restored in a fully anaerobic control experiment. Thus, further to the earlier studies, the electrochemical results show that H_{ox}^{inact} is unreactive to O_2 (Figure 6B).

7.1.4. Summary: Hydrogenases Operating in Air?

Protein film voltammetry provides precise details on H_2 oxidation activity for hydrogenases in air (this is not easy to measure in other ways) and on the extent of and conditions for recovery after removal of air. For the [NiFe]-hydrogenases from *D. fructosovorans* and *A. vinosum*, O_2 leads to a mixture of inactive states, Ni-A and Ni-B, and to some permanent damage. Repeated cycles of exposure to O_2 in the microanaerobic environment of these organisms (Figure 3) would lead to a build-up of enzyme that is very slow to reactivate under ambient conditions (hours), along with increased amounts of "dead" enzyme. Access to the Ni-B state that is readily activated may be important in providing protection against O_2 inhibition and/or damage in semi-aerobic growth conditions. For the [FeFe]-hydrogenase (from *D. desulfuricans*), the anaerobically generated inactive state, H_{ox}^{inact}, appears to be the only form of the enzyme that can survive exposure to O_2.

As might be expected, the hydrogenases from the aerobic Knallgas bacteria *Ralstonia* (Figure 3) behave very differently to the hydrogenases from anaerobes under O_2-rich conditions, maintaining substantial H_2-oxidation activity and recovering rapidly on removal of O_2. At the time of writing this Review, it is still not clear how the states of *Ralstonia* MBH enzymes relate to those shown in Figure 6A. The gas atmospheres employed in Figure 38 are still far less challenging than the conditions that may be experienced *in vivo* ($\rho(H_2)$ may be in the microbar range, and $\rho(O_2)$ may be in the millibar range and above; section 2.1); further challenges to H_2 oxidation by the *Ralstonia* hydrogenases are addressed in section 8.2, in which we explore the technological possibilities arising from a catalyst that will oxidize H_2 in air.

Determining whether hydrogenases are able to *produce* H_2 in air will be important for applications involving aerobic

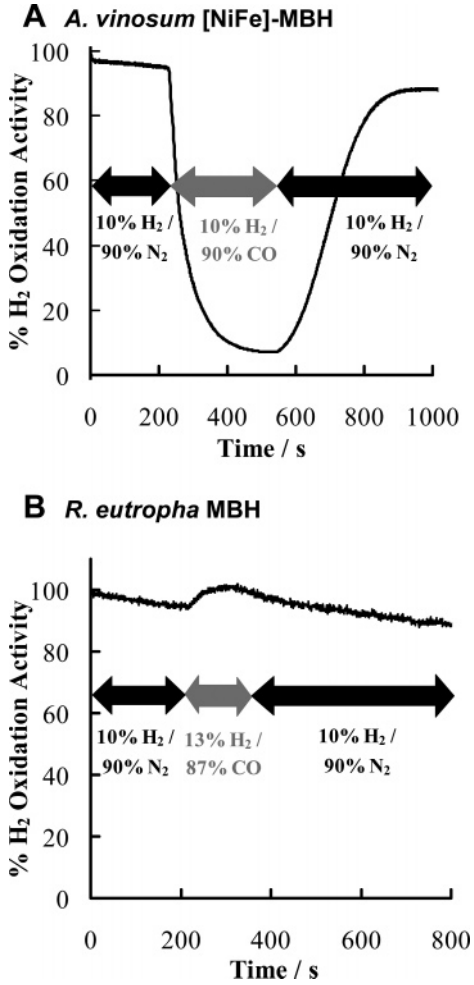

Figure 40. Effect of CO on H_2 oxidation activity measured for a PGE electrode modified with (A) *A. vinosum* [NiFe]-MBH at 142 mV and (B) *R. eutropha* [NiFe]-MBH at 100 mV. A continual slow drop in current during both experiments is attributed to film loss from the electrode. In each case, the gas composition in the headspace of the electrochemical cell was varied as indicated, the electrode was rotated at 2000 rpm, and the cell solution was pH 5.6 buffer at 30 °C. Reprinted with permission from ref 128. Copyright 2005 National Academy of Sciences, U.S.A.

photosynthetic H_2 production that exploit either intact cells or biologically derived or inspired constructs.

7.2. Inhibition of Hydrogenases by CO

In 1943 Hoberman and Rittenberg first reported that hydrogenase activity is inhibited by CO.[138] Unlike Pt catalysts which require harsh oxidative treatment to remove bound CO, typical hydrogenases are inhibited in a quite reversible manner by CO, and some CO-insensitive [NiFe]-hydrogenases have been identified.[2] According to structural and spectroscopic studies carried out on the [NiFe]-hydrogenase from *D. vulgaris* (Miyazaki F), the exogenous (inhibitory) CO molecule binds to the Ni atom,[70] and the crystal structure reported by Peters et al. for CO-inhibited *C. pasteurianum* [FeFe]-hydrogenase I shows CO bound as a terminal ligand at active site Fe.[139]

7.2.1. [NiFe]-hydrogenases and CO

Figure 40 compares the effect of CO on two [NiFe]-hydrogenases studied as films on a rotating PGE electrode.[128] For *A. vinosum* [NiFe]-MBH, changing the gas environment from 10% H_2/90% N_2 to 10% H_2/90% CO results in almost complete inhibition of current (H_2 oxidation activity), but activity is restored rapidly as CO is flushed out of solution (Figure 40A). Similarly, reversible CO inhibition of *T. roseopersicina* hydrogenase was reported by Karyakin et al. on the basis of direct electrochemical measurements.[140] In contrast, the H_2 oxidation activity of *R. eutropha* [NiFe]-MBH (Figure 40B) is unaffected by CO.[128] In this case, the gas composition of the cell was changed from 10% H_2/90% N_2 to 13% H_2/87% CO, and this actually resulted in an *increase* in activity due, most likely, to the slightly higher H_2 content of the gas environment. In other words, the H_2 oxidation activity of *R. eutropha* MBH is not inhibited by CO, even in large excess over H_2.

Léger and colleagues studied how CO inhibits the [NiFe]-hydrogenase from *D. fructosovorans* and measured how the equilibrium constant for CO inhibition varies with $\rho(H_2)$ and electrode potential.[66] They recorded the recovery of activity as CO is flushed from the cell solution, analogous to the experiment carried out to measure the K_M for H_2 oxidation (see Figure 17). In contrast to O_2, CO is fully competitive with H_2, and the data were analyzed according to eqs 18 and 19, which arise from standard equations for competitive inhibition.[66,94] Equation 18 shows the relationship between activity and the concentrations of CO and H_2.

$$i(t) = \frac{i_{max}}{1 + \frac{K_M}{C_{H_2}(t)}\left(1 + \frac{C_{CO}(t)}{K_I(CO/H_2)}\right)} \quad (18)$$

In eq 18, $K_I(CO/H_2)$ is the dissociation constant for CO as an inhibitor of H_2 oxidation. The time dependence is simple because the concentration of H_2 will remain constant throughout the transient (cf. Figure 17), provided the amount of CO injected is small. This yields eq 19,

$$i(t) = \frac{i(0)}{1 + \frac{C_{CO}(t)\exp(t/\tau)}{K_I^{app}(CO/H_2)}} \quad (19)$$

where $i(0) = i_{max}/(1 + K_M/C_{H_2})$ is the initial current (before adding CO) and

$$K_I^{app}(CO/H_2) = K_I(CO/H_2)\frac{C_{H_2}}{K_M}\left(1 + \frac{K_M}{C_{H_2}}\right) \quad (20)$$

As expected from the way that H_2 oxidation activity decreases as H_2 is flushed from the cell, the recovery of activity after CO injection is also sigmoidal. Equation 21 shows how the data are manipulated in a linear form by logarithmic transform.

$$\log_{10}\left(\frac{i(0)}{i(t)} - 1\right) = \log_{10}\left(\frac{C_{CO}(0)}{K_I^{app}}\right) + \frac{t}{2.3\tau} \quad (21)$$

Values of K_I^{app} determined for different values of electrode potential and H_2 partial pressure are shown in Figure 41 and reveal a complex pattern of CO inhibition that depends both on H_2 pressure and electrode potential. The value of $K_I(CO/H_2)$ decreases about 10-fold as the H_2 level is lowered from 1 to 0.1 bar. Notably, at 1 bar H_2 (red data points), $K_I^{app}(CO/H_2)$ is almost independent of electrode potential (the

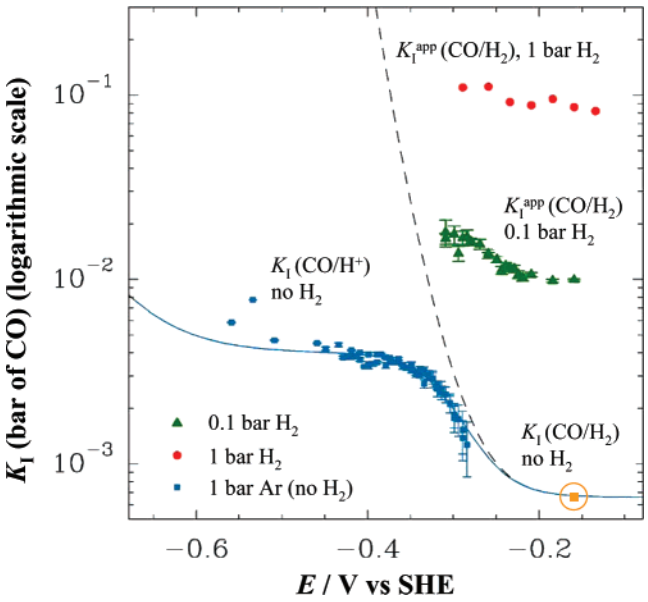

Figure 41. Summary of all the constants for the inhibition by CO of H_2 oxidation and H^+ reduction by *D. fructosovorans* [NiFe]-hydrogenase, at pH 6, 40 °C. Values of $K_I^{app}(CO/H_2)$ measured at 1 bar H_2 are shown in red, and values measured at 0.1 bar H_2 are shown in green. The corresponding value of $K_I(CO/H_2)$ once the competition with H_2 is accounted for is shown as a circled orange point. Blue points denote $K_I(CO/H^+)$ data obtained for experiments without H_2 (at 1 bar Ar). The lines are from fits to equations given in ref 66 and the Supporting Information given therein. Reprinted and adapted with permission from ref 66. Copyright 2004 American Chemical Society.

value is approximately 10^{-1} bar) whereas, at 0.1 bar H_2 (green data points), $K_I^{app}(CO/H_2)$ increases slightly as the potential is lowered. A similar set of experiments was performed to examine the effect of CO on H^+ reduction under an atmosphere of Ar (blue data points): in this case, it was found that inhibition is strong and potential dependent.

Of the three active states that have been spectroscopically characterized (see Figure 6A), Léger and co-workers favored assignment of Ni-SI (also known as Ni_a-S) as the state which binds CO.[66] This state has been isolated and crystallized for two [NiFe]-enzymes from sulfate-reducing bacteria.[141,142] It was considered by Léger and co-workers that Ni-R is unlikely to bind CO because no CO-adduct has yet been detected spectroscopically. A reversible CO-adduct with Ni-C was also considered to be very unlikely. (In Ni-C, the Ni atom is formally Ni(III)-H^-, but H^- dissociation as H^+ would leave Ni(I), which could then bind CO.[143]) However, their assertion that Ni-SI is the target for competitive inhibition by CO presents a problem because others have reported that its reaction with H_2 to give Ni-C is *irreversible* on the time scale of catalytic turnover (the back reaction—formation of Ni-SI from Ni-C—occurs very slowly).[36] In other words, the fact that CO appears to be a *competitive* inhibitor of H_2 oxidation and the suggestion that it binds to Ni-SI must be weighed against spectroscopically derived evidence that Ni-SI is probably not a catalytic intermediate.[118] Nonetheless, the analysis and proposals of Léger and co-workers are given here. The dotted line in Figure 41 shows the dependence of K_I on E expected for a model in which CO can bind only to state Ni-SI and electron transfer to the Ni Fe site is very fast. Clearly, this line predicts that binding will be very weak below about −0.4 V, where very little Ni-SI exists at equilibrium with the electrode. The fact that the rate levels off to a limiting value (rather than decreases to zero) as the potential is lowered was explained in terms of electron transfer being sufficiently slow that some Ni-SI could persist even under low-potential conditions. Léger et al. extended this argument to explain why CO inhibits H_2 evolution in solution assays: intermolecular electron transfer from electron donors is too slow to maintain a steady state with the enzyme in the more reduced states that do not bind CO. The answer may be that true catalytic intermediates are being missed: as discussed earlier, the turnover frequency is too high to allow easy detection of true intermediates and, whereas Ni-SR may be a reactive precursor, the states Ni-C and Ni-R might be better regarded as "active cul-de-sacs".

7.2.2. [FeFe]-hydrogenase: CO Inhibition

Hatchikian and co-workers reported a value of $K_I = 0.16$ μM for CO binding to *D. desulfuricans* [FeFe]-hydrogenase at 30 °C, with 20% H_2 in Ar.[136] The crystal structure of the CO-inhibited form of *C. pasteurianum* [FeFe]-hydrogenase I by Peters et al. showed that the inhibitory action of CO results from binding to the active site.[139] From EPR spectroscopy on the CO-bound crystals, it was confirmed that the structurally determined inhibited state is analogous to the H_{ox}-CO state formed when *D. desulfuricans*, *D. vulgaris*, and *C. pasteurianum* II [FeFe]-hydrogenases are inhibited by CO.[136,144−146] In the first voltammetric study of an [FeFe]-hydrogenase, from *M. elsdenii*, Butt and Hagen used their observation of CO inhibition as evidence that the enzyme was the electrocatalyst.[74] We have carried out various voltammetry experiments to study the inhibition of *D. desulfuricans* [FeFe]-hydrogenase by CO, and in accordance with previous reports, injection of CO-saturated buffer at 40 mV causes immediate loss of H_2 oxidation activity and injection at −460 mV causes immediate loss of H^+ reduction activity.[71] In the course of these experiments, we noted that the inactive, anaerobically oxidized state, H_{ox}^{inact}, is unable to bind CO. Generating the H_{ox}^{inact} state from active enzyme and then subjecting it to rapid activation is difficult using redox mediators, but the sequence of operations is easy to execute with PFV. This is clearly demonstrated in Figure 42, which compares the amount of reactivation observed when H_{ox}^{inact} is reactivated at different scan rates in the presence of CO. Data from control experiments (black lines) are included to show the current response when H_{ox}^{inact} is reactivated under 1 bar H_2 in the absence of CO (the decrease in current as the potential is taken below −0.2 V is simply due to the loss of thermodynamic driving force). In the presence of CO (red lines), the activity reaches a maximum and then drops sharply to zero as CO binds to the reactivated enzyme. The peak current increases in magnitude at faster scan rates because the faster the scan rate, the more H_{ox}^{inact} is activated to H_{ox} before CO has a chance to bind and block catalysis.

7.2.3. [FeFe]-hydrogenase: CO Recovery and Light

The light sensitivity of CO-inhibited [FeFe]-hydrogenase was first reported by Thauer in 1974, when it was noted that H_2 oxidation activity could proceed in the presence of CO if the sample was illuminated.[147] The photolability of exogenous CO in various [FeFe]-hydrogenases has since been investigated using a variety of techniques. Most recently, Albracht and co-workers presented a comprehensive study of the [FeFe]-hydrogenase from *D. desulfuricans*, in which EPR and IR spectroscopy revealed that, in the absence of H_2, the H_{ox}-CO state is stable in light.[120,148] Cryogenic

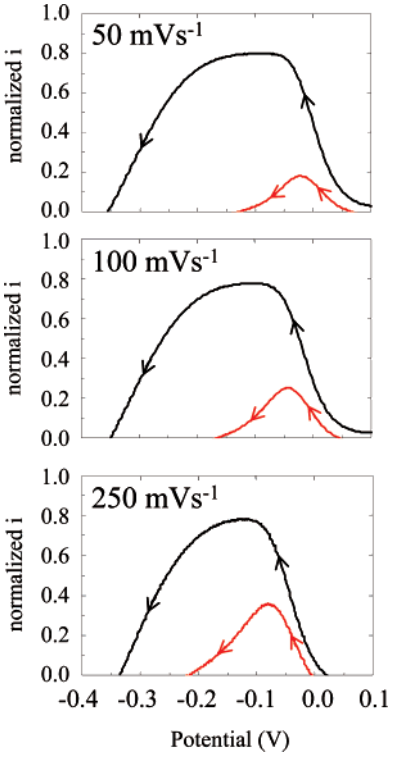

Figure 42. Reaction of CO with *D. desulfuricans* [FeFe]-hydrogenase as the enzyme is reactivated from the H_{ox}^{inact} state. Arrows show the direction of the scan. The film was first inactivated by poising the electrode potential at 241 mV for 300 s. In each case the current is normalized with respect to the level of activity measured on the previous scan; black lines indicate the level of reactivation expected if CO is absent; red lines show the responses observed when 30 μL of CO-saturated solution (final concentration 14 μM) is injected before the scan. Other conditions: rotation rate 2500 rpm, pH 6.0, 10 °C, 1 bar H_2. The current transient obtained in the presence of CO, which intensifies at a higher scan rate, reflects the enzyme's opportunity to catalyze H_2 oxidation before CO inhibition. Reprinted with permission from ref 71. Copyright 2006 American Chemical Society.

illumination caused photolysis of CO and generated the H_{ox} signal, but as observed for other [FeFe]-hydrogenases, raising the temperature caused complete recovery of the H_{ox}-CO signal.

In contrast to EPR studies which detect CO release through changes in spectra, investigations by PFV follow the recovery of catalytic activity. A study of the CO-inhibited [FeFe]-hydrogenase from *D. desulfuricans* revealed that light significantly enhances the rate of recovery of H_2 oxidation measured at −109 mV but does not enhance the rate of H^+ reduction, measured at −459 mV (Figure 43).[71] This behavior suggests the existence of (at least) two CO-bound forms, with the state that prevails at −109 mV (but not at −459 mV) displaying photolability.

7.2.4. Summary: Similarities and Differences between CO and O_2 Inhibition of [NiFe]- and [FeFe]-hydrogenases

In general, both [FeFe]- and [NiFe]-hydrogenases are susceptible to reversible inhibition by CO and more devastating attack by O_2. Although [FeFe]-hydrogenases may be permanently damaged by O_2, the anaerobically oxidized state, H_{ox}^{inact}, which does not bind CO, is also unreactive to O_2 and may represent a "resting" state that would allow the enzyme to survive under oxygenic conditions. The [NiFe]-MBH from *R. eutropha* is an important exception, even

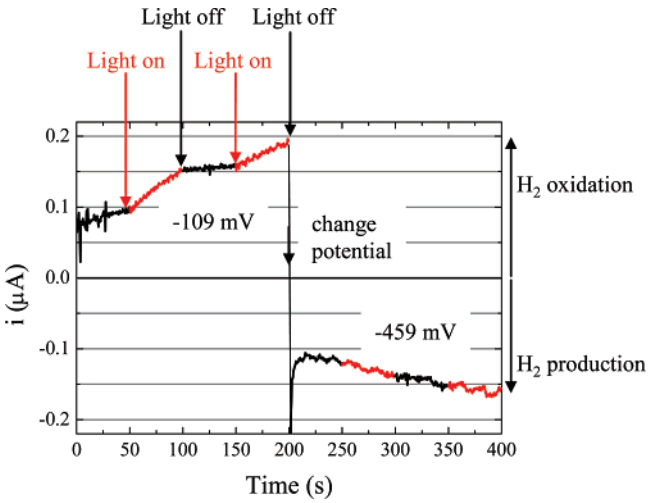

Figure 43. Effect of white light on the recovery of CO-inhibited *D. desulfuricans* [FeFe]-hydrogenase under conditions in which the electrode potential is driving either H_2 oxidation or H^+ reduction activity. Black lines indicate light off; red lines indicate light on. The electrode was soaked in CO-saturated buffer and then rinsed with water before commencing the experiment. The H_2 oxidation activity (0−200 s) was monitored by holding the electrode potential at −109 mV, whereas the H^+ reduction activity (201−400 s) was monitored at −459 mV. Other conditions: electrode rotation rate 2500 rpm, pH 6.0, 10 °C, 1 bar H_2. Reprinted with permission from ref 71. Copyright 2006 American Chemical Society.

though it shares >40% sequence identity with *D. gigas* [NiFe]-hydrogenase (based on ClustalW alignment of large subunit sequences). The *R. eutropha* MBH retains substantial H_2 oxidation activity even in the presence of an atmospheric level of O_2, and it is completely resistant to inhibition by CO even when a large excess over H_2 is used. Moreover, although this enzyme reacts with O_2 much more rapidly than it is inactivated anaerobically, the resulting inactive form is reactivated rapidly when a reductive potential step is applied. The latter observations suggest strongly that O_2 interacts at a redox center in the enzyme, most likely the active site (since reversible inhibition at iron−sulfur clusters is unlikely). Together, the results show that O_2 tolerance in this enzyme is due to the ease by which the product of O_2 attack is removed rather than due to restricted "gas channel" access to the active site. The hard sphere diameters of CO and O_2 calculated from gas viscosities are roughly the same (3.55 and 3.70 Å, respectively, compared with 2.71 Å for H_2),[128] so it follows that CO must be able to access, but not inhibit, the active site of *R. eutropha* MBH. Indeed, the fact that CO does not inhibit suggests an inability to form a metal−CO bond.

7.3. Reactions of [NiFe]-hydrogenases with Sulfide

Hydrogenases from sulfate reducing bacteria, *Desulfovibrio*, are likely to encounter H_2S under physiological conditions. In an early study by Higuchi et al., diffraction data obtained for certain crystals of the [NiFe]-hydrogenase from *D. vulgaris* Miyazaki F (MF) were interpreted in terms of a sulfur based bridging ligand between the active site Ni and Fe,[149] in place of the oxygenic ligands assigned to inactive forms of the enzymes from *D. gigas*, *D. fructosovorans*, and *A. vinosum*.[39,150−153] Higuchi and co-workers also detected H_2S upon incubation of as-isolated hydrogenase with H_2 and electron donors, at a level consistent with release of sulfide from >20% of the enzyme molecules,[124,154] and

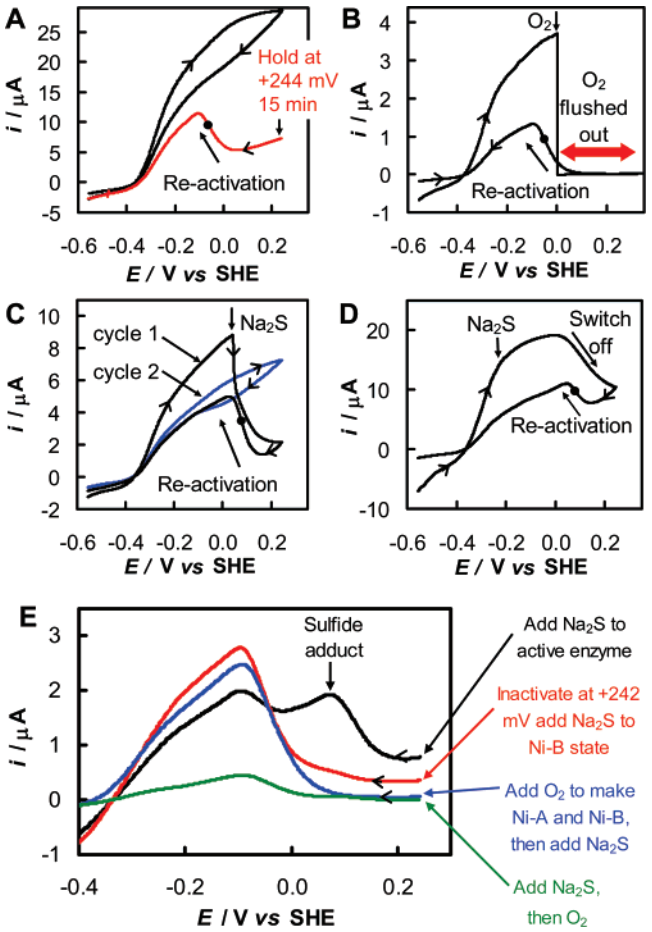

Figure 44. Inactivation of *D. vulgaris* Miyazaki F [NiFe]-hydrogenase by anaerobic high potential, O_2, or sulfide. The voltammograms in panel A show the behavior of a PGE film of enzyme at 1 bar H_2 under anaerobic conditions after pre-equilibration at either −556 mV (black) or +244 mV (red). In panel B, an aliquot of O_2-saturated buffer is introduced at 0 V on the forward scan (toward more positive potentials) and the O_2 is flushed out so the enzyme reactivates under anaerobic conditions on the reverse scan. In panel C, an aliquot of Na_2S solution, adjusted to the same pH as the experimental buffer, pH 6, was introduced at about 0 V (indicated by a vertical arrow) to give a final concentration of 1 mM. Flushing the headspace with H_2 then removes the sulfide (as H_2S). In panel D, the same amount of Na_2S is added at a lower potential. For experiments shown in panel E, the potential was swept from +242 mV to −400 mV after various pretreatments designed to generate specific active or inactive states before injecting sulfide and removing it as H_2S. Other conditions: pH 6.0, 45 °C, 1 bar H_2, electrode rotation rate = 2500 rpm, scan rate (A−D) 3 mV s^{-1}, (E) 1 mV s^{-1}. Reprinted with permission from ref 10. Copyright 2006 American Chemical Society.

further X-ray crystallography showed that the bridging S atom was absent in the reduced form.[142]

Following this lead, we undertook electrochemical investigations of the reaction of *D. vulgaris* MF [NiFe]-hydrogenase with H_2S and studied the properties of the inactive product that is formed.[10] The experiments shown in Figure 44 were carried out at pH 6, conditions under which H_2S ($pK = 6.8$) is conveniently produced by dissolution of solid Na_2S. A control experiment (Figure 44A, black line) carried out at a scan rate of 3 mV s^{-1} shows that anaerobic inactivation is slow. Full inactivation is achieved by poising the electrode potential at 244 mV for 15 min, and a negative potential sweep (red line) reveals that reactivation occurs at ca. −50 mV (the "switch" potential, as defined in section 6, is indicated by •). In Figure 44B, O_2 is injected at about 0 V on the forward sweep, and the switch potential for reactivation on the reverse sweep is again about −50 mV. The effect of adding an aliquot of sulfide solution at an electrode potential of about 0 V is shown in Figure 44C. The immediate drop in current shows that sulfide inhibits the enzyme. Activity is restored on the return sweep, with a switch potential of about 80 mV, which is 130 mV more positive than the switch potential for reactivation of the anaerobically oxidized or O_2-inactivated state. If sulfide is added at a more negative potential (Figure 44D), no effect on activity is observed until the potential is taken above about 0 V. Thus, we concluded that sulfide generates a new, inactive state of the *D. vulgaris* MF [NiFe]-hydrogenase—a sulfide adduct that is stable only above 80 mV. When experiments were carried out at higher pH (not shown), the inactivation by sulfide was much slower, suggesting (but not proving) that H_2S is the attacking species.[10]

These results can be discussed with reference to a more recent paper by Higuchi and co-workers,[124] who carried out a detailed crystallographic and EPR study of the reactions of the *D. vulgaris* MF [NiFe]-hydrogenase with Na_2S and O_2. The EPR spectra of the as-isolated enzyme indicated a mixture of species which they attributed to Ni-B (Ready) and a small amount of Ni-A (Unready). Anaerobic addition of a high concentration (50 mM) of Na_2S resulted first in spectral changes consistent with reduction of the [3Fe-4S] cluster, and then the Ni-B signals converted to signals indicative of a new state that they termed Ni-B′ while the Ni-A signals remained essentially unchanged. These results suggest that the high level of sulfide introduced in these experiments acts first as a reductant and then as an inhibitor, presumably generating the sulfide adduct observed in the electrochemical experiments shown in Figure 44C and D. Introduction of O_2 resulted in conversion of the new Ni-B′ EPR signals to Ni-A signals, and reductive activation with methyl viologen was slow (>40 min), consistent with activation of Ni-A.[124]

The experiments in Figure 44E show how these observations are addressed electrochemically. All the scans were performed on different films of hydrogenase, so the current magnitudes vary, and a low scan rate (1 mV s^{-1}) was used. During the reductive scan (black line) with the sulfide adduct (formed after adding sulfide to active enzyme), the slow scan rate provides time for the enzyme to inactivate for a second time after the sulfide adduct is reactivated (at the higher potential). The second reactivation process is observed at the lower potential expected for the Ni-B state. The high-potential reactivation process corresponding to the sulfide adduct is not observed when sulfide is added to enzyme that has been inactivated anaerobically (Ni-B (Ready), red line) or by O_2 (Ni-A and Ni-B (Unready and Ready), blue line).[10] Note that the exact positions for the switch potentials E_{switch} are shifted to slightly higher values than in panels A−D because the scan rate is slower. Finally, in the experiment represented by the green line, active enzyme was first exposed to Na_2S and then to O_2. The high potential reactivation process is absent, but limited recovery occurs at the same E_{switch} value as Ni-A or Ni-B and further activity is recovered during subsequent potential cycles (not shown).[10] These results are consistent with formation of Ni-A being particularly favored if the active enzyme is first exposed to sulfide (giving Ni-B′) and then O_2, as suggested by Ogata et al.[124] The possibility of a slowly reactivating

species with an S−O bridge cannot be ruled out. The inactivation/reactivation reactions proposed for *D. vulgaris* MF [NiFe]-hydrogenase based on interpretation of the electrochemical results[10] in light of EPR and crystallographic data[124] are summarized in Figure 45.

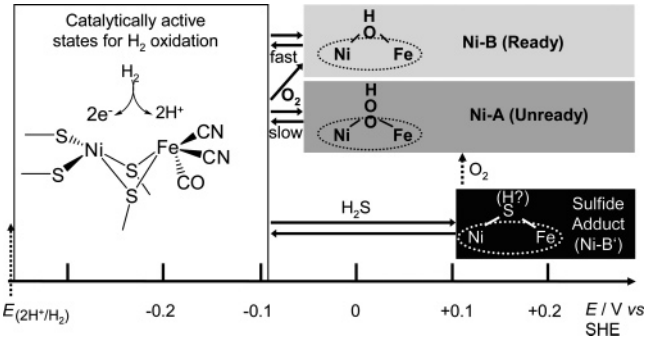

Figure 45. Representation of proposed reaction scheme for potential-dependent inactivation and reactivation reactions of [NiFe]-hydrogenases under anaerobic conditions or in the presence of O_2 and/or sulfide. The approximate potential regions indicated refer to *Desulfovibrio vulgaris* Miyazaki F [NiFe]-hydrogenase and apply for 45 °C, pH 6, 1 bar H_2, and scan rate 1 mV s^{-1}. Reprinted and adapted with permission from ref 10. Copyright 2006 American Chemical Society.

Other [NiFe]-hydrogenases also react with sulfide. The enzymes from other *Desulfovibrio* species, *D. gigas* (Figure 46A) and *D. fructosovorans* (not shown), show similar although slower reactivity compared to the *D. vulgaris* MF enzyme. The *A. vinosum* [NiFe]-MBH (Figure 46B) reacts much more slowly with sulfide, and to a lesser extent.

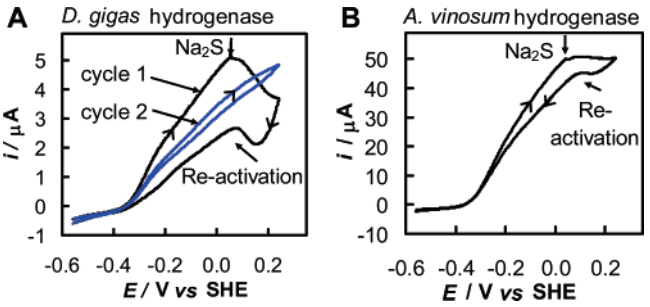

Figure 46. Cyclic voltammograms recorded to explore the effect of sulfide on [NiFe]-hydrogenases from (A) *D. gigas* and (B) *A. vinosum*. Other conditions: pH 6.0, 45 °C, 1 bar H_2, electrode rotation rate 2500 rpm, scan rate 3 mV s^{-1}. Reprinted with permission from ref 10. Copyright 2006 American Chemical Society.

Sulfate-reducing bacteria such as *Desulfovibrio* and purple sulfur bacteria such as *Allochromatium* couple H_2 oxidation to the reduction of sulfur (or sulfate) to sulfide. The PFV results show that sulfide (H_2S) is unable to inhibit [NiFe]-hydrogenases at potentials more negative than about +100 mV, and it is unlikely that potentials higher than this would be experienced *in vivo*. However, during cell disruption and aerobic purification, it is possible that hydrogenase may be exposed to sulfide at appropriate redox potentials and may therefore be isolated, at least partially, in a sulfur-trapped state. This reaction would be difficult to diagnose in solution experiments without good potential control. Further, the reaction of the sulfide adduct with O_2 could result in Ni-A because an HS-ligand should be easier to displace than an HO-ligand (in Ni-B) and this would occur under more oxidizing conditions, predicted (see section 7.1.1) to produce Ni-A (Unready) rather than Ni-B (Ready). The information on reactions with sulfide provided by voltammetric experiments is therefore highly relevant to spectroscopic and crystallographic studies. Hydrogen sulfide contaminates H_2 prepared by steam reforming of hydrocarbons,[155] and the resistance of hydrogenases to sulfides at mild oxidizing potentials may enable them to be exploited as catalysts for oxidation of impure H_2.

8. Applications of Hydrogenases

8.1. Replacing Pt in Fuel Cells with Biological Catalysts

The high electrocatalytic H_2 oxidation activity of electrodes modified with hydrogenase has suggested to several groups the possibility of employing hydrogenases in place of the Pt particles generally used as the anode catalyst in proton-exchange membrane H_2/O_2 fuel cells.[82,100,140] The high O_2 tolerance of the H_2-oxidation activity of *Ralstonia eutropha* H16 [NiFe]-MBH, which retains about 20% activity in air (see section 7.1.2), suggested to us that an anode modified with this enzyme should be able to function in a membraneless fuel cell using a second enzyme, laccase, a high-potential O_2-reducing enzyme, as the electrocatalyst at the cathode.[128] The optimum pH for H_2 oxidation by *R. eutropha* [NiFe]-MBH is around 5, close to the pH 3−5 region favored by laccase from *Trametes versicolor*, a "white rot" wood fungus.[156]

As shown in Figure 47A, electrodes coated with these enzymes were placed in an open beaker of aqueous buffer (0.1 M citrate, pH 5). It was thus possible to generate electricity from H_2 and air without a separating membrane, providing that the gas streams were directed close to the anode and cathode, respectively.[128] The open circuit voltage was about 980 mV, dropping as a load was connected across the cell to draw a current, giving rise to the power vs load curve shown in Figure 47B. For comparison, the power/load curve is shown also for a control experiment in which the more active but O_2-sensitive *Allochromatium vinosum* [NiFe]-MBH is employed at the anode (open circles). Since the *R. eutropha* [NiFe]-MBH is completely insensitive to carbon monoxide, introduction of CO in the fuel supply has no effect on the cell voltage or power (Figure 47C).[128]

8.2. "Wireless Hydrogen"?

We next pose the question, "can a certain hydrogenase be sufficiently O_2-tolerant that it will function as an electrocatalyst in a fuel cell that can extract useful electrical power from air containing benign, low-levels of H_2?" This alternative concept, which we term "wireless H_2", offers an extreme challenge for an O_2-tolerant hydrogenase, demanding operation at <4% H_2 in air, a level that is noncombustible.[157]

As discussed in section 7.1.2, the membrane-bound hydrogenase from the heavy metal resistant aerobe *Ralstonia metallidurans* CH34 is so tolerant to O_2 that >40% of the anaerobic level of H_2-oxidation activity is retained at ambient levels of O_2, provided that the H_2 partial pressure is high.[157] However, activity is detectable even at just 3% H_2 in air. This led us to explore the possibilities of a fuel cell operating on a still mixture of trace H_2 in air, as shown in Figure 48A. An open circuit voltage of 950 mV was recorded, and a maximum power of 5 μW cm^{-2} was achieved at a cell voltage of approximately 500 mV.

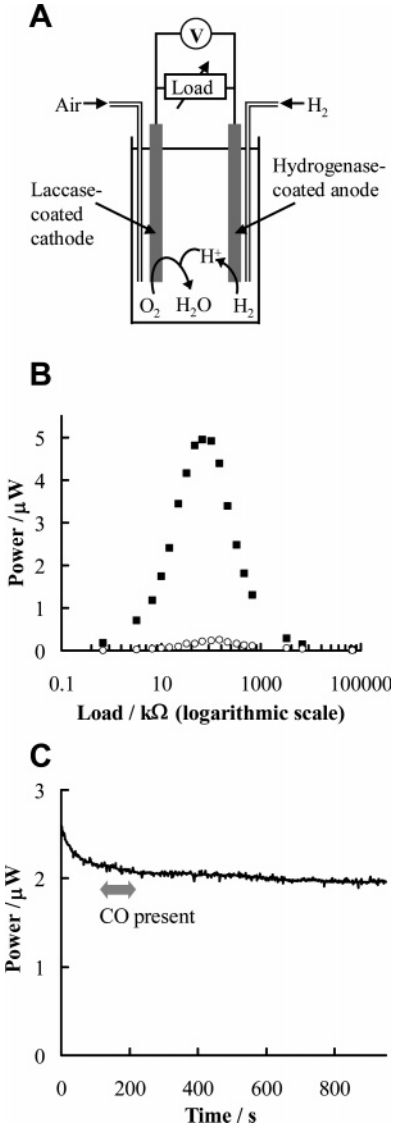

Figure 47. Operation of a membraneless H_2/O_2 fuel cell, in which H_2 is directed at a PGE anode modified with *R. eutropha* [NiFe]-MBH and air is directed at a PGE cathode modified with laccase from *T. versicolor*. Each electrode has a surface area of 0.7 cm^2, and the electrolyte is aqueous citrate, 0.1 M, pH 5. The cell is operated at room temperature. Panel A: diagram of the cell. Panel B: a plot of power vs applied load (V^2/R vs R, where V = cell voltage and R = load) for the fuel cell (filled squares, ■) and for a control experiment (open circles, ○) in which the O_2-tolerant *R. eutropha* MBH-modified electrode is replaced by an electrode modified with the O_2-sensitive *A. vinosum* [NiFe]-MBH. Panel C shows the power versus time course recorded with a 330 kΩ load: introduction of CO has no effect on the power output. Reprinted wtih permission from ref 128. Copyright 2005 National Academy of Sciences, U.S.A.

Three cells connected in series provided sufficient power to allow a wristwatch to run for 24 h, fueled by the energy contained within a tank (12 L, a large volume relative to the amount of fuel consumed) of just 3% H_2 in air (Figure 48B). The power curve shown in Figure 48C reflects the behavior of just one cell as the applied load is successively lowered. The power was fairly stable (>10 min) at each load above about 100 kΩ, but below this, the power dropped very rapidly and the open circuit voltage was not recovered when the circuit was disconnected.

This behavior can be understood with reference to the voltammogram in Figure 48D, for *R. metallidurans* [NiFe]-

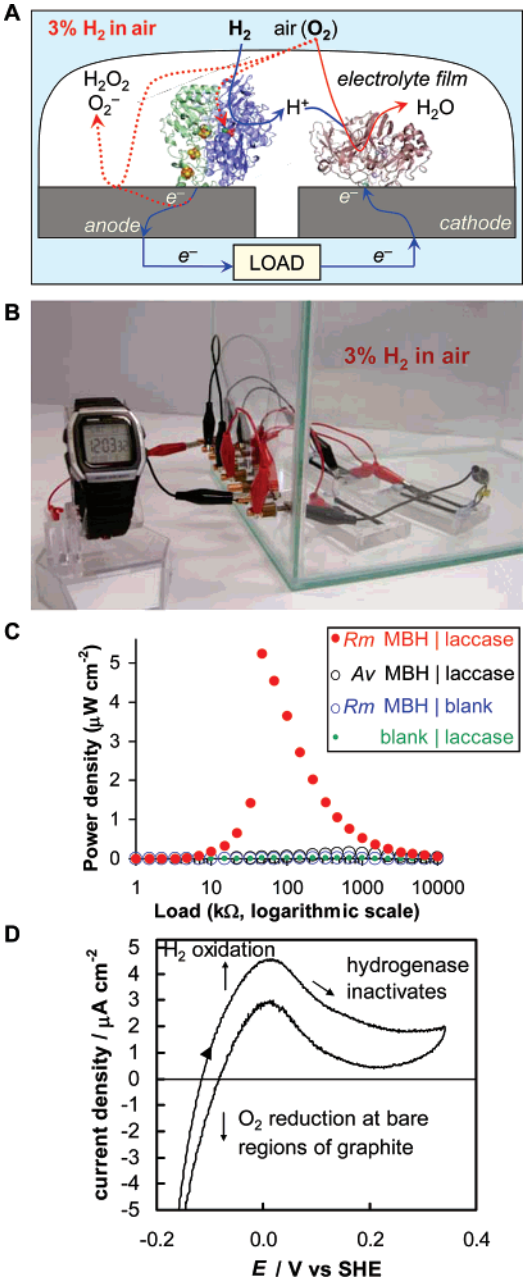

Figure 48. "Wireless hydrogen"—fuel cell experiments under demanding conditions. Panel A: Schematic representation of an enzyme fuel cell open to the gas atmosphere of 3% H_2 in air contained within a glass tank. The anode is modified with the *R. metallidurans* [NiFe]-MBH, and the cathode is modified with laccase. The hydrogenase must be sufficiently active and tolerant to O_2 to compete with direct reduction of O_2 at bare regions of the PGE anode, which generates peroxide and superoxide species that could potentially damage the enzymes. Panel B: A wrist watch powered by three of these cells operated in series. Panel C: Power vs load curve for a single fuel cell recorded as the load was stepped to progressively lower values (red solid circles). Data from control experiments are also shown in which the anode is modified with an O_2-sensitive hydrogenase, *A. vinosum* [NiFe]-MBH (black open circles), or is left bare (small green dots). Alternatively, a bare PGE cathode is combined with the *R. metallidurans* [NiFe]-MBH-modified anode (open blue circles). Panels A−C are reproduced from ref 157 by permission of The Royal Society of Chemistry. Panel D: Cyclic voltammogram recorded for a rotating PGE electrode modified with *R. metallidurans* [NiFe]-MBH (electrode area = 0.03 cm^2, rotation rate = 6000 rpm) at 2 mV s^{-1} in 0.1 M citrate buffer, pH 6, in contact with 3% H_2 in air. (K. A. Vincent, J. A. Cracknell, M. Ludwig, O. Lenz, B. Friedrich, F. A. Armstrong. Unpublished data.)

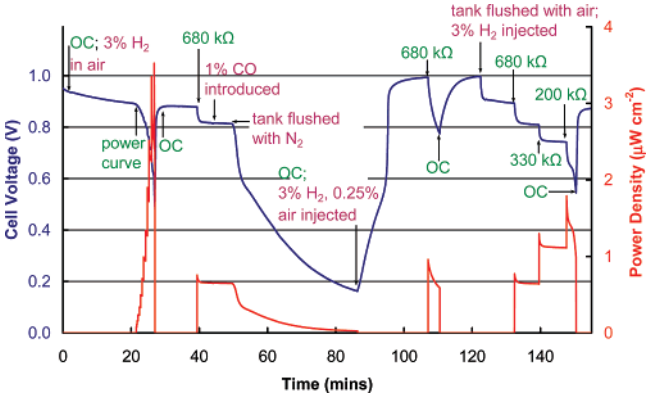

Figure 49. Variation in fuel cell voltage (blue) and power output (red) with time, in response to changes in the gas environment (purple labels) or applied load (green labels) for a fuel cell operated as shown in Figure 48A. OC = Open circuit. Reproduced from ref 157 by permission of The Royal Society of Chemistry.

MBH on a rotating graphite electrode under 3% H_2 in air. Under these demanding conditions, H_2 oxidation is sustained only over a very narrow potential range, bounded at more negative potentials by competing O_2 reduction at bare regions of the graphite and at high potentials by inactivation of the hydrogenase that is rapid under these conditions and causes the current to drop almost to zero at potentials higher than 200 mV. Application of a low load in the fuel cell causes the potential at the anode to rise into the region where the enzyme inactivates. Depletion of H_2 close to the anode as larger currents are drawn at low loads will make these conditions even more challenging.

Fuel cell experiments not only explore ways in which hydrogenases may be applied in energy technologies, but they also provide information on the ability of hydrogenases from aerobic Knallgas bacteria to sustain activity under the highly demanding conditions that may be experienced *in vivo*. Figure 49 shows the effect of various manipulations of gas environment or applied load on the cell voltage and power output for a single fuel cell as described above. The electrolyte was first saturated with H_2, and then the cell was placed in an atmosphere of 3% H_2 in air under open-circuit conditions. The open-circuit potential decreased over 20 min from 0.94 to 0.88 V as the gas composition of the electrolyte equilibrated with that of the environment. A variable load was then connected to measure a power vs load curve, causing the cell voltage to drop as current was drawn (power increases). When open-circuit conditions were restored, the voltage climbed back to 0.87 V and remained stable. After 10 min, a 680 kΩ load was applied, causing the cell voltage to drop; the voltage then remained stable at 0.82 V even after introduction of 1% CO. After a further 5 min, the tank was flushed with N_2, causing the cell voltage to drop below 0.2 V. After reapplying open-circuit conditions and introducing 3% H_2 and just 0.25% air to the N_2 atmosphere, the voltage climbed to 1 V. Under these conditions, the open-circuit voltage was reproducibly slightly higher than the value recorded at 3% H_2 and 97% air, although the power output dropped rapidly when a load was applied to draw current. After flushing the tank with air and readmitting 3% H_2, sequential decreases in load gave decreases in voltage (with increases in current). Finally, restoration of open-circuit conditions gave 0.86 V, close to the initial value after equilibration with the gas environment.

The fuel cell experiments described in this section clearly demonstrate that *R. metallidurans* [NiFe]-MBH is able to oxidize dilute H_2 in air, consistent with the physiological role of this enzyme in an aerobes living at low H_2 partial pressures (see Figure 3). The advantages of certain hydrogenases as H_2 oxidation catalysts, in comparison to Pt, include their high affinity for H_2, their ability to oxidize H_2 in air, and their high selectivity for H_2 over other small molecules such as CO or H_2S. Hydrogenases functioning at mild temperatures in aqueous conditions are unlikely to compete with Pt in proton exchange membrane (PEM) fuel cells in which the catalyst is operated at elevated temperatures (sometimes >100 °C) in a humidified gaseous environment. However, the selectivity of hydrogenases may open up novel possibilities for energy technologies that exploit H_2 sources that are too dilute or contaminated to be suitable for conventional Pt fuel cells.

9. Conclusions and Outlook

The high catalytic H^+ reduction and H_2 oxidation activities of hydrogenases translate into high catalytic currents in direct electrochemical experiments, making protein film voltammetry (PFV) a sensitive and powerful technique for addressing these enzymes. Whereas high turnover rates lead to rapid depletion of substrate near the electrode (and the current response for a hydrogenase at a stationary electrode generally reports on little more than the rate of mass transport of H_2), rotation of the electrode provides a convenient means to supply substrate and remove product at the electrode surface. Providing interfacial electron transfer between the electrode and the enzyme is fast, the electrocatalytic current response provides significant insight into the potential profiles for activity and reactions of hydrogenases. The PGE electrode has proved to be an excellent conducting substrate for direct adsorption of proteins, and highly electroactive films of a number of [NiFe]- and [FeFe]-hydrogenases have been studied. The minimal sample requirement and ease of film preparation on this kind of electrode have enabled detailed comparisons of the properties of hydrogenases from different organisms or of the effect of site-directed mutations—comparative studies that would be difficult to achieve by spectroscopic or crystallographic methods that demand much larger quantities of enzyme. Remarkable variation in the properties of hydrogenases has been revealed through PFV experiments, in particular differences in their sensitivity to oxidative inactivation and small molecule inhibition, even for enzymes with very high sequence similarity. Only a small number of hydrogenases have so far been purified and examined in detail, and the discovery and isolation of new hydrogenases is likely to lead to a library of enzymes with diverse catalytic properties.

The electrochemical response is sensitive to potential-dependent variations in catalytic activity or other reactivities, all of which might be overlooked in conventional solution methods. Notable examples include the higher overpotential for H_2 oxidation of *Ralstonia eutropha* [NiFe]-MBH compared with other hydrogenases (approximately 80 mV), the high potential window for stability of the sulfide adduct of *Desulfovibrio vulgaris* Miyazaki F [NiFe]-hydrogenase, and the potential dependence of CO inhibition constants for *D. fructosovorans* [NiFe]-hydrogenase. A voltammogram resembles a spectrum with recognizable features, such as a fast or slow "switch off" in activity at high potential, or the potential-dependent release of an inhibitor. Protein film voltammetry thus provides much more than just values of reduction potentials, and where potentials are provided by

PFV, they may refer to conditions in which the substrate is present, which is not possible in equilibrium potentiometric titrations.

Electrochemical results can rarely be interpreted in isolation: PFV provides information on reactions but not the structures of species that react or form. Consider the "CEEC" reversible inactivation−reactivation cycle of hydrogenases: inactivation involves first a chemical reaction, i.e., a rearrangement/removal of atoms, and then the resulting arrangement is trapped by loss of an electron. The conditions required for generating specific states determined from electrochemical experiments provide insight into conditions that may be employed to generate well-defined states for structural measurements. Electrochemical diagnosis of reactions, including *potentials* (thermodynamics) and *rates* (kinetics), therefore, goes hand-in-hand with spectroscopic or crystallographic structure elucidation. Challenges remain for comparing the inherent activities of different hydrogenases on an electrode, since the overall electroactivity depends both on the rate of enzyme turnover and on electroactive coverage, which is rarely known. Details of the actual mechanisms still remain unclear: the turnover frequencies are very high, and intermediates that can be inferred from PFV experiments, evident in the pH and potential dependencies of current, are likely to remain elusive and difficult to characterize structurally.

Whereas most studies of hydrogenase activity have employed high levels of H_2 (typically >0.1 mM), the sensitivity of electrochemical measurements to activity at low H_2 concentrations has permitted evaluation of activities under conditions more closely resembling those encountered by hydrogenases *in vivo*. The high activity of hydrogenases, high affinity for H_2, and high selectivity for H_2 over other small molecules have been exploited in small-scale proof-of-concept novel fuel cells to produce electricity from H_2 at low levels in air or with high levels of contaminating CO. These experiments not only highlight opportunities for hydrogenases in future technologies but also explore the challenge of aerobic H_2 oxidation in biology. The activity per active site for hydrogenases on graphite compares favorably with that of Pt, and together with the impressive resistance of certain hydrogenases to small molecule poisons (O_2, CO, H_2S), this may lead to application of hydrogenase-modified electrodes in novel fuel cells or H_2 production or H_2 sensing applications. While the enzymes themselves are inherently fairly stable, these applications will demand robust electrode attachment and improvements in coverage.

Knowledge of the reactions of hydrogenases with small molecules provides a benchmark for the desirable properties of future hydrogen-cycling catalysts. Synthetic clusters inspired by hydrogenase chemistry may be developed to catalyze H_2 oxidation and H^+ reduction, but challenges clearly arise not only in synthesis of catalytic sites but also in providing the "plumbing" for gas access and "wiring" for electrons that subtly tune the chemistry of these enzymes.

10. Full Names and Strains of the Main Micro-organisms Mentioned in the Text

Allochromatium vinosum
Aquifex aeolicus
Clostridium pasteurianum
Desulfomicrobium baculatum
Desulfovibrio desulfuricans
Desulfovibrio gigas
Desulfovibrio vulgaris (strains Miyazaki F or Hildenborough)
Megasphaera elsdenii
Pyrococcus furiosus
Ralstonia eutropha H16
Ralstonia metallidurans CH34
Thiocapsa roseopersicina

11. Abbreviations

EPR	electron paramagnetic resonance
MBH	membrane-bound hydrogenase
PFV	protein film voltammetry
PGB	pyrolytic graphite basal plane
PGE	pyrolytic graphite "edge" surface
RHE	real hydrogen electrode
SCE	saturated calomel electrode
SHE	standard hydrogen electrode

12. Acknowledgments

The authors acknowledge the BBSRC (BB/D52222X/1) and EPSRC (Supergen 5 and quota award) for funding. F.A.A., K.A.V. and A.P. are grateful for the support of St. John's College, Wadham College, and Jesus College, Oxford, respectively. The authors thank collaborators for productive discussions, in particular, C. Léger, J. C. Fontecilla-Camps, B. Friedrich, O. Lenz, W. Lubitz, and S. P. J. Albracht.

13. References

(1) Wiberg, N. *Inorganic Chemistry*; Academic Press: London, 2001.
(2) Cammack, R.; Frey, M.; Robson, R. *Hydrogen As a Fuel: Learning From Nature*; Taylor and Francis: London and New York, 2001.
(3) Conrad, R. *Microbiol. Rev.* **1996**, *60*, 609.
(4) Armstrong, F. A. *J. Chem. Soc., Dalton Trans.* **2002**, 661.
(5) (a) Léger, C.; Elliott, S. J.; Hoke, K. R.; Jeuken, L. J. C.; Jones, A. K.; Armstrong, F. A. *Biochemistry* **2003**, *42*, 8653. (b) Elliott, S. J.; Léger, C.; Pershad, H. R.; Hirst, J.; Heffron, K.; Ginet, N.; Blasco, F.; Rothery, R. A.; Weiner, J. H.; Armstrong, F. A. *Biochim. Biophys. Acta* **2002**, *1555*, 54.
(6) Vincent, K. A.; Armstrong, F. A. *Inorg. Chem.* **2005**, *44*, 798.
(7) Hirst, J. *Biochim. Biophys. Acta* **2006**, *1757*, 225.
(8) Cammack, R.; Fernández, V. M.; Hatchikian, E. C. *Methods Enzymol.* **1994**, *243*, 43.
(9) Long, M.; Liu, J.; Chen, Z.; Bleijlevens, B.; Roseboom, W.; Albracht, S. P. J. *J. Biol. Inorg. Chem.* **2006**, *12*, 62.
(10) Vincent, K. A.; Belsey, N. A.; Lubitz, W.; Armstrong, F. A. *J. Am. Chem. Soc.* **2006**, *128*, 7448.
(11) Bleijlevens, B.; Broekhuizen, F. A.; Lacey, A. L.; Roseboom, W.; Fernández, V. M.; Albracht, S. P. J. *J. Biol. Inorg. Chem.* **2004**, *9*, 743.
(12) De Lacey, A. L.; Pardo, A. L. A.; Fernández, V. M.; Dementin, S.; Adryanczyk-Perrier, G.; Hatchikian, E. C.; Rousset, M. *J. Biol. Inorg. Chem.* **2004**, *9*, 636.
(13) Edwards, P.; Kuznetsov, V.; David, W. *Philos. Trans. R. Soc. London, Ser. A*, in press.
(14) Sigfusson, T. *Philos. Trans. R. Soc. London, Ser. A*, in press.
(15) Melis, A.; Zhang, L. P.; Forestier, M.; Ghirardi, M. L.; Seibert, M. *Plant Physiol.* **2000**, *122*, 127.
(16) Martinez-Perez, N.; Cherryman, S. J.; Premier, G. C.; Dinsdale, R. M.; Hawkes, D. L.; Hawkes, F. R.; Kyazze, G.; Guwy, A. J. *Biomass Bioenergy* **2007**, *31*, 95.
(17) Fouchard, S.; Hemschemeier, A.; Caruana, A.; Pruvost, J.; Legrand, J.; Happe, T.; Peltier, G.; Cournac, L. *Appl. Environ. Microbiol.* **2005**, *71*, 6199.
(18) Tsygankov, A. A.; Kosourov, S. N.; Tolstygina, I. V.; Ghirardi, M. L.; Seibert, M. *Int. J. Hydrogen Energy* **2006**, *31*, 1574.
(19) Melis, A.; Happe, T. *Plant Physiol.* **2001**, *127*, 740.
(20) Ihara, M.; Nishihara, H.; Yoon, K.-S.; Lenz, O.; Friedrich, B.; Nakamoto, H.; Kojima, K.; Honma, D.; Kamachi, T.; Okura, I. *Photochem. Photobiol.* **2006**, *82*, 676.
(21) Tromp, T. K.; Shia, R.-L.; Allen, M.; Eiler, J. M.; Yung, Y. L. *Science* **2003**, *300*, 1740.
(22) Schuler, S.; Conrad, R. *FEMS Microbiol. Ecol.* **1990**, *73*, 77.
(23) Schuetz, K.; Happe, T.; Troshina, O.; Lindblad, P.; Leitao, E.; Oliveira, P.; Tamagnini, P. *Planta* **2004**, *218*, 350.
(24) Ghirardi, M. L. *Indian J. Biochem. Biophys.* **2006**, *43*, 201.
(25) Lovley, D. R. *Appl. Environ. Microbiol.* **1985**, *49*, 1530.

(26) Klueber, H. D.; Lechner, S.; Conrad, R. *FEMS Microbiol. Ecol.* **1995**, *16*, 167.
(27) Arras, T.; Schirawski, J.; Unden, G. *J. Bacteriol.* **1998**, *180*, 2133.
(28) Wilson, M. *Microbial Inhabitants of Humans: their ecology and role in health and disease*; Cambridge University Press: Cambridge, 2005.
(29) Olson, J. W.; Maier, R. J. *Science* **2002**, *298*, 1788.
(30) Stefano, M. D.; Missanelli, A.; Miceli, E.; Strocchi, A.; Corazza, G. R. *J. Lab. Clin. Med.* **2004**, *144*, 313.
(31) Nemati, M.; Mazutinec, T. J.; Jenneman, G. E.; Voordouw, G. *J. Ind. Microbiol. Biotechnol.* **2001**, *26*, 350.
(32) Nagpal, S.; Chuichulcherm, S.; Peeva, L.; Livingston, A. *Biotechnol. Bioeng.* **2000**, *70*, 370.
(33) Conrad, R.; Aragno, M.; Seiler, W. *FEMS Microbiol. Lett.* **1983**, *18*, 207.
(34) Vignais, P. M.; Colbeau, A. *Curr. Iss. Mol. Biol.* **2004**, *6*, 159.
(35) Garcin, E.; Vernede, X.; Hatchikian, C.; Volbeda, A.; Frey, M.; Fontecilla-Camps, J. C. *Structure* **1999**, *7*, 557.
(36) Armstrong, F. A.; Albracht, S. P. J. *Philos. Trans. R. Soc. London, Ser. A* **2005**, *363*, 937.
(37) This methanogen hydrogenase was formerly thought to contain no metal. In the older literature, the class of hydrogenases with a di-iron active site is often termed Fe-hydrogenases. However, for clarity, we now call the di-iron enzymes [FeFe]-hydrogenases to distinguish them from the methanogen [Fe]-hydrogenases.
(38) Korbas, M.; Vogt, S.; Meyer-Klaucke, W.; Bill, E.; Lyon, E. J.; Thauer, R. K.; Shima, S. *J. Biol. Chem.* **2006**, *281*, 30804−30813.
(39) Volbeda, A.; Martin, L.; Cavazza, C.; Matho, M.; Faber, B. W.; Roseboom, W.; Albracht, S. P. J.; Garcin, E.; Rousset, M.; Fontecilla-Camps, J. C. *J. Biol. Inorg. Chem.* **2005**, *10*, 239.
(40) Nicolet, Y.; Piras, C.; Legrand, P.; Hatchikian, C.; Fontecilla-Camps, J. C. *Structure* **1999**, *7*, 13.
(41) Fareleira, P.; Santos, B. S.; Antonio, C.; Moradas-Ferreira, P.; LeGall, J.; Xavier, A. V.; Santos, H. *Microbiology* **2003**, *149*, 1513.
(42) Grapperhaus, C. A.; Darensbourg, M. Y. *Acc. Chem. Res.* **1998**, *31*, 451.
(43) Claiborne, A.; Mallett, T. C.; Yeh, J. I.; Luba, J.; Parsonage, D. *Adv. Protein Chem.* **2001**, *58*, 215.
(44) Heidelberg, J. F.; Seshadri, R.; Haveman, S. A.; Hemme, C. L.; Paulsen, I. T.; Kolonay, J. F.; Eisen, J. A.; Ward, N.; Methe, B.; Brinkac, L. M.; Daugherty, S. C.; Deboy, R. T.; Dodson, R. J.; Durkin, A. S.; Madupu, R.; Nelson, W. C.; Sullivan, S. A.; Fouts, D.; Haft, D. H.; Selengut, J.; Peterson, J. D.; Davidsen, T. M.; Zafar, N.; Zhou, L.; Radune, D.; Dimitrov, G.; Hance, M.; Tran, K.; Khouri, H.; Gill, J.; Utterback, T. R.; Feldblyum, T. V.; Wall, J. D.; Voordouw, G.; Fraser, C. M. *Nature Biotechnol.* **2004**, *22*, 554.
(45) Valente, F. M. A.; Almeida, C. C.; Pacheco, I.; Carita, J.; Saraiva, L. M.; Pereira, I. A. C. *J. Bacteriol.* **2006**, *188*, 3228.
(46) Denoted simply *Allochromatium vinosum* [NiFe]-hydrogenase in earlier work, this enzyme is now called MBH to distinguish it from the soluble hydrogenase of *A. vinosum* which was recently isolated and characterized. The "membrane-bound" [NiFe]-hydrogenases are associated with the surface of the membrane by an anchor and are not integral membrane proteins.
(47) Burgdorf, T.; Lenz, O.; Buhrke, T.; van der Linden, E.; Jones, A. K.; Albracht, S. P. J.; Friedrich, B. *J. Mol. Microbiol. Biotechnol.* **2005**, *10*, 181.
(48) Pereira, I. A. C.; Romao, C. V.; Xavier, A. V.; Le Gall, J.; Teixeira, M. *J. Biol. Inorg. Chem.* **1998**, *3*, 494.
(49) Lemon, B. J.; Peters, J. W. In *Handbook of metalloproteins*; Messerschmidt, A., Huber, R., Poulos, T., Wieghardt, K., Eds.; John Wiley & Sons: Chichester, U.K., 2001; Vol. 2.
(50) Vignais, P. M.; Billoud, B.; Meyer, J. *FEMS Microbiol. Rev.* **2001**, *25*, 455.
(51) Tamagnini, P.; Axelsson, R.; Lindberg, P.; Oxelfelt, F.; Wunschiers, R.; Lindblad, P. *Microbiol. Mol. Biol. Rev.* **2002**, *66*, 1.
(52) Stephenson, M.; Stickland, L. H. *Biochem. J. (London)* **1931**, *25*, 205.
(53) Seefeldt, L. C.; Arp, D. J. *Biochemistry* **1989**, *28*, 1588.
(54) Teixeira, M.; Fauque, G.; Moura, I.; Lespinat, P. A.; Berlier, Y.; Prickril, B.; Peck, H. D., Jr.; Xavier, A. V.; Le Gall, J.; Moura, J. J. G. *Eur. J. Biochem.* **1987**, *167*, 47.
(55) Ikeda, T.; Takagi, K.; Tatsumi, H.; Kano, K. *Chem. Lett.* **1997**, 5.
(56) Tatsumi, H.; Takagi, K.; Fujita, M.; Kano, K.; Ikeda, T. *Anal. Chem.* **1999**, *71*, 1753.
(57) Lojou, E.; Giudici-Orticoni, M. T.; Bianco, P. *J. Electroanal. Chem.* **2005**, *579*, 199.
(58) Verhagen, M. F.; Wolbert, R. B.; Hagen, W. R. *Eur. J. Biochem.* **1994**, *221*, 821.
(59) Page, C. C.; Moser, C. C.; Chen, X.; Dutton, P. L. *Nature* **1999**, *407*, 47.
(60) Montet, Y.; Amara, P.; Volbeda, A.; Vernede, X.; Hatchikian, E. C.; Field, M. J.; Frey, M.; Fontecilla-Camps, J. C. *Nature Struct. Biol.* **1997**, *4*, 523.
(61) Cohen, J.; Kim, K.; Posewitz, M.; Ghirardi, M. L.; Schulten, K.; Seibert, M.; King, P. *Biochem. Soc. Trans.* **2005**, *33*, 80.
(62) Teixeira, V. H.; Baptista, A. M.; Soares, C. M. *Biophys. J.* **2006**, *91*, 2035.
(63) Buhrke, T.; Lenz, O.; Krauss, N.; Friedrich, B. *J. Biol. Chem.* **2005**, *280*, 23791.
(64) Duche, O.; Elsen, S.; Cournac, L.; Colbeau, A. *FEBS J.* **2005**, *272*, 3899.
(65) Armstrong, F. A. *Curr. Opin. Chem. Biol.* **2004**, *8*, 133.
(66) Léger, C.; Dementin, S.; Bertrand, P.; Rousset, M.; Guigliarelli, B. *J. Am. Chem. Soc.* **2004**, *126*, 12162.
(67) Guiral, M.; Tron, P.; Belle, V.; Aubert, C.; Léger, C.; Guigliarelli, B.; Giudici-Orticoni, M.-T. *Int. J. Hydrogen Energy* **2006**, *31*, 1424.
(68) Johnston, W.; Cooney, M. J.; Liaw, B. Y.; Sapra, R.; Adams, M. W. W. *Enzyme Microb. Technol.* **2005**, *36*, 540.
(69) Armstrong, F. A.; Bond, A. M.; Büchi, F. N.; Hamnett, A.; Hill, H. A.; Lannon, A. M.; Lettington, O. C.; Zoski, C. G. *Analyst (Cambridge, U.K.)* **1993**, *118*, 973.
(70) Ogata, H.; Mizoguchi, Y.; Mizuno, N.; Miki, K.; Adachi, S.; Yasuoka, N.; Yagi, T.; Yamauchi, O.; Hirota, S.; Higuchi, Y. *J. Am. Chem. Soc.* **2002**, *124*, 11628.
(71) Parkin, A.; Cavazza, C.; Fontecilla-Camps, J. C.; Armstrong, F. A. *J. Am. Chem. Soc.* **2006**, *128*, 16808.
(72) Varfolomeev, S. D.; Yaropolov, A. I.; Berezin, I. V.; Tarasevich, M. R.; Bogdanovskaya, V. A. *Bioelectrochem. Bioenerg.* **1977**, *4*, 314.
(73) Varfolomeyev, S. D.; Yaropolov, A. I.; Karyakin, A. A. *J. Biotechnol.* **1993**, *27*, 331.
(74) Butt, J. N.; Filipiak, M.; Hagen, W. R. *Eur. J. Biochem.* **1997**, *245*, 116.
(75) Pershad, H. R.; Duff, J. L. C.; Heering, H. A.; Duin, E. C.; Albracht, S. P. J.; Armstrong, F. A. *Biochemistry* **1999**, *38*, 8992.
(76) Vincent, K. A.; Parkin, A.; Lenz, O.; Albracht, S. P. J.; Fontecilla-Camps, J. C.; Cammack, R.; Friedrich, B.; Armstrong, F. A. *J. Am. Chem. Soc.* **2005**, *127*, 18179.
(77) Bianco, P.; Haladjian, J. *J. Electrochem. Soc.* **1992**, *139*, 2428.
(78) Blanford, C. F.; Armstrong, F. A. *J. Solid State Electrochem.* **2006**, *10*, 826.
(79) Armstrong, F. A.; Cox, P. A.; Hill, H. A. O.; Lowe, V. J.; Oliver, B. N. *J. Electroanal. Chem. Interfacial Electrochem.* **1987**, *217*, 331.
(80) Morozov, S. V.; Vignais, P. M.; Cournac, L.; Zorin, N. A.; Karyakina, E. E.; Karyakin, A. A.; Cosnier, S. *Int. J. Hydrogen Energy* **2002**, *27*, 1501.
(81) Morozov, S. V.; Voronin, O. G.; Karyakina, E. E.; Zorin, N. A.; Cosnier, S.; Karyakin, A. A. *Electrochem. Commun.* **2006**, *8*, 851.
(82) Karyakin, A. A.; Morozov, S. V.; Karyakina, E. E.; Zorin, N. A.; Perelygin, V. V.; Cosnier, S. *Biochem. Soc. Trans.* **2005**, *33*, 73.
(83) Guiral-Brugna, M.; Giudici-Orticoni, M. T.; Bruschi, M.; Bianco, P. *J. Electroanal. Chem.* **2001**, *510*, 136.
(84) Haladjian, J.; Bianco, P.; Nunzi, F.; Bruschi, M. *Anal. Chim. Acta* **1994**, *289*, 15.
(85) Lojou, E.; Durand, M. C.; Dolla, A.; Bianco, P. *Electroanalysis* **2002**, *14*, 913.
(86) Noda, K.; Zorin, N. A.; Nakamura, C.; Miyake, M.; Gogotov, I. N.; Asada, Y.; Akutsu, H.; Miyake, J. *Thin Solid Films* **1998**, *327*−*329*, 639.
(87) Qian, D. J.; Nakamura, C.; Zorin, N.; Miyake, J. *Colloids Surf., A* **2002**, *198*−*200*, 663.
(88) Rüdiger, O.; Abad, J. M.; Hatchikian, E. C.; Fernández, V. M.; De Lacey, A. L. *J. Am. Chem. Soc.* **2005**, *127*, 16008.
(89) Hirst, J.; Armstrong, F. A. *Anal. Chem.* **1998**, *70*, 5062.
(90) Armstrong, F. A.; Camba, R.; Heering, H. A.; Hirst, J.; Jeuken, L. J. C.; Jones, A. K.; Léger, C.; McEvoy, J. P. *Faraday Discuss.* **2000**, *116*, 191.
(91) Jeuken, L. J. C.; Armstrong, F. A. *J. Phys. Chem. B* **2001**, *105*, 5271.
(92) Jones, A. K.; Lamle, S. E.; Pershad, H. R.; Vincent, K. A.; Albracht, S. P. J.; Armstrong, F. A. *J. Am. Chem. Soc.* **2003**, *125*, 8505.
(93) Bard, A. J.; Faulkner, L. R. *Electrochemical Methods. Fundamentals and Applications*, 2nd ed.; John Wiley: New York, 2001.
(94) Fersht, A. *Enzyme Structure and Mechanism*; W.H. Freeman and Company: New York, 1985.
(95) Elliott, S. J.; McElhaney, A. E.; Feng, C. J.; Enemark, J. H.; Armstrong, F. A. *J. Am. Chem. Soc.* **2002**, *124*, 11612.
(96) Mondal, M. S.; Goodin, D. B.; Armstrong, F. A. *J. Am. Chem. Soc.* **1998**, *120*, 6270.
(97) Hudson, J. M.; Heffron, K.; Kotlyar, V.; Sher, Y.; Maklashina, E.; Cecchini, G.; Armstrong, F. A. *J. Am. Chem. Soc.* **2005**, *127*, 6977.
(98) Turner, K. L.; Doherty, M. K.; Heering, H. A.; Armstrong, F. A.; Reid, G. A.; Chapman, S. K. *Biochemistry* **1999**, *38*, 3302.
(99) Roessler, M.; Parkin, A.; Armstrong, F. A. Unpublished data.

(100) Jones, A. K.; Sillery, E.; Albracht, S. P. J.; Armstrong, F. A. *J. Chem. Soc., Chem. Commun.* **2002**, 866.
(101) Léger, C.; Jones, A. K.; Albracht, S. P. J.; Armstrong, F. A. *J. Phys. Chem. B* **2002**, *106*, 13058.
(102) Dementin, S.; Belle, V.; Bertrand, P.; Guigliarelli, B.; Adryanczyk-Perrier, G.; De Lacey, A. L.; Fernández, V. M.; Rousset, M.; Léger, C. *J. Am. Chem. Soc.* **2006**, *128*, 5209.
(103) Limoges, B.; Saveant, J. M. *J. Electroanal. Chem.* **2004**, *562*, 43.
(104) Léger, C.; Jones, A. K.; Roseboom, W.; Albracht, S. P. J.; Armstrong, F. A. *Biochemistry* **2002**, *41*, 15736.
(105) Ottaway, J. M. In *Indicators*; Bishop, E., Ed.; Pergamon Press: Oxford, U.K., 1972.
(106) Hamnett, A.; Christensen, P. A. *Techniques and Mechanisms in Electrochemistry*; Blackie Academic and Professional: London, 1994.
(107) Sørensen, B. *Hydrogen and Fuel Cells*, 3rd ed.; Elsevier Academic Press: Burlington, MA, 2004.
(108) Conway, B. E.; Jerkiewicz, G. *Electrochim. Acta* **2000**, *45*, 4075.
(109) Trasatti, S. *Electrochim. Acta* **1994**, *39*, 1739.
(110) Petrii, O. A.; Tsirlina, G. A. *Electrochim. Acta* **1994**, *39*, 1739.
(111) Fauque, G. D.; Berlier, Y. M.; Czechowski, M. H.; Dimon, B.; Lespinat, P. A.; LeGall, J. *J. Ind. Microbiol.* **1987**, *2*, 15.
(112) Lamle, S. E.; Vincent, K. A.; Halliwell, L. M.; Albracht, S. P. J.; Armstrong, F. A. *J. Chem. Soc., Dalton Trans.* **2003**, 4152.
(113) Albracht, S. P. J. *Biochim. Biophys. Acta* **1994**, *1188*, 167.
(114) Rousset, M.; Montet, Y.; Guigliarelli, B.; Forget, N.; Asso, M.; Bertrand, P.; Fontecilla-Camps, J. C.; Hatchikian, E. C. *Proc. Natl. Acad. Sci. U.S.A.* **1998**, *95*, 11625.
(115) Mege, R. M.; Bourdillon, C. *J. Biol. Chem.* **1985**, *260*, 14701.
(116) Roberts, L. M.; Lindahl, P. A. *J. Am. Chem. Soc.* **1995**, *117*, 2565.
(117) De Lacey, A. L.; Hatchikian, E. C.; Volbeda, A.; Frey, M.; Fontecilla-Camps, J. C.; Fernández, V. M. *J. Am. Chem. Soc.* **1997**, *119*, 7181.
(118) (a) Coremans, J. M. C. C.; Van der Zwaan, J. W.; Albracht, S. P. J. *Biochim. Biophys. Acta* **1992**, *1119*, 157. (b) George, S. J.; Kurkin, S.; Thorneley, R. N. F.; Albracht, S. P. J. *Biochemistry* **2004**, *43*, 6808.
(119) Patil, D. S.; Moura, J. J. G.; He, S. H.; Teixeira, M.; Prickril, B. C.; DerVartanian, D. V.; Peck, H. D., Jr.; Le Gall, J.; Huynh, B. H. *J. Biol. Chem.* **1988**, *263*, 18732.
(120) Roseboom, W.; De Lacey, A. L.; Fernández, V. M.; Hatchikian, E. C.; Albracht, S. P. J. *J. Biol. Inorg. Chem.* **2006**, *11*, 102.
(121) Peters, J. W.; Lanzilotta, W. N.; Lemon, B. J.; Seefeldt, L. C. *Science* **1998**, *282*, 1853.
(122) Nicolet, Y.; Lemon, B. J.; Fontecilla-Camps, J. C.; Peters, J. W. *Trends Biochem. Sci.* **2000**, *25*, 138.
(123) Lamle, S. E.; Albracht, S. P. J.; Armstrong, F. A. *J. Am. Chem. Soc.* **2004**, *126*, 14899.
(124) Ogata, H.; Hirota, S.; Nakahara, A.; Komori, H.; Shibata, N.; Kato, T.; Kano, K.; Higuchi, Y. *Structure* **2005**, *13*, 1635.
(125) Lamle, S. E.; Albracht, S. P. J.; Armstrong, F. A. *J. Am. Chem. Soc.* **2005**, *127*, 6595.
(126) Baek, J.-S.; Choi, E.-H.; Yun, Y.-S.; Kim, S.-C.; Kim, M.-S. *J. Microbiol. Biotechnol.* **2006**, *16*, 1210.
(127) Maness, P.-C.; Smolinski, S.; Dillon, A. C.; Heben, M. J.; Weaver, P. F. *Appl. Environ. Microbiol.* **2002**, *68*, 2633.
(128) Vincent, K. A.; Cracknell, J. A.; Lenz, O.; Zebger, I.; Friedrich, B.; Armstrong, F. A. *Proc. Natl. Acad. Sci. U.S.A.* **2005**, *102*, 16951.
(129) Albracht, S. P. J. Personal communication.
(130) Rakhely, G.; Colbeau, A.; Garin, J.; Vignais, P. M.; Kovacs, K. L. *J. Bacteriol.* **1998**, *180*, 1460.
(131) Camba, R.; Armstrong, F. A. *Biochemistry* **2000**, *39*, 10587.
(132) Tilley, G. J.; Camba, R.; Burgess, B. K.; Armstrong Fraser, A. *Biochem. J.* **2001**, *360*, 717.
(133) Crack, J.; Green, J.; Thomson, A. J. *J. Biol. Chem.* **2004**, *279*, 9278.
(134) Adams, M. W. W. *Biochim. Biophys. Acta* **1990**, *1020*, 115.
(135) Van der Westen, H. M.; Mayhew, S. G.; Veeger, C. *FEBS Lett.* **1978**, *86*, 122.
(136) Hatchikian, C.; Forget, N.; Fernández, V. M.; Williams, R.; Cammack, R. *Eur. J. Biochem.* **1992**, *209*, 357.
(137) Van Dijk, C.; Van Berkel-Arts, A.; Veeger, C. *FEBS Lett.* **1983**, *156*, 340.
(138) Hoberman, H. D.; Rittenberg, D. *J. Biol. Chem.* **1943**, *147*, 211.
(139) Lemon, B. J.; Peters, J. W. *Biochemistry* **1999**, *38*, 12969.
(140) Karyakin, A. A.; Morozov, S. V.; Karyakina, E. E.; Varfolomeyev, S. D.; Zorin, N. A.; Cosnier, S. *Electrochem. Commun.* **2002**, *4*, 417.
(141) Garcin, E.; Vernède, X.; Hatchikian, C.; Volbeda, A.; Frey, M.; Fontecilla-Camps, J. C. *Structure* **1999**, *7*, 557.
(142) Higuchi, Y.; Ogata, H.; Miki, K.; Yasuoka, N.; Yagi, T. *Structure* **1999**, *7*, 549.
(143) Happe, R. P.; Roseboom, W.; Albracht, S. P. J. *Eur. J. Biochem.* **1999**, *259*, 602.
(144) Bennett, B.; Lemon, B. J.; Peters, J. W. *Biochemistry* **2000**, *39*, 7455.
(145) Patil, D. S.; Czechowski, M. H.; Huynh, B. H.; LeGall, J.; Harry D. Peck, J.; DerVartanian, D. V. *Biochem. Biophys. Res. Commun.* **1986**, *137*, 1086.
(146) Telser, J.; Benecky, M.; Adams, M.; Mortenson, L.; Hoffman, B. *J. Biol. Chem.* **1987**, *262*, 6589.
(147) Thauer, R. K.; Kaufer, B.; Zahringer, M.; Jungermann, K. *Eur. J. Biochem.* **1974**, *42*, 447.
(148) Albracht, S. P. J.; Roseboom, W.; Hatchikian, E. C. *J. Biol. Inorg. Chem.* **2006**, *11*, 88.
(149) Higuchi, Y.; Yagi, T.; Yasuoka, N. *Structure* **1997**, *5*, 1671.
(150) Volbeda, A.; Garcia, E.; Piras, C.; De Lacey, A. L.; Fernández, V. M.; Hatchikian, E. C.; Frey, M.; Fontecilla-Camps, J. C. *J. Am. Chem. Soc.* **1996**, *118*, 12989.
(151) Carepo, M.; Tierney, D. L.; Brondino, C. D.; Yang, T. C.; Pamplona, A.; Telser, J.; Moura, I.; Moura, J. J. G.; Hoffman, B. M. *J. Am. Chem. Soc.* **2002**, *124*, 281.
(152) van der Zwaan, J. W.; Coremans, J. M. C. C.; Bouwens, E. C. M.; Albracht, S. P. J. *Biochim. Biophys. Acta* **1990**, *1041*, 101.
(153) Volbeda, A.; Montet, Y.; Vernede, X.; Hatchikian, E. C.; Fontecilla-Camps, J. C. *Int. J. Hydrogen Energy* **2002**, *27*, 1449.
(154) Higuchi, Y.; Yagi, T. *Biochem. Biophys. Res. Commun.* **1999**, *255*, 295.
(155) Krebs, J. F. *Am. Inst. Phys. Conf. Proc.* **2003**, *671 (Hydrogen in Materials and Vacuum Systems*), 101.
(156) Eggert, C.; Temp, U.; Eriksson, K.-E. L. *Environ. Microbiol.* **1996**, *62*, 1151.
(157) Vincent, K. A.; Cracknell, J. A.; Clark, J. R.; Ludwig, M.; Lenz, O.; Friedrich, B.; Armstrong, F. A. *J. Chem. Soc., Chem. Commun.* **2006**, 5033.

CR050191U